SOMATOSENSORY PROCESSING BY RAT MEDIAL PONTOMEDULLARY RETICULAR FORMATION NEURONES: RESPONSES TO INNOCUOUS AND NOXIOUS THERMAL AND MECHANICAL STIMULI

A thesis submitted to
The Doctoral Degrees Board of the University of Cape Town
in fulfilment of the requirements for the degree of
Doctor of Philosophy

by

Craig Jeffrey Farham, B.Sc.(Hons.)

Department of Physiology
Medical School
University of Cape Town
Observatory 7925

December 1990

To Bridget
for endurance beyond the call of duty
with unfailing patience, humour, empathy and love

and to all our animal informants
for their contribution to the growth of knowledge.

ABSTRACT

This work examines somatosensory processing in "giant" neurones of the medial pontomedullary reticular formation (PMRF) in the rat, with particular emphasis on the response to cutaneous thermal stimuli. Thermal test stimuli were employed as these were deemed to be more precisely quantifiable than other forms of cutaneous stimulation.

Activity was recorded from 235 PMRF neurones in 94 female Long Evans rats (270 to 320 g) anaesthetised with urethane (1,25g/kg, i.p.). Rectal temperature was closely controlled at 38 ± 0,5°C. Standard stereotactic and extracellular recording techniques were employed. PMRF giant neurones were identified by their stereotactic location, large, stable spike amplitudes of long duration, responses to cutaneous mechanical stimuli and receptive field properties, and spontaneous discharge characteristics. Ramp, step and sine wave cutaneous thermal stimuli (35-48°C) were applied to the glabrous skin on the hindpaw by means of a computer-controlled Peltier device. The location of the units was confirmed by subsequent histology. One hundred and eleven neurones were located in nucleus reticularis pontis caudalis (NPC), and 124 in nucleus reticularis gigantocellularis (NGC).

Mechanical stimulation excited 188 of 235 (80%) PMRF neurones (ON-m cells), and inhibited 40 (17%, OFF-m cells). Seven cells (3%) had mosaic receptive fields of excitation and inhibition (complex responses, CX-m). Twenty-eight percent of neurones were responsive to both weak and intense stimuli (mixed neurones). The remainder (72%) responded only to intense mechanical stimulation of the skin (high threshold neurones). The (excitatory or inhibitory) response of the mixed neurones to intense stimuli was generally greater than to mild stimuli. Receptive fields ranged in size from restricted (hindlimbs only) to very extensive (covering the entire body surface). Neurones with small receptive fields were almost exclusively of the high threshold type, and tended to be located in NGC, while mixed neurones tended to have larger receptive fields, and were located predominantly in NPC. Some portion of the hind limbs were represented in the receptive fields of all but one of the neurones studied, while the tail and/or trunk were represented in 77%, and the forelimbs and face in 28% of receptive fields. Most of the cells responding to cutaneous mechanical stimulation had bilateral (usually symmetric) receptive fields.

Spontaneous (background) activity occurred in the absence of any deliberate sensory stimulation in 72% of PMRF neurones. The frequency of spontaneous discharge rates ranged from 0 to 47 spikes/s. The coefficient of variation of the spontaneous discharge rate of a given neurone was generally less than 20% (range 0 to 85%).

Of the 235 identified mechanosensitive PMRF neurones, 203 (86%) also responded to cutaneous thermal stimulation (43-48°C) of the ipsilateral hindpaw. Eighty percent of these responded with increased discharge rates (ON-t cells), and 20% were inhibited (OFF-t cells). The polarities of response of individual PMRF neurones to mechanical and thermal stimuli, and to repeated ipsilateral and contralateral thermal stimuli, did not differ significantly. Following transient thermal stimulation, spontaneous discharge rates largely returned to pre-stimulus levels.

The thresholds of response to slow ramp (0,15°C/s) and stepped (2°C/s) thermal stimui occurred both in the innocuous and noxious temperature ranges (below and above 42°C, respectively). The threshold temperatures showed large variability to repeated identical thermal stimuli. Despite the poor reproducibility of the threshold responses, the

distribution of thresholds to thermal ramp stimuli was consistently bimodal, with peaks occurring at 39 and 43°C. The bimodality persisted even when the ipsilateral and contralateral data were pooled. The modes of these threshold distributions conform to the maximum discharge ranges for warm and noxious cutaneous receptors. Thus, it is likely that thermal input to individual PMRF neurones is derived from both types of receptors.

The responses of PMRF neurones to repeated thermal stimuli were stable and reproducible with respect to magnitude and time course. The average (static) and maximum (dynamic) responses to thermal stimuli were generally small: for example, the mean of the average responses to ramp stimuli was 5,9 spikes/s ± 11,0 SD, (range -28 to 40 spikes/s), and the mean of the maximum responses was 9,3 spikes/s ± 16,1 SD, (range -46 to 65 spikes/s). The absolute change in firing rate of individual PMRF neurones, and of the population, increased monotonically as a function of the intensity of stepped cutaneous thermal stimuli in the range 40 to 48°C. However, their resolution, based on their average and maximum responses, was poor. Incorporating the post-stimulus responses into the comparisons between different stimulus intensities marginally increased the resolution of these neurones. Thus, while the majority of PMRF neurones are able to distinguish innocuous from noxious stimuli, few are capable of encoding stimulus intensity within the noxious range (above 43°C).

The majority (70%) of PMRF neurones responded to sustained thermal stimuli with a slow increase or decrease to a new static discharge rate which was maintained with little or no adaptation. Latency to onset of response to stepped thermal stimuli varied from 1 to 50 seconds, and the time to maximal response between 5-60 seconds. Many PMRF neurones also showed marked afterdischarge for periods of up to 5 minutes after removal of the stimulus.

The thermal receptive fields of over 90% of PMRF neurones were large, incorporating at least both hindlimbs. The extensive receptive field sizes of individual PMRF neurones provides evidence against them having a role in stimulus location.

The large number of PMRF neurones showing multimodal convergence, their small magnitude responses, their slow response times, and their large receptive fields strongly suggest that these neurones are not participating in classical sensory discrimination. Rather, they may function as stimulus detectors or alternatively play a role in associative processes.

ACKNOWLEDGEMENTS

Professor Peter Belonje: for providing the excellent research facilities at the Department of Physiology.

Professor Rodney Douglas: for planting the seed, writing the original data capture and analysis programs, and supervising the project.

Professor Johann Koeslag: for sagacious criticism and editorial comment, and for staging multiple rescue operations at the blue event horizon.

Professor Leon Isaacson: for discussion and editorial comment, and for cultivating a nephrologist's perspective of the nervous system (and the world).

Jan Pepler: for the design and construction of the thermal stimulator, and assistance with all electronic and technical matters.

Riyaat Terblanche: for assistance with histology.

Barbara Young: for proof-reading and editorial assistance.

Prakash Kara: for discussion and late-night sustenance.

My Parents: for their loving support.

The Cats: for sanity, spontaneity and spaced oddity.

The Harry Crossley Foundation: for travel expenses.

This research was supported by a grant from the South African Medical Research Council to Prof. R. J. Douglas.

CONTENTS

Chapter 1

GENERAL INTRODUCTION

Since Moruzzi and Magoun discovered the arousal properties of the "ascending reticular activating system" in 1949, the brainstem reticular core has occupied a prominent location in the literature concerning the neuroanatomical and physiological foundations of behaviour. The reticular formation is recognized to be an important component of the extrapyramidal motor systems, and has also been implicated in a variety of functions including the control of sleep and wakefulness, simple forms of behavioural plasticity such as habituation and sensitization, and the mediation of somatic and visceral noxious stimuli. The extensive involvement of brainstem neurones with both sensory and motor functions and in a variety of behavioural contexts suggests that they are involved in global co-ordination of sensory-motor function. Because of its position, connectivity and gross physiology, the reticular formation is also thought to play a key role in the neural mechanisms of behavioural state control.

This study examines the responses of "giant" neurones in the rat medial pontomedullary reticular formation (PMRF) to innocuous and noxious cutaneous thermal stimuli. Although some aspects of the architecture and function of the PMRF have been well described, the role of these neurones in sensory processing is poorly understood. There is little information available on the sensory properties of reticular formation neurones in the rat, but there have been several reports on the sensory properties of neurones in the mesencephalic and lower regions of the reticular formation in cats (see Chapter 2). These latter studies have shown that while a few of these neurones do not respond to sensory stimulation, most do respond to mechanical, visual, auditory, proprioceptive or other stimuli over wide receptive fields. A large proportion of these are convergent neurones characterized by their capacity to respond to multimodal sensory information from cutaneous, visceral and muscular origin. There is also abundant anatomical and electrophysiological evidence suggesting that the giant neurones in the PMRF could play an important role in the processing of nociceptive information. Many PMRF neurones respond either exclusively or preferentially to mechanical, electrical or chemical noxious stimuli. Large numbers of these cells are also activated by Aδ or Aδ- and C-fibre peripheral volleys from any part of the body. Focal stimulation of some areas in the

region of the PMRF can modulate and suppress pain transmission systems in the spinal cord, and also elicits escape behaviour in cats trained to avoid painful electric shocks. However, the responses of reticular formation units to noxious stimuli are often inconsistent, their receptive fields are typically large and difficult to delimit, and their excitability frequently changes.

Since PMRF neurones characteristically receive polymodal sensory input over extensive receptive fields, investigation of the role of these neurones in sensory processing requires a well defined stimulus. Of all the methods used to study somatosensory and pain processes experimentally, temperature is perhaps of the greatest value. Thermal stimuli can be accurately controlled, quantitatively administered and recorded, and generated in such a manner as to produce little or no tissue damage. This study shows that cutaneous heat stimuli can reliably alter the discharge patterns of PMRF neurones in both the innocuous and noxious temperature ranges. Thus, temperature is a suitable probe for studying the somatosensory response properties of these neurones. The responses of PMRF neurones to graded cutaneous thermal stimuli have not previously been investigated in any species.

The experiments reported here were performed in two stages. In order to establish consistency between this and previous studies, "giant" cells in the PMRF were first identified by their stereotactic location, electrophysiological characteristics, and responses to tactile and mechanical stimuli over wide receptive fields (Chapter 3). Thereafter, the responses of these neurones to graded and repeated cutaneous thermal stimuli were studied in detail (Chapter 4). These experiments addressed the following questions:

1. Are mechanosensitive PMRF neurones also responsive to cutaneous thermal stimuli (i.e. what fraction of these neurones exhibit multimodal convergence)?
2. How do their responses to thermal and mechanical stimuli compare (i.e. what are their response polarities, their adequate stimuli and their receptive field characteristics to each stimulus type)?
3. Are PMRF neurones capable of encoding thermal stimulus parameters (i.e. what are their temperature thresholds; and does the magnitude and time course of response vary as a function of the intensity, rate, and/or duration of the thermal stimulus)?
4. Do these neurones exhibit spatial convergence, and if so, to what extent?

Answers to these questions provide information about the intensive, temporal and spatial aspects of the neuronal spike discharge patterns of the PMRF giant neurones (Chapter 5).

This work forms part of a combined laboratory research program to study the electrophysiology, microanatomy and neuropharmacology of the PMRF. The program comprises a number of projects which have examined, inter alia, (a) the temporal structure of action potential discharge in PMRF neurones (R. Douglas), (b) the somatosensory properties of PMRF neurones (this study; and P. Francis), (c) the functional circuitry of these neurones, using combined electrophysiology, micro-ionophoresis and HRP tract tracing (L. Kellaway), (d) possible interactions between neurones within the PMRF, using multicellular recording and interspike interval analysis (A. George), and (e) their rostral projections (B. Sefton) and (f) cholinoceptive properties (H. Markram). The significance of this program lies in the probable role of the PMRF as a major brainstem controller of sensory input to spinal and supraspinal sensory pathways. In this view the PMRF affects sensory attention selection by mechanisms analogous to the brainstem pain control system. We are examining the physiology and microcircuitry of the PMRF in this context.

The original data capture and analysis programs used in this project were written by Professor Rodney Douglas, and are gratefully acknowledged. I performed all other facets of this work, including extensive revisions and additions to the data analysis programs as the project evolved. All experiments were performed on anaesthetized rats, which were sacrificed at the end of the experiment. All animal experimental methods and techniques met with criteria acceptable to the University of Cape Town Medical Animal Research Review Committee.

Aspects of the work have been presented at meetings of the Physiological Society of Southern Africa and the European Neurosciences Association. Some of the results presented in this thesis, and a technical report describing the thermal stimulator designed and constructed in this laboratory, have been published (Farham and Douglas, 1985; Pepler, Farham and Douglas, 1985).

Chapter 2

THE ROLE OF THE PMRF IN SENSORY AND PAIN MECHANISMS

2.1 INTRODUCTION

The term "reticular formation" is most commonly used to refer to the complex of neuronal cell pools and associated fibre systems making up the central core of the brainstem; the tegmentum of the midbrain and pons and its continuation into the medulla and upper spinal cord. Originally, the reticular formation was thought to be a "nonspecific system" comprising diffuse, unpatterned groups of neurones and fibres (Hobson, 1980). However, this concept has changed markedly in recent years, and many studies have emphasized the specificity of projections and neurotransmitter coding as key features of the anatomy and function of this region. Thus, for example, Hobson and Scheibel (1980) describe the brainstem reticular core as "a complex and highly organized interdigitation of individually signatured cell systems [each having] its own idiosyncratic morphology, synaptic chemistry, input-output relations, and functional roles" (p. 10). The "nonspecific systems" are therefore recognized to be, in many respects, more highly ordered and more complex than the "specific systems".

The reticular formation is truly multifunctional. Neurones in this system receive many afferent collaterals from long ascending (sensory) tracts, the visual, olfactory, auditory and trigeminal nerve systems, as well as from the cerebellum, basal ganglia, hypothalamus, limbic system and cerebral cortex. The efferent projections from the reticular formation conduct impulses both to higher brain centres and caudally to the spinal cord. The reticular formation thus constitutes a polysynaptic pathway for sensory input of all types, and contains fairly localized regions which are essential for the control of muscle tone and movements of all parts of the body, eye movements, vestibulo-ocular reflexes, several autonomic functions, and modulation of spinal nociceptive inputs. There is no topographic organization of the input-output relationships within this region, and the nature of the processing is not understood. There is, however, evidence of topographically organized polysensory convergent patterns in the mesencephalic reticular formation which may provide summed outputs that control thalamic gating

mechanisms, thereby producing an active focusing of the conscious state (for references, see Hobson and Brazier, 1980; Hobson and Scheibel, 1980; Brodal, 1981; Hobson and Steriade, 1986). Studies of the behavioural correlates of activity in reticular formation cells have found units whose discharge relates to sensory stimuli, pain and escape behaviour, conditioning and habituation, arousal and complex motivational states, REM sleep, and others (Siegel, 1979, 1983; Siegel and Tomaszewski, 1983; Siegel et al., 1983, 1986). The comprehensive sensory and motor processing roles of the reticular formation suggests that it might be a primitive integration region for the selection of behavioural states (Hobson and Brazier, 1980; Hobson and Steriade, 1986).

Most reticular nuclei have indistinct boundaries and heterogeneous cytoarchitecture, and the projections of the component nuclei differ in ways that, to some extent, reflect involvement in different behaviours. Furthermore, functional areas often do not conform to the cytoarchitectural borders of the reticular formation (Brodal, 1981; Andrezik and Beitz, 1985). Thus, individual reticular nuclei may have diverse functions, and, conversely, functional groups of neurones may be distributed among several nuclei.

All reticular formation neurones are interneurones, since their axons and dendrites reach neither the receptive periphery of the organism, nor the organs of motor performance, such as muscles and glands (Scheibel, 1984). Neurones comprising the brainstem reticular core appear organized to distribute information quickly to multiple targets throughout most of the neuraxis, from the diencephalon to the spinal cord. The effector functions of the reticular formation are mediated mainly by neurones in the medial two-thirds of the brainstem, where incomplete segregation is found between levels exerting their main action on the spinal cord and those acting chiefly on more rostral parts of the brain. The small cells in the lateral third of the brainstem appear to act to a large extent on the medial two-thirds by medially directed processes. The lateral reticular formation may therefore function as an "area of association" (Brodal, 1981).

The following account focuses primarily on the architecture and functions of the giant neurones of the medial pontomedullary reticular formation (PMRF) as related to sensory functions and pain mechanisms. Other aspects of the anatomy and physiology of the brainstem reticular formation have been reviewed, directly or indirectly, by a number of authors (anatomy - Brodal, 1981; Andrezik and Beitz, 1985; Martin et al., 1985; motor functions - Peterson, 1979; Holstege and Kuypers, 1987; REM sleep - Vertes, 1984a; neurochemistry - Sjölund and Björklund, 1982; behavioural functions - Siegel, 1979, 1983;

Hobson and Brazier, 1980; Hobson and Scheibel, 1980; Hobson and Steriade, 1986). The volume edited by Jasper et al. (1958) is a major synopsis of earlier work on the reticular formation.

2.2 NUCLEI, CYTOARCHITECTURE AND DENDRITIC DOMAINS OF THE PMRF

The PMRF, as defined in this study, is composed of nucleus gigantocellularis (NGC) and nucleus reticularis pontis caudalis (NPC; Figure 2.1). NGC occupies the medial two-thirds of the reticular formation, extending in the rat from the midpoint of the inferior olive to the caudal pole of the superior olive. This nucleus fuses rostrally with NPC and caudally with nucleus reticularis ventralis (NRV). The medial boundary abuts the hypoglossal nerve and paramedain reticular nucleus caudally, and the predorsal fibre bundles rostrally. The parvocellular reticular nucleus occupies the lateral one-third of the reticular formation adjacent to NGC. Ventrally, NGC borders on nucleus gigantocellularis pars alpha and nucleus paragigantocellularis, and dorsally on the nuclei that comprise the dorsomedial surface of the medulla (Andrezik and Beitz, 1985).

The giant neurones (somata 65 µm x 30 µm) which give NGC its name in fact comprise only a small proportion of the neurones in this nucleus. Most of the neurones are medium-sized or small, with 69% having a major axis length of 20-40 µm, and only 12% exceeding 50 µm (Newman and Kiddy, 1981; Andrezik and Beitz, 1985). The large neurones are predominantly involved in controlling motor nuclei and spinal cord operations, whereas small neurones have ascending projections. This relative dichotomy is characteristic of both bulbar and pontine reticular formations (Hobson and Steriade, 1986). There are few giant neurones in the lateral portions of NGC, where the cells are smaller and more densely packed than in other regions of this nucleus.

Nucleus reticularis pontis caudalis (NPC) extends from the level of the caudal pole of the trapezoid body to the level of the junction between the middle and rostral thirds of the trigeminal nerve. Rostrally, NPC is continuous with nucleus reticularis pontis oralis (NPO) in the medial pontine tegmentum. There is a prominent collection of giant neurones in the medial portion of NPC. These are among the largest cells in the reticular formation, with some somata measuring up to 65 µm x 50 µm in their longest dimension (Valverde, 1962; Andrezik and Beitz, 1985). There are no giant cells in NPO, but the histological transition between NPC and NPO is indistinct.

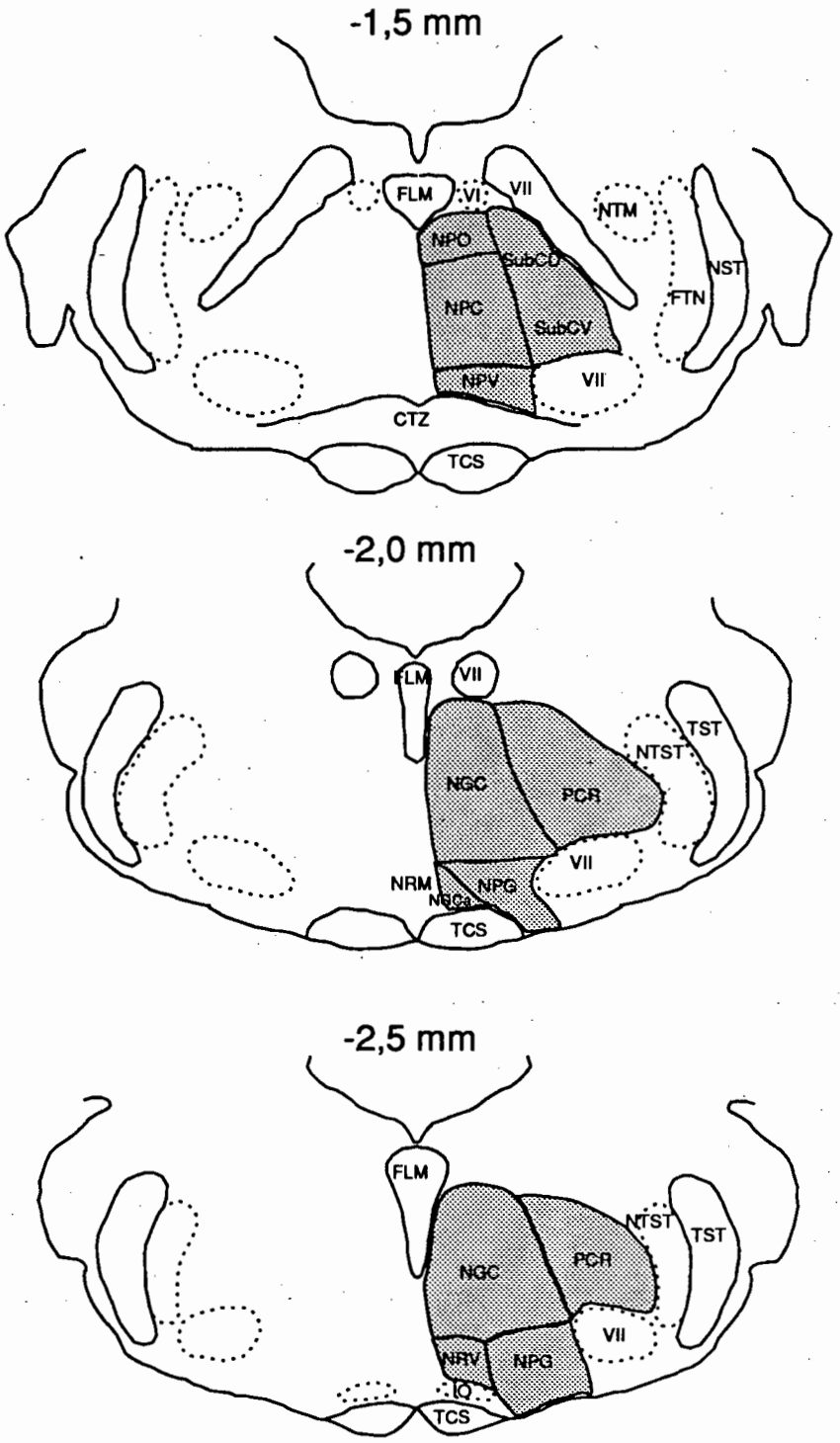

FIGURE 2.1 Major anatomical structures in rat medial pontomedullary reticular formation. The nuclei of the reticular formation are redrawn primarily from Andrezik and Beitz (1985). CTZ, fibres of the trapeziod body; FLM, longitudinal fasciculus; FTN, fibres of the trigeminal nerve; NGC, nucleus gigantocellularis; NPC, nucleus pontis caudalis; NST, sensory nucleus of trigeminal; NTM, motor nucleus of trigeminal; NTST, spinal tract of trigeminal; TCS, corticospinal tract; TST ascending spinal tract of trigeminal; VI, abducens nucleus; VII, facial nerve nucleus. The numbers above each section indicate the anterior-posterior stereotaxic coordinates in millimetres.

The dendritic trees of the large and medium-sized PMRF neurones radiate from the cell body in the coronal plane to form round or slightly oval dendritic trees with marked rostrocaudal compression (Scheibel and Scheibel, 1958; Valverde, 1961; Edwards et al., 1987). This radial spread of dendrites with the primary orientation perpendicular to the long axis of the brainstem provides these cells with numerous sources of heterogenous afferent input, and serves to limit presynaptic input within circumscribed regions. This suggests that the brainstem reticular core has a modular organization such that cells at a given level interdigitate extensively, but interaction along the rostrocaudal plane is very much less (Scheibel and Scheibel, 1958; Scheibel, 1984).

Edwards et al. (1987) distinguished two morphological types of medial reticular cells on the basis of dendritic branching patterns of neurones filled with horseradish peroxidase (HRP): densely branched and sparsely branched. Densely branched cells were larger, had more spines on distal dendrites, and were confined to NGC. Sparsely branched cells were small, medium or large, had few spines, and were found in NGC, nucleus reticularis magnocellularis (NMC) and nucleus raphe magnus (NRM). No spines were seen on the cell somas of either cell type.

2.3 AFFERENT PROJECTIONS TO THE RETICULAR FORMATION

Spinoreticular fibres terminate in virtually all regions of the medial bulbar and pontine reticular formation. The medullary terminations are predominantly ipsilateral, while those in the pons tend to be bilateral. The terminations are most dense in the ventrocaudal NGC, NPC and NRV, and are less prevalent in NPO. The spinoreticular projection is not somatotopically organized (Willis and Coggeshall, 1978; Brodal, 1981).

The spinoreticular tract ascends in the ventrolateral funiculus of the cord, interspersed with spinothalamic, spinocerebellar and spinotectal fibres. In the brainstem the terminal branches and collaterals of the spinoreticular fibres run dorsomedially, approximately perpendicular to the long axis of the brainstem in the same plane as the dendritic trees of the PMRF neurones (Scheibel and Scheibel, 1958).

HRP deposited in NGC leads to retrograde labelling of somata in both the dorsal and ventral grey of the cervical cord (Gallager and Pert, 1978; Kevetter et al., 1982; Chaouch et al., 1983). Kevetter and co-workers found greater numbers of HRP-labelled spinoreticular cells in the ventromedial cord, particularly laminae VII and VIII, while labelled cells of the dorsal horn were confined mainly to the lateral reticulated aspect of

lamina V. Ipsilaterally projecting neurones are more prevalent in cervical segments, but they are found in all levels of the spinal cord studied so far (Maunz et al., 1978; Menétrey et al., 1980; Kevetter et al., 1982). Attempts to identify spinoreticular tract somata by means of antidromic recordings have yielded equivocal results (Albe-Fessard et al., 1974; Fields et al., 1977; Maunz et al., 1978).

While the spinoreticular fibres probably comprise the major ascending input to the PMRF, there are also collaterals from other ascending systems, particularly the spinothalamic tract (Scheibel and Scheibel, 1958; Kevetter and Willis, 1982, 1983; Albe-Fessard et al., 1985). There is considerable overlap in the distribution of spinothalamic and spinoreticular cells, especially in laminae VII and V (Kevetter and Willis, 1984). However, the spinal neurones projecting to the reticular formation, thalamus and diencephalon appear to constitute predominantly separable populations (Fields et al., 1977; Giesler et al., 1981; Haber et al., 1982; Kevetter et al., 1982, 1983).

The PMRF receives afferents conveying pain, temperature, touch and pressure arising from all regions of the periphery (see below), as well as proprioceptive (Pompeiano and Barnes, 1971) and visceral sensory input (Pavlasek et al., 1977; Schulz et al., 1983; Ammons, 1987; Blair, 1987). There is no input from the dorsal column nuclei (Bowsher et al., 1968) or the medial lemniscus (Valverde, 1961). Thus, the PMRF probably does not respond to discriminative touch or vibration.

Sensory input from the cranial nerves to the PMRF is not well understood. A few primary sensory fibres have been traced to it, for example from the vagus, glossopharyngeal and trigeminal nerves, but these appear to be scarce and restricted in their distribution. There are, however, many collaterals of secondary sensory fibres from the vestibular pathway, ascending auditory pathways, and visual system via tectoreticular connections (Brodal, 1981).

Descending afferents converge onto the medullary and pontine reticular formation via largely monosynaptic connections from the cerebral cortex (Rossi and Brodal, 1956; Kuypers, 1958a, 1958b; Valverde, 1962, 1966), cerebellum (Walberg et al., 1962), superior colliculus (Kawamura et al., 1974) and vestibular nuclei (Ladpli and Brodal, 1968). Most of the terminations of these afferents coincide with the sites of origin of reticulospinal fibres, mainly in NGC and NPC (see below). There is considerably less overlap with reticular regions giving off long ascending axons and with the terminal distribution of

spinoreticular fibres. Thus, it would appear that these convergent descending inputs primarily influence reticular control of the spinal cord (Brodal, 1981).

2.4 EFFERENT OUTFLOW FROM THE RETICULAR FORMATION

The interneuronal nature of cells in the reticular core is revealed by the length and distribution of their axonal systems. There are no local circuit (Golgi type II) neurones in the reticular formation, and all axons appear to project at least some distance rostrally and/or caudally. A spectrum of axonal lengths is found, ranging from relatively limited trajectories (but not true short-axoned cells), to the predominant class of intermediate-length elements. A small fraction of cells in NGC, NPC, NPO and possibly nucleus cuneiformis generate long bifurcating axons running for long distances both rostrally and caudally (Scheibel, 1984; Martin et al., 1985). Double-labelling experiments have shown that some of the neurones in NGC which innervate the spinal cord also project to either the cerebellum or the diencephalon (Waltzer and Martin, 1984). The long axons give off several collaterals, the majority of which spread out among the radiating dendrites in the coronal plane (Brodal, 1981). Studies in this laboratory indicate that some of these collaterals loop back to the area of origin of their cell somas (Kellaway and Douglas, 1985). Thus, in addition to their projecting roles, these neurones may also function in a similar manner to local circuit neurones.

Both the descending reticulospinal fibres and the majority of long ascending fibres arise in two clusters in the pons (NPO and NPC) and medulla (NGC and NRV). While there is considerable overlap of these two efferent systems, descending axons appear to arise somewhat more rostral than do ascending fibres. These efferent axon systems are both crossed and uncrossed, except for fibres descending from the pons, which are uncrossed (Brodal, 1957). Collateral interactions between these fibres indicate that impulses passing to the cord may act on rostrally projecting cells and vice versa. This implies that there is very close integration between the influences exerted by the reticular formation in the rostral and caudal directions.

Reticulospinal axons from NGC descend bilaterally in the ventral and lateral funiculi, but with a distinct ipsilateral predominance (Zemlan and Pfaff, 1979; Martin et al., 1985). Axons of the gigantocellular neurones distribute throughout the length of the spinal cord, primarily to medial parts of laminae VII, VIII and X (Zemlan et al., 1982; Martin et al., 1985), and to a lesser extent to lateral parts of laminae III to VII, lamina IX, the intermediolateral cell column and the sacral parasympathetic nucleus (Martin and

Waltzer, 1984; Martin et al., 1985). Spinal axons from NPC project primarily via the ipsilateral ventral funiculus to lamina VIII and medial parts of lamina VII (Martin et al., 1985). There is evidence in the opossum that the ventral NPC innervates the dorsal horn, possibly via serotonergic neurones (Martin et al., 1979, 1982).

The axons of many neurones in the medulla and pons extend the entire length of the spinal cord, and a relatively large percentage of these give rise to collaterals distributed both to the cervical and lumbar spinal cord (Peterson et al., 1975a; Huisman et al., 1981). Electrophysiological findings have shown that some of the medullary reticulospinal fibres make direct connections with motoneurones (Peterson, 1979). A spatial segregation of pontomedullary reticular neurones into various zones exerting differential excitatory or inhibitory effects on motoneurones innervating eye, limb and axial musculature has been clearly demonstrated (Cohen and Henn, 1972; Keller, 1974; Graybiel, 1977; Peterson et al., 1978; Tohyama et al., 1979; see Section 2.8).

Serotonergic neurones found in NGC, nucleus raphe magnus and other brainstem nuclei apparently contribute to the dense serotonergic innervation found within laminae IX and X, the intermediolateral cell column and autonomic nuclei (Bowker et al., 1982). Peptides such as enkephalin and substance P are also present within neurones in NGC and the raphe nuclei, and many of these innervate the spinal cord. Some of these peptides co-exist with serotonin (Hökfelt et al., 1982). Noradrenergic neurones are found in the dorsolateral pons, in locus coeruleus (LC, not classically regarded as a reticular nucleus) and nucleus subcoeruleus (SubC). Many of these project to the intermediate areas of the cord (laminae V to VIII), to lamina X, to autonomic nuclei, and to laminae I and II (Martin et al., 1985). It has been suggested that in highly motivated behaviours (such as fight and flight), serotonergic projections from NGC to the spinal cord modulate motor activity, whereas noradrenergic projections from the dorsolateral pons modulate both pain processing and motor behaviour (Kuypers, 1982, 1985). Catecholamine projections to layers I, II and V are thought to play a role in centrally induced analgesia (Basbaum and Fields, 1978, 1980; Fields and Basbaum, 1989).

The ascending projections of the PMRF are directed to the cerebellum (Martin and Waltzer, 1984), diencephalon (Takagi et al., 1980; Loewy et al., 1981; Vertes, 1984b, 1984c) and selected cranial nerve motor nuclei (Graybiel, 1977). Both NGC and NPC contribute axons to the median forebrain bundle. Axons from NGC divide into dorsal and ventral branches, with the dorsal branch projecting to the dorsal thalamus and the ventral one

innervating the zona incerta, the hypothalamus and more rostral areas (Nauta and Kuypers, 1958; Vertes et al., 1984). Diencephalic projections of the NPC and NPO innervate certain intralaminar nuclei and the dorsomedial nucleus of the thalamus, as well as various hypothalamic, subthalamic and basal forebrain areas (Graybiel, 1977; Robertson and Feiner, 1982).

2.5 RESPONSE OF PMRF NEURONES TO SENSORY STIMULI

The anatomical evidence indicating convergence of terminal and/or collateral fibres on neurones in the brainstem reticular formation is strongly supported by physiological data. Both extracellular (Amassian and DeVito, 1954; Bell et al., 1964; Wolstencroft, 1964; Bowsher et al., 1968) and intracellular (Magni and Willis, 1963; Ito et al., 1970) single unit recordings have emphasized polysensory convergence on individual reticular formation cells. Patterns of convergence vary markedly among individual units, but they are clearly not unlimited (Scheibel et al., 1955; Bowsher et al., 1968) or random (Peterson et al., 1975b), and each reticular unit appears to have its own unique mix of input terminals (Scheibel, 1984).

Early electrophysiological studies demonstrated convergence of inputs from several parts of the body and from multiple neural systems on individual PMRF units (Amassian and DeVito, 1954; Scheibel and Scheibel, 1958; Wolstencroft, 1964; Segundo et al., 1967). Thus, for example, a given medullary or pontine neurone could be shown to respond to ipsilateral or bilateral electrical stimulation of the sciatic or saphenous nerve, to somatic stimuli from all parts of the body, to auditory and visual stimuli, and/or to cortical stimulation. Response latency to electrical stimulation of receptive field ranged from 12 to 80 ms (Amassian and DeVito, 1954). In some units, cutaneous stimuli applied to different parts of the body were not equally effective in eliciting a response, resulting in graded or restricted receptive fields. Most PMRF units were excited by natural stimuli, others exhibited inhibition, and a small fraction were excited from some parts of the body and inhibited from others (Wolstencroft, 1964).

Reticular formation neurones respond potently to vestibular inputs. Stimulation of the vestibular nerve produces EPSP's or IPSP's in 75% of medial reticular neurones (Peterson et al., 1975b), and over 50% of these units receive monosynaptic input from the vestibular nuclei (Peterson and Abzug, 1975). Specific responses to vaginal and other sexual stimuli have been demonstrated throughout the brainstem reticular formation (Rose, 1975a, 1975b, 1978; Hornby and Rose, 1976). Unit responses to vaginal stimulation

are increased during oestrous (Rose, 1975b; Rose and Michael, 1978) and by oestrogen treatment in ovariectomized animals (Kow and Pfaff, 1982). Neurones sensitive to brainstem and/or hypothalamic temperature have been detected in midbrain reticular formation (Cronin and Baker, 1977) and caudal medulla (Lee et al., 1977). Units responsive to cutaneous thermal stimuli have been located in bulbar reticular formation (Burton, 1968), medial mesencephalon and rostral pons (Eickhoff et al., 1978), midline medullary neurones (Young and Dawson, 1987) and in NGC and NPC (Farham and Douglas, 1985). The responses of medial PMRF neurones to cutaneous thermal stimuli are described in detail in Chapter 4.

There is some evidence for a relatively high degree of organization of somatic afferent terminals within the reticular formation. Bell et al. (1964) found that the face and the forelimbs were the most commonly represented body components in the lower two-thirds of the brainstem. The majority of their terminals projected ipsilaterally and were concentrated in highly restricted fields. The hindlimb, trunk and tail constituted the least frequently represented zones and involved bilateral projections characterized by wide receptive fields. Groves et al. (1973) reported differences in the anatomical distribution of different sensory modalities throughout the reticular core. Although there was considerable overlap between regions and even within neurones, in general units responding to the face and anterior body regions were located both in the mesencephalic reticular formation and at the level of the pontomedullary junction (the most posterior region studied), the middle of the body was represented at the mesencephalo-pontine junction, and the posterior zones were represented in the rostral pons. Thus there appear to be subtle differences between the pontomedullary and mesencephalic areas for the face and anterior and posterior body regions, respectively.

These results contrast with those of Bowsher et al. (1968), who reported that all cells encountered in the gigantocellular region could be driven by somatic stimulation and about 60% of these showed heterosensory convergence with sound or light, or both. Over 90% of these neurones had receptive fields that included all four limbs. Thus, while there may be regions of functional specialization in the reticular core, there is also evidence for substantial interaction and a heterogenous functional arrangement in this region, which could provide a basis for unified operations (Casey, 1980).

These patterns of sensory representation along the reticular core probably reflect dynamic configurations, with potential for widespread variation under certain

conditions (Scheibel, 1984). For example, most reticular formation neurones show a progressive decrease in their response to repeated cutaneous stimulation. This process of adaptation or habituation has been studied by several investigators (Bell et al., 1964; Scheibel and Scheibel, 1965a, 1965b, 1965c; Segundo et al., 1967; Groves et al., 1973; Peterson et al., 1975a; Fox and Wolstencroft, 1976). The percentage of reticular cells showing response habituation varies from 60% to 90%, depending on the technique and the animal species used. This high percentage of response habituation underscores the plasticity of reticular formation neurones and their afferent sensitivity to the transitory nature and relevance of a stimulus (Scheibel, 1984). The cyclic variation in the responsiveness to several types of stimuli in lower brainstem reticular formation neurones known to be involved in multiple somatic and autonomic functions further suggest that these neurones may periodically function as part of one neural net and then another (Scheibel and Scheibel, 1965c).

2.6 RESPONSE OF PMRF NEURONES TO NOXIOUS STIMULI

There is substantial evidence that nociceptor afferents are among the most effective inputs influencing the discharge of a sizable population of reticular formation neurones (Bowsher, 1976). Many investigators have demonstrated that medullary and mesencephalic units respond exclusively or differentially to noxious stimuli (Wolstencroft, 1964; Bowsher et al., 1968; Burton, 1968; Casey, 1969; Benjamin, 1970; Goldman et al., 1972; Guilbaud et al., 1973; Casey et al., 1974; LeBlanc and Gatipon, 1974; Young and Gottschaldt, 1976; Eickhoff et al., 1978; Pearl and Anderson, 1978, 1980). Those neurones showing differential responsiveness to noxious stimuli generally have large, often bilateral receptive fields, and are therefore unlikely to subserve somatesthetic discriminative functions (Casey, 1980).

Pearl and Anderson (1978) used electrical stimulation of radial, sciatic and trigeminal nerves to study the responses of NGC neurones to noxious stimuli. The type of response (excitation, inhibition or mixed) appeared to correlate with the spontaneous discharge rates of each cell. Approximately half of the neurones responded with excitation followed by a period of suppressed activity. These cells had high (35-70/s) or medium (10-35/s) spontaneous discharge rates. Twenty-five percent had low spontaneous rates (0-20/s), and responded only with excitation. Six percent responded by decreasing their discharge rates. These units had relatively high (35-70/s) spontaneous discharge rates. The remainder showed mixed responses (excitation and inhibition) and had a wide range of discharge rates.

The responses of NGC neurones to noxious peripheral stimuli are similar. LeBlanc and Gatipon (1974) reported that 60% were excited, and the remainder inhibited, by noxious pressure and pinch stimuli. The excitatory response outlasted the duration of the applied stimulus. The inhibition was a prolonged (up to 40 s) depression of ongoing spontaneous activity, with or without ensuing excitation. NGC neurones have also been shown to respond to noxious stimulation of the gallbladder (Pavlasek et al., 1977), kidneys (Ammons, 1987) and heart (Blair, 1987).

Many spinoreticular neurones projecting to NGC and other medial reticular structures are excited by noxious stimuli (Fields et al., 1975, 1977; Maunz et al., 1978; Haber et al., 1982; Blair et al., 1984). The receptive fields of spinoreticular cells vary from quite small to large, with the latter sometimes bilateral regions of the skin or deep tissue (Haber et al., 1982). As noted above, some spinal neurones project both to the thalamus and to the reticular formation and thus provide the same information to both brain structures (Giesler et al., 1981; Haber et al., 1982; Kevetter and Willis, 1982). It is not clear if the comparatively discrete sensory information transmitted by some spinoreticular afferents is preserved in the postsynaptic responses of reticular formation neurones or if these responses are made less discriminative by convergent input from other afferent neurones (Willis, 1989).

Casey (1971a) studied the discharge of NGC cells in cats trained to escape painful electric shock. He found that unit discharge rates increased as stimulus intensities were raised to levels eliciting escape behaviour. Electrical stimulation in the same area produces escape or avoidance behaviour in these animals (Keene and Casey, 1970, 1973; Casey, 1971b; Casey et al., 1974). In the rat, some of these escape-related neurones develop responses to innocuous stimuli which have been paired with noxious shock, but not to a neutral conditioned stimulus (Vertes and Miller, 1976). The responsive neurones were located primarily in NPC, but also in NGC. There was no correlation between the activity of the cells to the conditioned response and gross movement of the animal.

Halpern and Halverson (1974) found that destructive lesions in NGC significantly increased the latency and electrical shock threshold of escape behaviour in cats. Control observations indicated that the effect was not due to motor impairment. Similar findings have been reported by Anderson and Pearl (1975). These effects may be due to damage to cell bodies, passing axons, or both.

2.7 CONTROL OF SENSORY INPUT BY THE PMRF

The brainstem reticular formation is capable of modulating and suppressing nociceptor systems in the spinal cord, possibly under the control of enkephalin-binding neurones of the periaqueductal grey matter (PAG). Ascending spinal sensory pathways can be controlled by at least two separate systems originating in the caudal brainstem - NGC projecting via the reticulospinal tract, and nucleus raphe magnus (NRM) acting via the raphespinal projections in the dorsolateral funiculi. Both affect transmission in spinothalamic fibres. Stimulation of NGC evokes both inhibition and excitation in spinothalamic neurones (Haber et al., 1978, 1980), with the Aδ and Aβ inputs equally affected. The control persisted after lesions of the dorsolateral funiculi, suggesting that the effect is mediated by reticulospinal rather than raphespinal projections. Haber et al. (1980) found no topographic organization in NGC with respect to regions causing inhibition or excitation of spinothalamic neurones. Stimulation in NRM appears to selectively inhibit activity in neurones of laminae I and V, and preferentially affects conduction in Aδ rather than Aβ fibres (Liebeskind et al., 1973; Besson et al., 1974; Willis et al., 1977). Responses to both tactile and noxious stimuli are inhibited. Lamina I cells are selectively activated by slowly conducting Aδ or C fibres, or both (Christensen and Perl, 1970; Trevino et al., 1973), and appear to be primarily responsive to intense mechanical, thermal or noxious stimuli (Price and Mayer, 1974; Willis et al., 1974). Lamina V cells are responsive both to noxious stimuli and wide field convergent cutaneous stimuli (Price and Browe, 1973; Willis et al., 1974). McCreery et al. (1979) reported that stimulation in both NRM and NGC produced a much greater suppression of the response of spinothalamic tract neurones to slowly changing or sustained mechanical stimuli than to transient stimuli. They suggest that the effects of both descending systems are at least as dependent on the time course of the mechanical stimulus as they are on its intensity.

Local injection of morphine into NGC produces analgesia (Takagi et al., 1978), while formalin-induced and thermal but not mechanical noxious stimuli increased the tonic release of met-enkephalin in this nucleus (Kuraishi et al., 1984). Analgesia-producing electrical stimulation of the periaqueductal gray alters the spontaneous activity in 80% of neurones in NGC and nucleus paragigantocellularis (both excitation and inhibition are observed) and inhibits stimulus-evoked excitation in 75% of these neurones (Morhland and Gebhart, 1980). Microinjection of morphine into the PAG also increases (50%) or decreases (17%) the spontaneous activity and inhibits the noxious-evoked excitation of

47% of these neurones. These effects are specific for analgesia produced by PAG manipulations and are partially reversed by naloxone, an opiate antagonist (Morhland and Gebhart, 1980).

Repetitive stimulation in NRM and in the dorsal raphe nucleus of the midbrain has been shown to modify the threshold of the jaw-opening reflex obtained by tooth pulp stimulation, and suppresses behavioural reactions elicited by strong pinches to the tail or to the limbs (Mayer and Price, 1976; Oliveras et al., 1977). Stimulation in these areas also produces profound behavioural analgesia when assessed by the tail-flick test (Vanegas et al., 1984a, 1984b; Barbaro et al., 1986). These inhibitory responses are attenuated by naloxone (Oliveras et al., 1977).

2.8 CONTROL OF MOTOR OUTPUT BY THE PMRF

NGC is known to be involved in posture and balance, and the pontine reticular formation to effect somatic motor functions (Peterson, 1980). A number of studies have provided evidence for selective projections from the PMRF to spinal motoneurones. Direct excitatory effects from neurones in NPC and NGC have been demonstrated on flexors and extensors of the hindlimb (Grillner and Lund, 1968), and on motoneurones supplying head, neck, back and forelimbs (Wilson and Yoshida, 1969; Wilson et al., 1970). Peterson et al. (1978, 1979) identified five functional zones in medial PMRF on the basis of their somatomotor connections. Zone 1 includes NPC and a portion of NGC, and appears to exert an excitatory effect on motoneurones at all levels of the spinal cord. Zone 2 comprises the ventral NGC and the rostral part of NRV, and zone 3 the bulk of caudal NRV. Neurones in zone 2 and 3 both evoke direct excitation of motoneurones supplying the axial musculature of the back, while the cervical motoneurones are excited by zone 2 and powerfully inhibited by zone 3. Zone 4, which lies dorsal to zones 1 and 2, exerts its maximal effect on cervical motoneurones, providing both excitation and inhibition. Zone 5 primarily occupies NPO, and appears to have little effect on spinal motoneurones. Peterson et al. (1979) suggest that zones 1 and 2 are involved in whole body postural reflexes, with zone 2 providing greater emphasis on the axial muscles. Zone 3 is thought to generate the postural atonia of sleep, and zone 4 to coordinate head and neck movements with gaze. Zone 5 receives afferents from the optic tectum, and contains many neurones whose discharge rate is synchronized with the sleep-wake cycle. These cells may therefore be involved in functions such as startle reactions and/or arousal.

2.9 ASCENDING SYSTEMS

The existence of an extensive spinoreticular pathway in cat, rat and monkey (see above), and of reticulothalamic projections in cats and possibly other species (Brodal, 1981) has been well documented. However, there is very little information available about the relationship between these two pathways. While there is some evidence for a spino-reticulo-thalamic pathway relaying in NGC of the cat and rat, the details and characteristics of this and other possible indirect pathways from the spinal cord via the brainstem to thalamus are poorly understood (Albe-Fessard et al., 1985). Bowsher et al. (1968) showed that neurones in the vicinity of NGC of the cat could be activated by fibres projecting in the anterolateral quadrant, and that electrical stimulation in the same region could activate neurones in the thalamic centre median nucleus (CM) of the intralaminar complex. In an anatomical study, Peschanski and Besson (1984) injected HRP conjugated with wheat germ agglutinin into rat NGC, and analyzed the retrogradely labelled axons in the spinal cord and the anterogradely labelled terminals in the diencephalon. Their results showed the existence of a pathway originating in the spinal ventral horn, terminating in NGC and projecting from NGC to the intralaminar complex, including the centre median nucleus. The origin and termination of this pathway appears to be clearly distinguished from those of the direct spinothalamic tract. Peschanski and Besson (1984) suggest that unlike the spinothalamic pathway relaying in the ventrobasal thalamus, the spino-reticulo-thalamic pathway does not have the features required of a structure playing a role in the sensory-discriminative aspects of pain transmission. This indirect pathway is thought likely to be involved in some motor and/or behavioural responses related to pain.

2.10 THE ROLE OF THE PMRF IN SENSORY AND PAIN MECHANISMS

The evidence reviewed above indicates that the PMRF is an important component of the central mechanisms activated by noxious stimuli (cf. Bowsher, 1976; Mayer and Price, 1976; Casey, 1980; Albe-Fessard et al., 1985). A large fraction of PMRF neurones are strongly influenced by noxious stimuli, and many of these play a significant role in aspects of pain behaviour and perhaps also pain perception. Although the reticular formation may not be critical for processing sensory-discriminative information for pain sensation (Mayer and Price, 1976; however, cf. Bowsher 1976), it is likely to trigger arousal and to contribute to neural activity underlying affective-motivational aspects of pain (Casey 1980).

Clearly, the functions of reticular formation cells are not restricted to pain mechanisms or to any single dimension of pain, since many PMRF neurones contribute to various other aspects of continuing behaviour when noxious input is absent. For example, the activity of some of these neurones is highly correlated with REM sleep (Hobson et al., 1974; Siegel and McGinty, 1977; Vertes, 1977, 1979, 1984c), while others are likely to be related to control of autonomic reflexes (Henry and Calaresu, 1974; Langhorst et al., 1983; Schulz et al., 1983; Blair, 1985, 1987). A significant number of reticular neurones responding to noxious inputs also respond to innocuous stimuli, and may show appreciable attenuation of responsiveness with repetition of these stimuli (Fox and Wolstencroft, 1976). It is probably also an oversimplification that the descending brainstem systems are involved exclusively in suppressing or filtering ascending nociceptive signals. Furthermore, the activity of brainstem reticular neurones is modulated in awake animals by behavioural factors such as the level of arousal, attention to a particular stimulus, relevance of the stimulus to the particular or general behaviour, and the motivational state of the animal. Thus, the particular response properties of a neurone at any one time can be misleading if these properties are used to identify the sensory function of that neurone, for example, pain or no pain.

Casey (1980) argues that in the absence of input from nociceptors, the activity of reticular formation neurones showing differential responsiveness to noxious stimuli must be determined by the unique activity patterns of that population. Tissue damage, on the other hand, would appear to recruit a strongly interdependent, but functionally diverse, population of reticular formation neurones to a high level of coherent activity. It is not known whether this interactive mode of operation results from direct input to specific groups of reticular cells from spinoreticular neurones differentially responsive to noxious stimuli, or whether these same spinoreticular neurones distribute to interneurones such as those found in NGC, which in turn modify and coordinate the activity of specific functional neuronal groups. Both mechanisms may be available (Casey 1980).

This review indicates that current knowledge of the role of PMRF neurones in the processing somatosensory and pain information is rather fragmentary. It is also clear that the role of the reticular formation will not be satisfactorily understood purely in terms of sensory and pain mechanisms. However, if it is the case that these neurones are performing a co-ordinating role in sensorimotor function and behavioural arousal, then it is essential to understand in detail how they process sensory information. In fact, there

have been surprisingly few quantitative studies of the sensory functions of these neurones. This is in sharp contrast with their motor and behavioural functions, which have been the subject of a great deal of research in the past two decades (for example, see Hobson and Steriade, 1986; Holstege and Kuypers, 1987). This study goes some way towards redressing this imbalance, by providing quantitative information about the intensity, temporal and spatial characteristics of the responses of single PMRF neurones to innocuous and noxious cutaneous stimuli. This, in turn, is seen as a necessary, but preliminary, step towards understanding how these neurones interact locally and with distant neuronal populations to provide coherent output control.

Chapter 3

IDENTIFICATION OF PMRF GIANT NEURONES

3.1 INTRODUCTION

It is well documented that "giant neurones" in the medial PMRF respond to innocuous and noxious mechanical stimuli over large receptive fields (see Chapter 2). In order to establish consistency between this and previous studies, the receptive field characteristics of all neurones encountered in the region of the PMRF were routinely evaluated by means of natural somatic stimuli. Only cells exhibiting large spike amplitudes, and responding to a variety of sensory stimuli over extensive receptive fields, were selected as being physiologically indistinguishable from giant PMRF neurones. Thereafter, the spontaneous discharge rates of these neurones were assessed at a skin temperature of 35°C. The detailed responses to cutaneous heat stimuli (Chapter 4) were studied only in neurones which remained silent, or maintained a regular background discharge rate, at this temperature.

The location of the tip of the electrode in the PMRF was always determined at post-mortem. However, no detailed histology of individually studied neurones was performed. This is therefore a purely physiological study of giant neurone-like activity in the PMRF.

3.2 METHODS

3.2.1 ANIMAL PREPARATION AND SURGERY

Experiments were performed on 94 female Long-Evans rats weighing between 280 and 350 g. The animals were anaesthetised with urethane at an initial dose of 1,25 g/kg (i.p.). Supplementary doses were administered as required to maintain a depth of anaesthesia sufficient to prevent any somatic or respiratory reflexes, even during the strongest noxious stimuli. Rectal temperature was monitored and maintained at 37,5 ± 0,5°C using an electrical heating pad controlled by an intra-rectal thermistor probe.

The animals were mounted in a Narishige SR-6 stereotactic instrument, with the palatal bar positioned 5 mm below the level of the interaural line. In this orientation, the neck is flexed such that the surface of the skull is approximately horizontal. This allows vertical access to the brainstem reticular formation without penetrating the transverse sinus. A burrhole of 3-5 mm diameter was drilled in the occipital bone to expose the transverse sinus and anterior pole of the cerebellum, and the dura overlying the cerebellum was carefully removed. The cerebellum was left intact to minimise respiratory movements of the brainstem. In a few animals, further reduction of brainstem respiratory movements was achieved by cementing a 10 mm diameter, thin-walled perspex cylinder to the skull surrounding the burrhole with dental acrylic, and filling the chamber to a depth of about 5 mm with 4% agar in 0,9% sodium chloride. The reference electrode was attached to a screw mounted in the parietal bone.

3.2.2 RECORDING PROCEDURES AND DATA ACQUISITION

Extracellular single unit recordings were obtained with low impedance (5-10 MΩ DC, 1-4 µm tip diameter) glass microelectrodes (1 mm OD, Clark GC100F-10) filled with 3M NaCl. A silver wire inserted into the micropipette solution was connected to a custom built high input impedance (10^{12} Ω) preamplifier. The signals were then led to a high-gain bandpass (100 Hz - 20 kHz) amplifier, and were monitored on an audio-monitor and by continuous display on a dual-beam oscilloscope (Telequipment D1011 or Iwatsu SS-5702). The signals were also led to a discriminator circuit, which transformed the action potentials of the unit under investigation into a series of 0,5 ms logic pulses. These output pulses were displayed on the second channel of the oscilloscope to ensure that the appropriate action potentials were being detected by the discriminator, and were

also led to a BBC B microcomputer which was programmed to compile peristimulus-time histograms (see Chapter 4).

A manual micromanipulator (Narishige SM11 or SM15) with a vertical displacement resolution of 2 µm was used to drive a microelectrode through the cerebellum and fourth ventricle into the brainstem reticular formation. Vertical electrode penetrations were made between 1,5 and 2,5 mm posterior to the interaural line, and within 1 mm of the midsagittal plane. Passage of the electrode through the cerebellum was characterised by complex spike activity from successive layers of Purkinje cells, while a sudden perceptible reduction of neuronal activity marked entry of the electrode into the fourth ventricle. The floor of the fourth ventricle exhibited slow, low amplitude activity. Putative PMRF cells were usually encountered about 1-4 mm ventral to this (approximately 6-9 mm from the cerebellar surface). Only units having the following electrophysiological characteristics were accepted for recording: (1) signal-to-noise ratios in excess of 3:1, (2) large, stable spike amplitudes (0,5 to 5 mV), and (3) durations longer than 0,5 ms (despite high-pass filtering). The electrode was carefully positioned to optimise signal-to-noise ratio and unit isolation. The activity of a given unit could usually be followed over a total of 70-250 µm or more of vertical electrode displacement. These values are all consistent with signals derived from the region of the neuronal soma, rather than axons (Douglas, 1984). Every effort was made to record from all putative PMRF units encountered in a penetration.

The shape of the extracellular action potentials was not an important consideration in these studies, since all subsequent data analyses were concerned only with the action potential discharge patterns of PMRF neurones, measured from logic pulses derived from discriminator level crossings. However, the shapes of the action potentials were carefully monitored during all data logging procedures to ensure (a) that the signal characteristics were suggestive of a somadendritic source rather than an axonal source, and (b) that the shape of action potentials being transformed into logic pulses remained constant during the observation period, as confirmation of the validity of the data being recorded.

Once well-isolated unitary activity was detected in the region of the PMRF, the cell was allowed to stabilise with the electrode in position for 2-5 minutes. The majority of cells exhibited continuous, regular discharge rates during this period (spontaneous units),

while other cells decayed to zero discharge, but could be reliably activated by peripheral stimulation (silent or quiescent units).

Typical signs of injury to the cell by the electrode included fluctuations in basal discharge rate and/or action potential amplitude, or complete cessation of all spontaneous and stimulus-evoked activity. If any signs of injury were apparent during the stabilization period, the unit was discarded.

3.2.3 CELL CLASSIFICATION: RECEPTIVE FIELD MAPPING AND SPONTANEOUS DISCHARGE RATES

If the cell appeared stable after 5 minutes, the cutaneous receptive field was estimated using a series of standard mechanical stimuli. These consisted of stroking the fur of the body and limbs with a blunt object, applying firm pressure or pinching the skin, achilles tendon, tail, forepaws and ears with fingers or forceps, and squeezing a fold of skin at these sites with serrated forceps. When tested on the experimenter's skin the pressure or pinching stimuli were mildly painful, while the squeezing stimuli were decidedly painful. A response of the neurone to any of these stimuli was defined as an increase or decrease in the spontaneous action potential discharge frequency, or the appearance of discharge in a quiescent unit.

The responses of PMRF neurones to mechanical stimulation were classified according to the following criteria: (1) polarity of response - excited (ON-m cells), inhibited (OFF-m cells) or complex (responding with combinations of excitation and inhibition in different regions of the receptive field); (2) receptive field location (subdivided into five body segments - tail, hindlimbs, trunk, forelimbs, head/neck) and size (number of body regions responding to mechanical stimuli); and (3) adequate stimulus - brushing the fur and skin (low threshold), pinching/squeezing the skin and/or achilles tendon (high threshold) or both (mixed). Neurones which did not respond to cutaneous mechanical stimuli were not studied further.

On completion of the receptive field assessment, the mechanosensitive PMRF units were left to fire spontaneously or remain quiescent for a further 2-5 minutes. The spontaneous discharge frequencies were then recorded for 30 to 100 s with the glabrous skin on the ipsilateral hindpaw held at a temperature of 35°C. There were no other intentional stimuli, including sound, vision, vibration and other cutaneous input. In order to simplify the statistical analysis of PMRF responses to natural (mechanical and thermal)

stimuli, only silent units or those exhibiting stable spontaneous discharge rates were included in the final data sample. On-line assessment of the stability of PMRF neuronal discharge rates was performed visually during the recording procedure: if any unit showed either unpredictably oscillating, or steadily increasing or decreasing, discharge rates during two consecutive control periods, recording was terminated and the unit was excluded from the sample. No attempt was made to quantify these discarded units. During subsequent data analysis, the control periods were divided into two equal time periods. If there was a statistically significant difference (Kolmogorov-Smirnov two sample test, $p<0,05$) between the discharge rates of the first and second periods, the neurone was also eliminated from the sample. The standard deviation (SD) and the coefficient of variation (CV = SD/MEAN) were measured in the remaining PMRF neurones as indices of the variability of the discharge rates of the sampled PMRF neurones in the "unstimulated" state.

3.2.4 HISTOLOGICAL PROCEDURES

On completion of electrophysiological recordings, the rat was overdosed with urethane and a thoracotomy performed. It was then perfused transcardially with 300-500 ml of 0,9% saline followed by approximately 500 ml 10% formaldehyde in 0,1 M phosphate buffer, pH 7,5. Thereafter the animal was decapitated and the occipital and parietal bones carefully prised away with rongeurs forceps. The head was then immersed in 100 ml 10% phosphate buffered formalin at room temperature for a minimum of 24 hours.

After post-fixation, the head was remounted in the stereotaxic instrument. A block of brain was cut in coronal section using a scalpel blade attached to the electrode holder on the stereotaxic microdrive. This ensured that the brain was cut in the same plane as the electrode penetrations. To prevent ice crystal artefact during subsequent sectioning, the blocks of brain were placed in 30% sucrose in phosphate buffer until they sank to the bottom of the container (typically a few days).

Coronal sections (100 µm) were cut on a microtome with a Pelcool thermoelectric freezing attachment (American Optical Company), or in some cases on a Campden Vibroslice. The sections were mounted on gelatinised slides and stained with cresyl fast violet (0,1% in Walpole's acetate buffer: 0,2 g in 165 ml 0,1 N acetic acid and 35 ml 0,1 M sodium acetate). Electrode penetrations and recording sites were then confirmed by histological examination.

Entire electrode tracts were often present in a single histological section. The location of each recording site was estimated from (a) anatomical landmarks in the region of the tracts, such as the abducens nucleus, the genu of the facial nerve, the shape of the fourth ventricle, and the position of the inferior or superior olives, (b) the known vertical displacement of the electrode as recorded from the microdrive, and (c) the coordinates of the fourth ventricle and the surface of the brainstem, which were routinely noted during each electrode penetration. The positions of the cells were mapped with reference to the atlas of Farham and Douglas (unpublished).

3.3 RESULTS

A total of 235 neurones were classified as putative PMRF giant neurones on the basis of their electrophysiological properties (Section 3.2.2), their physiological responses to mechanical cutaneous stimuli and spontaneous discharge characteristics (Section 3.2.3), and their gross anatomical location (Section 3.2.4). Extracellular spikes were generally biphasic and negative-positive in polarity, with spike amplitudes ranging from 200-5000 μV. Histological reconstruction of recording sites indicated that all neurones in this study were located in the region extending caudally from the level of the superior olivary complex to the border of the facial nerve nucleus, and within 1 mm of the midsagittal plane. The majority of units were located in relation to the nucleus and genu of the facial nerve (Figure 3.1).

3.3.1 RESPONSES TO MECHANICAL STIMULI AND RECEPTIVE FIELD CHARACTERISTICS

Many types of mechanical stimulation were effective in eliciting responses in PMRF neurones: hair bending, light touch, light and heavy pressure, pinching, or sometimes combinations of these stimuli. Deep afferents from joints and muscles were also effective, especially pinching the achilles tendon. Some units also responded to auditory and visual stimuli, while others varied their action potential discharge rates in relation to the respiratory cycle. No detailed accounts were taken of all of these responses since efforts were primarily directed at elucidating the temperature sensitivity of these neurones (Chapter 4). Neurones without identifiable cutaneous or deep (achilles pinch) mechanical receptive fields were not investigated further. No attempt was made to quantify these discarded cells.

Of the 235 mechanosensitive PMRF neurones, 188 were excited (80%, ON-m), 40 were inhibited (17%, OFF-m), and 7 units (3%) exhibited both excitation and inhibition in different parts of their receptive field (complex responses). Excitatory responses occurred in both spontaneously active and quiescent neurones (see Section 3.3.2). Most of these neurones responded vigorously for the duration of the stimulus and decreased their firing rates immediately after removal of the stimulus, while others exhibited long latencies and marked afterdischarges. Units with phasic responses to mechanical stimuli were occasionally observed. Inhibitory effects ranged from brief (2 s) interruption of a regular spontaneous rate to nearly complete cessation of the firing for the duration of the stimulation.

The receptive fields of individual PMRF neurones ranged in size from restricted (one receptive field region) to very extensive (all five regions: Figure 3.2, Table 3.1). There was a great deal of redundancy with respect to individual regions in the receptive field, with all but one of the PMRF neurones responding to stimulation of the hindlimbs (99,6%), 61% responding to the tail, 42% to the trunk, 17% to the forepaws, and 22% to the head (Table 3.2, across the rows; Figure 3.3). There was no somatotopic organization of the receptive fields of PMRF neurones, since each body segment was represented in approximately equal proportions within the NPC and NGC (Table 3.2, down the columns). Spatial convergence of the receptive fields was widespread, with 177 of 235 PMRF neurones (75%) responding to cutaneous stimuli of 2 or more body regions. However, this spatial convergence was not unlimited, as shown by the various combinations of body regions in the receptive fields of different PMRF neurones. For example, total body convergence was observed in only 14 neurones (6%), while four-limb convergence was seen in 39 neurones (17%). Unilateral responses were rare, comprising only 21 of 235 neurones (9%).

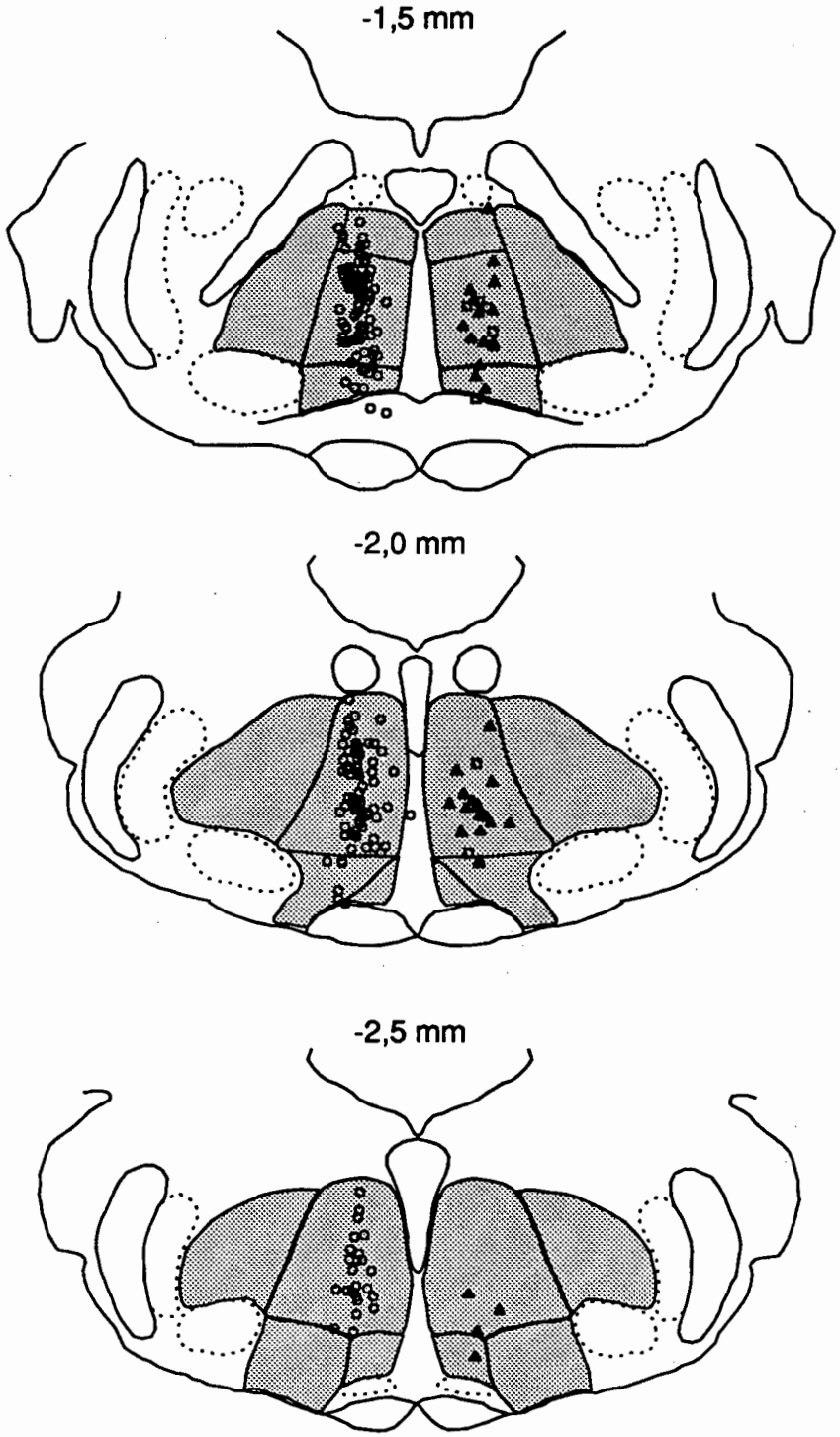

FIGURE 3.1 Anatomical location and response polarities of 235 mechanosensitive neurones (nuclei and tracts as in Figure 2.1). The drawings illustrate, on the left of each section, recording sites of units showing increased discharge rates in response to mechanical stimuli (open circles). The right of each section shows the location of units inhibited by cutaneous mechanical stimuli (closed triangles), and units with complex receptive fields (excitation and inhibition, open squares). Neurones with inhibitory or complex responses were all spontaneously active. In subsequent histological figures in this thesis, all NGC neurones (-2,0 and -2,5 mm posterior to inter-aural line) are represented on the more anterior section.

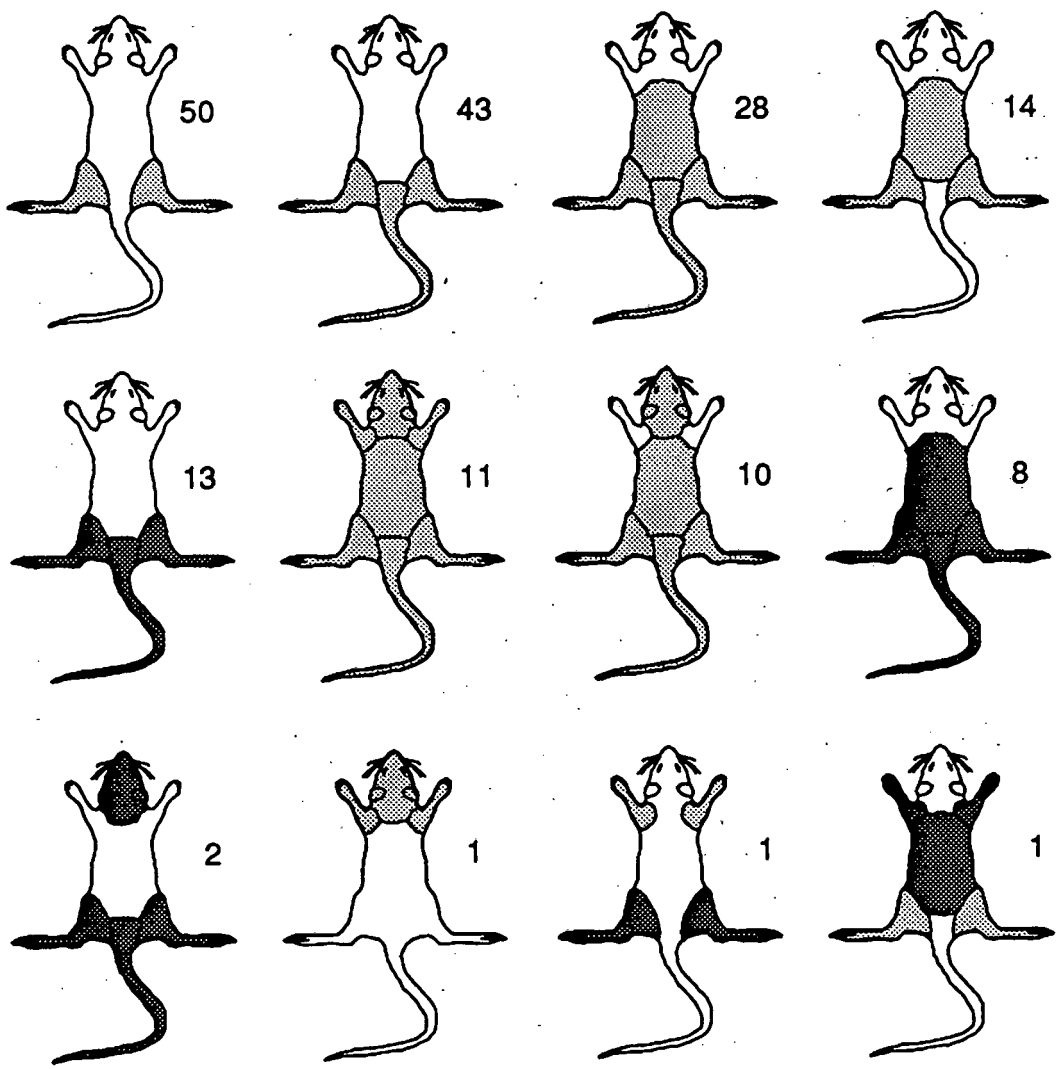

FIGURE 3.2 Representative receptive fields of PMRF neurones to cutaneous mechanical stimuli. The receptive fields are stylized to represent 5 dermatomal regions: the tail, hindlimbs, trunk, forelimbs and head/neck. Lightly shaded areas represent excited regions, while inhibited regions are shown as dark shading. The observed number of each receptive field configuration is shown to the right of the figures. The first eight examples show the most commonly represented receptive fields. The last four examples are of unusual receptive field types. Note the presence of continuous and discontinuous fields, and unipolar as well as complex responses.

TABLE 3.1 Receptive field organization of all mechanosensitive PMRF neurones.

	Body segment					Response				
Regions	TL	HP	TR	FP	HD	E	I	C	SUB	TOTAL
1	-	x	-	-	-	50	8	0	58	58
2	x	x	-	-	-	43	13	0	56	
	-	x	x	-	-	14	2	1	17	
	-	x	-	x	-	0	1	0	1	
	-	x	-	-	x	1	0	0	1	
	-	-	-	x	x	1	0	0	1	76
3	x	x	x	-	-	28	8	3	39	
	x	x	-	x	-	1	1	0	2	
	x	x	-	-	x	7	2	0	9	
	-	x	x	x	-	1	1	1	3	
	-	x	x	-	x	5	0	0	5	
	-	x	-	x	x	3	0	0	3	61
4	x	x	x	x	-	6	0	2	8	
	x	x	x	-	x	10	0	0	10	
	x	x	-	x	x	4	1	0	5	
	-	x	x	x	x	3	0	0	3	26
5	x	x	x	x	x	11	3	0	14	14
TOTAL						188	40	7		235

TL - tail; HP - hindpaws; TR - trunk; FP - forepaws; HD - head; E - excitatory response; I - inhibitory response; C - complex response (excitation and inhibition).

TABLE 3.2 Receptive fields in the PMRF: body segment participation and anatomical location.

	Body segment					
Anatomical location	TL	HP	TR	FP	HD	TOTAL
NGC	72	124	42	16	21	124
NPC	71	110	57	24	30	111
TOTAL	143	234	99	40	51	235

TL - tail; HP - hindpaws; TR - trunk; FP - forepaws; HD - head; NGC - nucleus gigantocellularis (-3 to -2 mm posterior to inter-aural line); NPC - nucleus pontis caudalis (-1,5 to -1 mm). Across a row, the sum of entries is greater than the total because each body segment is counted more than once whenever it is included in a receptive field. Down a column, the sum of entries equals the total since each anatomical location is counted only once.

A considerable fraction of PMRF neurones (64 of 235, 27%) were responsive to both light tactile and high intensity stimuli (mixed responses). The majority of neurones with mixed responses exhibited greater changes in their discharge rates (ON-m or OFF-m) following more intense stimuli. The remaining 171 neurones (73%) responded exclusively to intense cutaneous stimuli (high threshold neurones). No PMRF neurones were found to respond only to light tactile stimulation (low threshold neurones).

The sizes of the receptive fields of PMRF neurones were correlated both with the adequate stimulus for mechanical response, and with the anatomical location of the units. Neurones with relatively small receptive fields (1 or 2 regions) had predominantly or exclusively high threshold responses, whereas neurones with larger receptive fields (3 or more regions) were approximately equally likely to be of the high threshold or mixed type (Chi-square, $p<0,0001$, Table 3.3). Furthermore, neurones with restricted receptive fields (1 region, high threshold) included only the hindlimbs, and were found in greater proportion in the posterior PMRF (nucleus gigantocellularis, NGC) than in the anterior PMRF (nucleus pontis caudalis, NPC), while a larger proportion of neurones exhibiting widespread convergence (4-5 regions, including the forelimbs and head) were found in NPC than in NGC (Chi-square, $p=0,006$; Table 3.4, Figure 3.4). Neurones with medium-sized receptive fields (2-3 regions) were approximately equally distributed throughout the PMRF.

FIGURE 3.3 (following page) Anatomical location of PMRF neurones as a function of body regions included in their receptive fields. Excitatory responses are represented on the left side of the sections as open circles, and inhibitory responses as closed triangles on the right side of the sections. Cells containing more than one body region in their receptive fields are plotted on each relevant anatomical section.

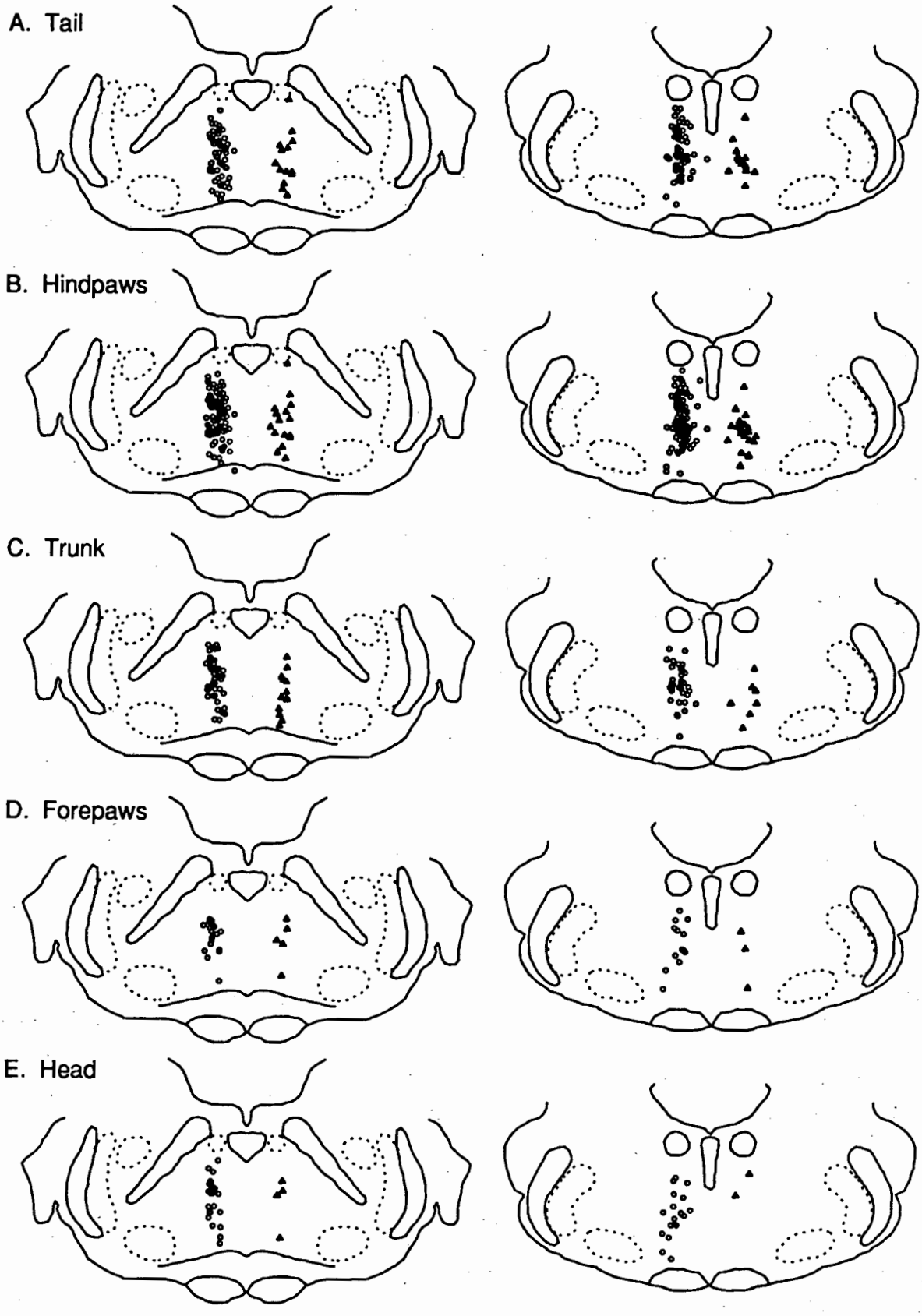
A. Tail
B. Hindpaws
C. Trunk
D. Forepaws
E. Head

TABLE 3.3 Relationship between the adequate stimulus for mechanical response, polarity of response and size of receptive field.

	MIXED					HIGH THRESHOLD					
Regions	E	I	C	SUB	%	E	I	C	SUB	%	TOTAL
1	0	0	0	0	(0)	50	8	0	58	(100)	58
2	10	0	0	10	(13)	49	16	1	66	(87)	76
3	23	3	4	30	(49)	22	9	0	31	(51)	61
4	15	0	2	17	(65)	8	1	0	9	(35)	26
5	5	2	0	7	(50)	6	1	0	7	(50)	14
TOTAL	53	5	6	64		135	35	1	171		235

E - excitatory response; I - inhibitory response; C - complex response (excitation and inhibition). Chi-square 66,89 (1 d.f.), p<0,0001. (The Chi-square test was performed on the sub-total columns.)

TABLE 3.4 Relationship between anatomical location and size of receptive field

RF regions	NPC	NGC	TOTAL
1	18	40	58
2-3	68	69	137
4-5	25	15	40
TOTAL	111	124	235

NPC - nucleus pontis caudalis (-1 mm to -1,5 mm); NGC - nucleus gigantocellularis (-2 mm to -3 mm). Chi-square 10,16 (2 d.f.), p=0,006.

FIGURE 3.4 (following page) Anatomical location of PMRF neurones as a function of receptive field size (number of mechanosensitive regions). The responses are represented as follows: open circles - excited; closed triangles - inhibited; open squares - complex responses (excitation and inhibition). Neurones with restricted receptive fields (hindlimbs only) were located predominantly in the posterior PMRF (NGC), whereas units showing widespread receptive field convergence (4-5 regions) were found in greater numbers anteriorly (NPC - see Table 3.4).

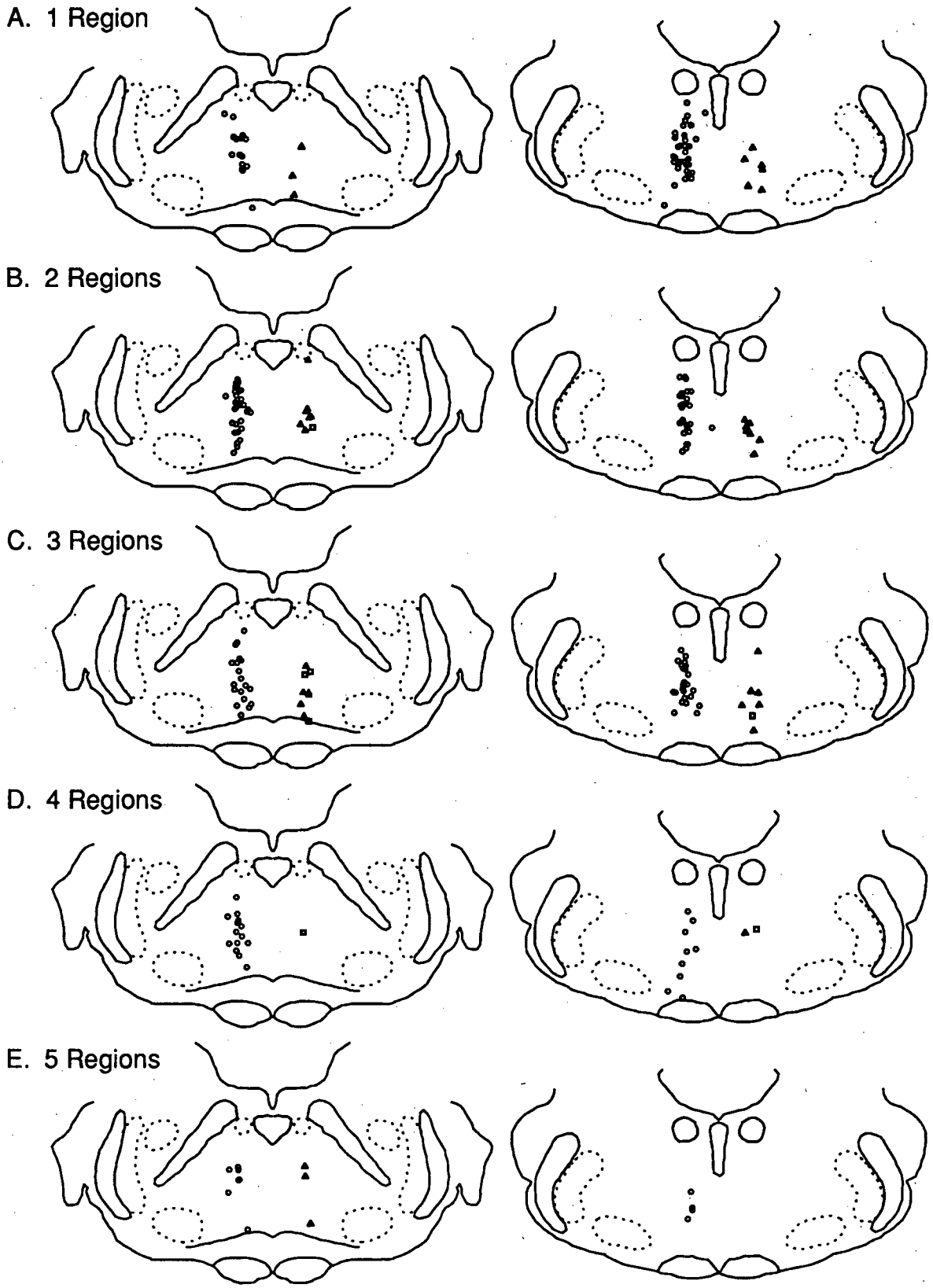
A. 1 Region
B. 2 Regions
C. 3 Regions
D. 4 Regions
E. 5 Regions

3.3.2 SPONTANEOUS DISCHARGE RATES

The spontaneous discharge frequencies of 201 PMRF neurones were analysed off-line. The majority of these (144 of 201, 72%) exhibited some spontaneous discharge (greater than 1 spike/s). The mode of the firing rates of spontaneously active PMRF neurones was 8,4 spikes/s, the median 12,0 spikes/s, and the range 1,5 to 46,6 spikes/s. The remaining 57 neurones (28%) either remained silent (n=41) or exhibited sporadic single discharges (n=16) when not appropriately stimulated (mean rate less than 1 spike/s); these neurones were classified as not spontaneously active or quiescent. The distribution of firing rates of the spontaneously active and quiescent neurones is shown in Figure 3.5A.

The standard deviations (SD) of the spontaneous firing rates ranged from 0 to 4,8 spikes/s (Figure 3.5B). The distribution of standard deviations closely resembled that of the spontaneous rates: i.e. the distribution was bimodal and skewed to the right. The first mode occurred at 0,2 spikes/s and the second at 1 spike/s. These peaks corresponded to the quiescent and spontaneously active neurones, respectively. The coefficients of variation (CV) of the spontaneously active neurones ranged from 2 to 87% (median 10%). The distribution of the individual coefficients of variation of spontaneously firing neurones is shown in Figure 3.5C.

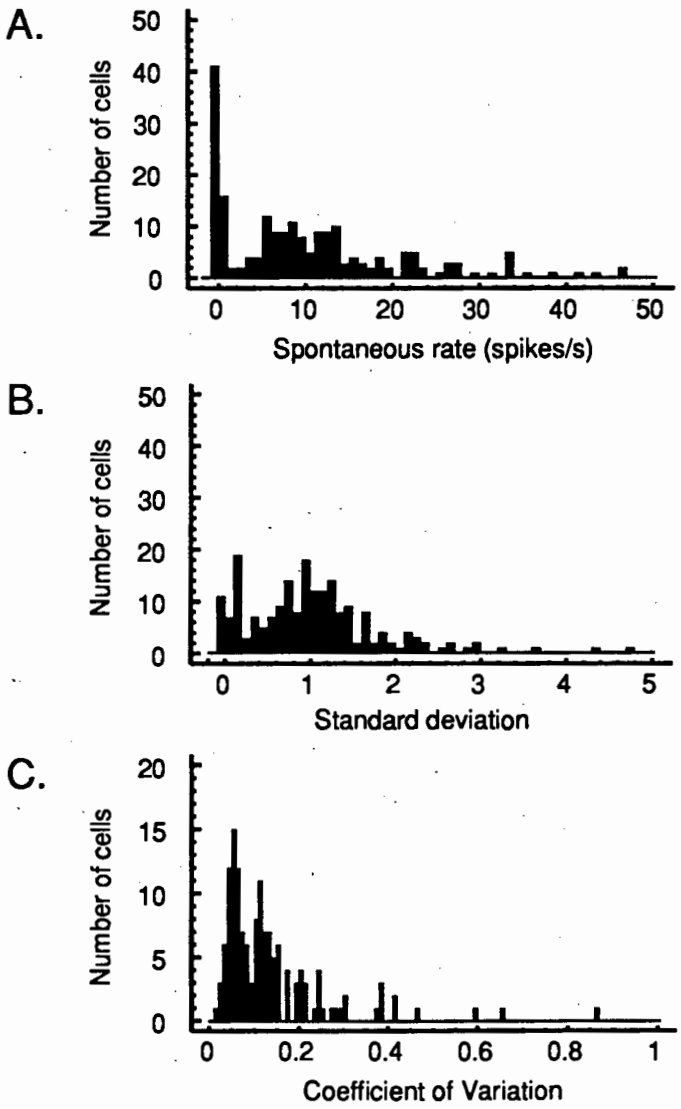

FIGURE 3.5 Statistical characteristics of spontaneous (background) discharge rates of PMRF neurones. A: Mean spontaneous rates (n=201). The first bin, plotted from -1 to 0, represents neurones exhibiting zero discharge in the unstimulated state (for at least 30 s). B: Standard deviation of spontaneous discharge rates. The first bin represents zero standard deviation. C: Coefficient of variation (CV) of spontaneously active PMRF neurones (n=144). The CV of neurones with spontaneous rates of less than 1 spike/s is meaningless.

3.4 DISCUSSION

The neurones in this study were located in the medial pontomedullary reticular formation (PMRF) - in the nucleus reticularis pontis caudalis (NPC) and nucleus reticularis gigantocellularis (NGC). They all showed one or more of the following physiological characteristics: (1) excitatory (ON-m), inhibitory (OFF-m) or complex (excitatory plus inhibitory) responses to cutaneous mechanical stimuli; (2) large continuous or discontinuous receptive fields involving different parts of the body; and (3) differential responsiveness to weak and intense stimuli. The electrophysiological characteristics, and these somatosensory responses and receptive fields were qualitatively similar to those obtained for giant PMRF cells in this region by earlier workers (Scheibel et al., 1955; Segundo et al., 1967; Bowsher et al., 1968; Bowsher, 1970; Groves et al., 1973; LeBlanc and Gatipon, 1974; Wolstencroft, 1974; Willis and Coggeshall, 1978; Siegel, 1979; Brodal, 1981). Consequently, their membership of the PMRF giant cell population is corroborated on both gross neuroanatomical and functional grounds.

The neurones under investigation in the PMRF are large and well separated spatially, which greatly simplifies their isolation and recording using extracellular techniques. In populations of neurones of different sizes, large neurones are expected to generate the largest current densities, and consequently the largest extracellular voltage fields (Douglas, 1984). Thus, large neurones have the greatest likelihood of being investigated both because of the increased probability of the electrode encountering their signal, and the relative ease of recording their signals well clear of the background noise. Units with very large spike amplitudes were commonly encountered in the PMRF, and signal-to-noise ratios of at least 3:1, and frequently in excess of 10:1, were routinely obtained. Since the giant neurones constitute a major cell type in the pontomedullary region (see Chapter 2), in this study any recording bias due to the size of the neurones is in favour of the neuronal population under investigation (Douglas, 1984).

Eighty percent of PMRF neurones were excited, and 17% inhibited, by cutaneous mechanical stimuli. Only 7 units in this study (3%) had both excitatory and inhibitory mechanical receptive fields (complex responses). These findings are similar to those of Burton (1968), who obtained 71% excitatory, 19% excitatory plus inhibitory, and 10% pure inhibitory responses in cat caudal medulla. On the other hand, these proportions of excitatory, inhibitory and complex responses contrast markedly with those of Benjamin

(1970), who found that 90% of high threshold units in rat caudal reticular formation exhibited both excitation and inhibition.

The receptive fields of PMRF neurones showed marked redundancy and widespread convergence. Some portion of the hindlimbs were represented in the receptive field of virtually all neurones observed, while the tail and trunk were also frequently represented. The forelimbs and face were least frequently represented in this study. Individual neurones were not subject to convergence from all types of physiological stimuli tested or from all parts of the body. In fact, only 14 units (6%) showed total body convergence (Table 3.1).

The sizes of the receptive fields of PMRF neurones were correlated both with the anatomical location of the cells and their adequate stimulus (high threshold or mixed responses). Neurones with small receptive fields (1 region) responded exclusively to noxious cutaneous stimuli, and were found in greater numbers in the caudal PMRF (NGC) than in the rostral PMRF (NPC). Small receptive fields were only found on the hindlimbs. Units with very large receptive fields (4 or 5 regions) predominated in NPC, and 60% of these responded to both innocuous and noxious mechanical stimuli. Neurones with medium-sized receptive fields (2 or 3 regions) were equally distributed throughout the PMRF.

Large redundancy of receptive fields of brainstem reticular formation neurones has previously been noted by several authors. Segundo et al. (1967) reported that the hindlimbs and tail were included in the receptive fields of 44% of brainstem reticular formation neurones. Their study area included regions more caudal to NGC and NPC. These authors also observed that neurones with widespread receptive fields (occupying more than half of the body surface) tended to be bilateral, and often excluded the ipsilateral face and forelimbs. Exclusively ipsilateral receptive fields were only seen in 33% (49/149) of their sample. Bowsher (1970) reported a greater degree of four-limb convergence in NGC than at reticular regions either rostral or caudal to it. He also reported a greater number of two-limb convergent units in NPC which responded only to stimulation of the forelimbs. Further rostral, Bell et al. (1964) reported that 80% of the mesencephalic reticular units had receptive fields that included one-quarter to one-half of the body surface. Mesencephalic units with unilateral fields almost always (35 of 39, 90%) had contralateral inputs.

Groves et al. (1973) examined the sensory responses of neurones in the mesencephalic and pontine reticular formation, from the superior colliculus to the entrance of the eighth nerve. They reported that some reticular formation cells responsive to light touch had receptive fields of widely differing sizes and configurations, and that about half of the cells had tactile receptive fields larger than one-third of the body surface. Multimodal cells were concentrated mainly in the mesencephalon. These authors also reported differential anatomical location of reticular formation neurones responding to different body regions. The posterior reticular formation received somatic input primarily from the posterior third of the body, the middle third of the body surface was represented at the mesencephalo-pontine junction, and the mesencephalic reticular formation responded mainly to stimuli on the anterior third of the body surface. Interpretation of the study of Groves et al. is complicated by their treatment of the pontomedullary and mesencephalic reticular formation as a functional whole. This is contrary to most of the commonly accepted anatomical and functional subdivisions of the brainstem. For example, the major input and output pathways to and from the cord are concentrated in the PMRF rather than in the mesencephalic reticular formation (Chapter 2). Thus, it is conceivable that the differential somatosensory responses observed by Groves et al. in the mesencephalic reticular formation and in the PMRF are functionally distinct. However, their results are consistent with the relative paucity of responses from the forepaws, head and neck observed in the present study. Although regions anterior to the superior olivary nuclei were not explored here, a greater proportion of neurones were found to exhibit widespread convergence (including the head and forelimbs) in NPC than in NGC (Figure 3.4, Table 3.4).

There is another possible explanation for the scarcity of the head, neck and forelimbs in the receptive fields of PMRF neurones. I was dealing with an anaesthetised animal mounted in a stereotactic frame to minimise movement. In this experimental arrangement, the hindlimbs, tail and trunk were more mobile than the forelimbs and head, and were often moved during mechanical or cutaneous stimulation. It is thus feasible that the PMRF neurones were responding to the movement of the limbs, exclusively or in addition to the stimulation of the cutaneous receptors. Studies in the behaving cat have shown a strong relationship between movement and PMRF discharge (Siegel, 1979, 1983; see Chapter 2). Responses of PMRF neurones to movement were not studied here.

Most PMRF neurones (73%) were responsive only to intense mechanical stimuli (during this phase of the experiment). The response amplitude of these neurones often differed with stimuli applied to different parts of the receptive field, but they all required noxious stimuli for activation. The remaining 27% of units were responsive to both light tactile and high intensity stimuli (mixed responses). These neurones usually exhibited greater responses to noxious than to innocuous stimuli. These findings are comparable to those of Casey et al. (1974), who reported that 59 of 85 (69%) somatically responsive units in rat NGC responded primarily or exclusively to strong mechanical stimuli delivered over wide body areas. Similarly, Burton (1968) reported that over 70% of neurones in the caudal bulbar reticular formation of anaesthetized or decerebrate cats responded specifically to noxious stimuli.

The range of discharge rates observed in spontaneously active PMRF neurones in this study is almost identical to those reported by MacGregor et al. (1973) for the mesencephalic reticular formation in conscious, paralysed rats (ignoring the ethical implications of this work). Firing rates in those animals ranged between 1 and 47 spikes/s, with 50% having discharge rates below 10 spikes/s. This compares with PMRF discharge rates in the present study of between 1,5 and 46,6 spikes/s, with the median at 12 spikes/s (Figure 3.5). By contrast, Douglas (1984) recorded higher discharge rates for the PMRF in urethane-anaesthetized rats, ranging from 3 to 70 spikes/s, with a population median of 22 spikes/s. Only 6% of PMRF neurones recorded by Douglas had rates below 10 spikes/s. However, he was studying the statistical properties of the spontaneous firing rates of PMRF neurones, and consequently did not include quiescent neurones in his sample. Neurones exhibiting discharge rates greater than 50 spikes/s were occasionally encountered in the present study, but they all exhibited erratic changes in firing rate and were consequently eliminated from the data sample.

Not only was there great variability in the spontaneous discharge rates of the different PMRF cells, but many neurones located within this area also showed large individual variability. For practical purposes, only those neurones which remained silent in the unstimulated state, or whose spontaneous firing rates were judged to be stable both by visual inspection during on-line data logging and by subsequent statistical analysis, were studied further (Section 3.2.3). The remaining spontaneously active cells had coefficients of variation ranging from 2 to 87%, with the median at 10% (Figure 3.5).

Twenty eight percent of PMRF neurones showed no spontaneous activity over periods of 30 to 100 s. This is similar to the findings of Siegel and McGinty (1976), who reported that approximately 30% of pontine reticular formation neurones were not spontaneously active in conscious behaving animals. Those neurones showed no activity during waking unless appropriately stimulated, and remained silent for periods of over 60 s during REM and slow wave sleep. Quiescent neurones were detected in their study by applying sensory stimuli while advancing the microelectrodes. No external stimuli were applied during the search procedure in these experiments, and "silent" PMRF neurones were detected only by their initial activation by the advancing electrode. However, once the baseline discharge of these neurones settled at zero, they were reliably activated by mechanical stimuli, and returned to their silent state between stimuli. This pattern could be repeated in some neurones for periods of up to 30 minutes.

The fraction of quiescent neurones recorded here and by Siegel and McGinty (1976) is probably an underestimate of the total population of quiescent neurones in the PMRF, since neurones not responding to the particular sensory stimulus being applied at that moment, go unnoticed. Douglas (1984) obtained an estimate of the proportion of quiescent neurones in the PMRF during urethane anaesthesia by comparing the distribution of vertical distances between spontaneously active PMRF neurones, and the spatial distribution of PMRF somata labelled retrogradely with horseradish peroxidase via the reticulospinal projections. He concluded that at least 75% of PMRF neurones do not exhibit spontaneous activity during urethane anaesthesia.

The existence of large numbers of quiescent neurones in the brainstem responding specifically to cutaneous sensory (and/or motor) events means that many PMRF neurones can only have unidirectional responses to specific stimuli. Although many of the remaining (spontaneously active) neurones had, at least superficially, consistently unidirectional responses to the same type of stimulus (either excitatory or inhibitory), a small number were found to exhibit bidirectional responses. Since there was nothing, prior to stimulation, to distinguish uni- from bidirectional responding neurones, it is possible that a larger proportion of spontaneously active PMRF neurones than found here (if not all) are capable of ambiguous responses under appropriate conditions.

Chapter 4

RESPONSES OF PMRF NEURONES TO GRADED INNOCUOUS AND NOXIOUS CUTANEOUS THERMAL STIMULI

4.1 INTRODUCTION

Pontomedullary reticular formation (PMRF) neurones typically respond to more than one sensory modality (see Chapter 2). These sensory modalities cover such diverse categories as cutaneous, visceral, proprioceptive, baro- and chemoreceptive sensation, as well as information from the special senses (hearing, balance, vision, taste etc). A chance observation that a faulty heating pad (used to maintain body temperature in anaesthetized rats) caused dramatic changes in the discharge rate of PMRF cells (Douglas, 1984) led us to study the responses of these neurones to thermal stimulation of the skin. Temperature is an ideal stimulus in that it can be accurately controlled and measured. This also provided the first opportunity to drive these neurones with precisely quantified cutaneous stimuli.

Temperatures were selected to cover the range which, in the conscious animal, would be expected to produce neutral to painful responses. The "neutral" stimulus was produced by heating the skin to 35°C (room temperature approximately 20°C). In humans this temperature, applied to the bare skin, is perceived to be neither warm nor cold (Hensel, 1981; Darian-Smith, 1984). The maximum temperature used was 48°C. This temperature produces non-adapting pain sensations in humans when applied for 30 s (Chéry-Croze, 1983). I call this the "noxious" stimulus. The middle of the range (40-41°C) is perceived by humans to be warm, but not painful (ie "innocuous"). It is presumed that conscious rats perceive these localized temperatures of hairless skin in essentially the same way as humans. This presumption is not critical, since my purpose was simply to study a range of stimuli that covers a large portion of the responsiveness of the warm/hot sensory mechanism. (This does not imply, however, that the PMRF neurones were driven to their maximum capacity.)

Three different stimulus waveforms were used: ramps, steps and sine waves.

4.2 METHODS

4.2.1 CONTROLLED THERMAL STIMULATION OF THE SKIN

Thermal stimuli were delivered by one of two contact thermal stimulators. In early experiments, an aluminium ohmic heating element with a total surface area of 315 mm^2 and a contact surface area in these experiments of approximately 200 mm^2 was used (Farham and Douglas, 1985). In all later experiments, a voltage controlled Peltier device with a surface area of 100 mm^2 was used (Pepler et al., 1985). The temperature of each stimulator was controlled by a feedback circuit, and was measured by a thermocouple mounted just below the thermode-skin interface. Stimulus temperatures were thus largely independent of varying thermal loads imposed by the underlying tissue. The temperature of the thermocouple was monitored by the BBC microcomputer via an analogue-to-digital converter. The resolution of the digitized temperature was less than 0,1 °C.

The ohmic device delivered an oscillating stimulus due to its slow feedback response. The amplitude of these oscillations in the steady-state was approximately 0,5 °C peak-to-peak. The power to drive the stimulator was kept low in order to minimize the oscillations, which resulted in a very slow heating response (maximum rate 0,2 °C/s). The command voltage to drive the stimulator was provided by a switch-selectable preset control on the front panel of the instrument. This stimulator could not be actively cooled, but required the device to be removed from the stimulation site to allow passive cooling of the skin.

The Peltier stimulator heated at a maximum rate of approximately 3 °C/s and cooled at 2 °C/s. The device had a linear response to external control voltages within this speed range for temperatures in these experiments of 35-50 °C, and exhibited minimal over- and undershoot and negligible steady-state oscillations. Heating and cooling stimuli could be generated successively without any associated mechanical stimulation of the skin. The BBC microcomputer was programmed to generate a variety of command voltage waveforms to drive the Peltier stimulator via a digital-to-analogue circuit.

Definition of stimulus series

Three types of stimulus waveforms were used to test the thermal responsiveness of PMRF neurones: (1) continuously increasing (ramp) stimuli, (2) constant-temperature (stepped) stimuli, and (3) low frequency sine wave stimuli. Prior to thermal stimulation the skin was adapted to a 35°C baseline temperature. Only units showing zero or approximately constant discharge during the control period were observed further (Chapter 3).

Slow ramp stimuli (Series SR) were used to determine the thresholds of response of PMRF neurones to skin heating. The activity of each neurone was recorded at the baseline temperature for approximately 100 s (control period). The temperature was then increased linearly from control to 48°C at a rate of 0,15 to 0,20°C/s. Thereafter the stimulator was removed from the foot to avoid tissue damage due to prolonged exposure to elevated temperatures.

The rate-sensitivity of PMRF neurones was examined following cutaneous temperature ramps from 35°C to 48°C at 0,2, 0,3, 0,5, 1 and 2°C/s (variable rates, Series VR). The temperature was held at 48°C for 20 s before being rapidly returned to baseline (2°C/s cooling rate in all cases). The order of presentation of the different rates of change of temperature was randomized.

Stepped thermal stimuli were used to determine the response of PMRF neurones to graded innocuous and noxious cutaneous temperatures. This series included two subgroups, double steps (Series DS) and single steps (Series SS).

Series DS comprised a 60 s control period at baseline temperature (35°C), followed by 2 consecutive steps (2°C/s, 60 s plateau) to 40°C and either 43°C or 45°C. The temperature was then returned to baseline. The order of presentation of the two temperature steps (ascending or descending) was randomized. The majority of cells in this series were exposed to at least two stimulus sequences spaced 5 minutes apart, during which the skin temperature was maintained at 35°C.

In Series SS, 30-second steps from 35°C to 40-48°C in 2°C steps were delivered in order of increasing intensity. The skin temperature was maintained at 35°C during the 5 minute

interstimulus interval. In some experiments a second set of heating pulses was applied to the skin.

Sine wave thermal stimuli from 36-45°C were delivered at frequencies of 0,02, 0,01 and 0,005 Hz (ie periods of 50, 100 and 200 s, respectively; Series SI). In a few cases, stimuli were presented in the range 38-42°C.

The PMRF neurones were not subjected to every thermal test, owing to (1) the duration of the experiments, (2) some differences in the design of individual experiments and (3) occasional problems with instability of the recording during the test period. Therefore, the actual numbers of PMRF neurones that were tested for each property investigated are listed below.

4.2.2 DATA ANALYSIS AND STATISTICS

Statistical analysis of data was performed using a suite of analysis programs developed in this laboratory for the BBC microcomputer (see Pepler et al., 1985), and on a PC microcomputer with commercially available statistical software (Statgraphics, Systat). Spontaneous discharge rates, magnitudes of response, thresholds and latencies were derived from the peristimulus time histograms (PSTHs) constructed during thermal stimulation.

The threshold of each PMRF neurone was defined as the temperature of the stimulator surface at the onset of a neuronal response. The thresholds to linear ramp stimuli were estimated to the nearest bin of the PSTH using the CUSUM technique (Muschaweck and Loevner, 1978). The threshold to stepped thermal stimuli was defined as the lowest temperature plateau at which a significant increase or decrease in discharge rate was observed, compared using the Kolmogorov-Smirnov two-sample test (Siegel, 1956). Since discontinuous intervals were used, the actual thresholds to temperature steps may have been between stimuli and therefore smaller than shown below. Latencies were measured during thermal steps from the onset of the stimulus to (a) the onset of the response, and (b) the maximum and minimum deviation from control.

Responses to thermal ramp and step stimuli were calculated by subtracting the average activity in the control period from the activity evoked during the stimulus. Post-stimulus responses (where applicable) were similarly computed by subtracting the control rate from the activity in the period following removal of the stimulus. Responses were

expressed either as the total difference or the mean difference in the number of spikes, as appropriate. Dynamic responses were calculated by subtracting the maximum (excitatory) or minimum (inhibitory) discharge rates from the average control discharge rate. The time taken to maximum response (i.e. to reach maximum or minimum discharge) was recorded as a measure of the speed of response.

Individual comparisons between two independent samples were made using the Mann-Whitney U-test. This non-parametric test is more conservative than the Student's t-test, and does not make any assumptions about the shape of the distributions (Gaussian or otherwise; see Siegel 1956). The relationship between independent samples was assessed by linear regression. Multiple comparisons among samples were completed using the one-way analysis of variance (ANOVA) followed by Newman-Keul's multiple range test.

4.3 RESULTS

4.3.1 GENERAL RESPONSE CHARACTERISTICS

Of the 235 PMRF neurones identified by their responses to mechanical stimuli (Chapter 3), 202 (86%) also responded to heat stimuli of 43-48°C applied to the glabrous skin on the ipsilateral hindpaw. Both excitatory (ON-t) and inhibitory (OFF-t) thermal responses were observed. The remaining 33 units (14%) were unaffected by thermal stimuli (non-responsive neurones, NR-t). All but one of the NR-t neurones were spontaneously active.

Of the 202 thermoresponsive units, 161 (80%) responded to cutaneous heating with an increase in discharge frequency (ON-t cells). These excitatory responses occurred both in spontaneously active and quiescent units. Forty-one neurones (20%) responded to heat stimuli by decreasing their discharge rates (OFF-t cells). There was no apparent spatial organization of the units with respect to excitatory and inhibitory responses (Figure 4.1).

The polarities of response of PMRF neurones to thermal and mechanical stimuli were significantly correlated (Chi-square 112,92, 6 d.f., $p<0,0001$; Table 4.1). Seventy-seven percent of all identified PMRF neurones (153 excited, 29 inhibited) responded with the same polarity to both stimuli. Considering the responses to mechanical stimulation as the independent variable (i.e. down the columns), 81% of neurones (153/188) were excited by both stimuli, while 73% (29/40) were inhibited by both stimuli. Regarding the thermal responses as the independent variable (i.e. across the rows), over 95% of PMRF units (153/161) increased their discharge rates in both experiments, while 71% (29/41) showed decreased discharge rates to mechanical and thermal cutaneous stimuli. The majority of PMRF neurones that were unresponsive to thermal stimuli, were excited by mechanical stimuli (26/33 or 79%). Only 14 of 235 neurones (6%) responded with opposite polarity to the two stimulus modalities.

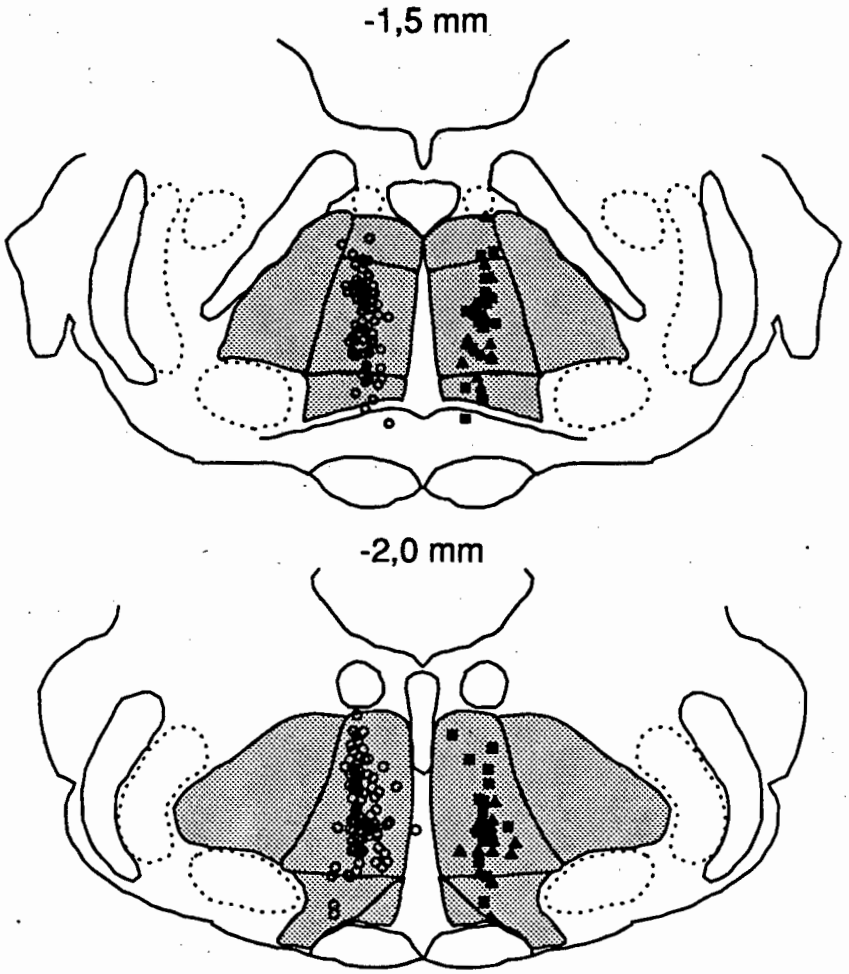

FIGURE 4.1 Anatomical location and response to cutaneous thermal stimuli of 235 units of the medial PMRF. Excitatory responses are represented on the left of each section as open circles. On the right of each section, inhibitory responses are represented as closed triangles, and neurones with no thermal response as open squares. No spatial organization is apparent with respect to polarity of response.

TABLE 4.1 Relationship between the polarities of response of PMRF neurones to thermal and mechanical stimuli.

		Mechanical			
		E	I	C	TOTAL
Thermal	E	153	5	3	161
	I	9	29	3	41
	N	26	6	1	33
TOTAL		188	40	7	235

E - excitatory response; I - inhibitory response; C - complex response (excitation and inhibition); N - no thermal response. Chi-square 112,92 (6 d.f.), $p < 0,0001$. Excluding the 7 complex responses from the Chi-square test had no appreciable effect on the result: the Chi-square value increased to 113,35 (2 d.f.), and the p-value remained unchanged.

4.3.2 RESPONSES TO CONTINUOUSLY INCREASING (RAMP) THERMAL STIMULI

One hundred and sixteen PMRF neurones were challenged with slow ramp thermal stimuli (0,2°C/s, 35-48°C) to the ipsilateral hindpaw. The firing rate of 91% (106 of 116) of these neurones changed in response to the ramp. Five representative responses of PMRF neurones to the thermal ramp stimuli are shown in Figure 4.2. In the following sections, the discharge patterns of these neurones are described in terms of their threshold temperatures (ie the temperature at the onset of the response), the size and time course of the evoked suprathreshold responses, and the effects of repeated thermal ramp stimuli.

4.3.2.1 Distribution of temperature thresholds

The threshold temperatures in the slow thermal ramp experiments ranged from 35,2°C to 47,9°C. The distribution of threshold temperatures of neither the ON-t, nor of the OFF-t, cells was Gaussian ($p<0,05$; Figure 4.3A and B). There were too few inhibitory responses (n=24) to discern the distribution of responses in the infinite population. The 82 excitatory responses were not randomly distributed over the entire stimulus range (Chi-square=48,32, 10 d.f., $p<0,0001$), but 78% of the responses clustered between 38,5 and 43,5°C. Within this range (38,5 to 43,5°C), there appeared to be two clearly separate peaks, at 39 and 43°C respectively. These were subsequently used as intermediary temperatures in the stepped stimulus series (Series DS; see Sections 4.2.1 and 4.3.3)

The threshold distribution of the excitatory responses was shifted significantly towards higher temperatures relative to that of the inhibitory responses (Mann-Whitney U-test, n_1=82, n_2=24, Z=2,56, p=0,01; Figure 4.3C). There was no anatomical organization of PMRF neurones as a function of their thermal response thresholds: neurones with thresholds below and above 42°C were encountered throughout the PMRF (Figure 4.4).

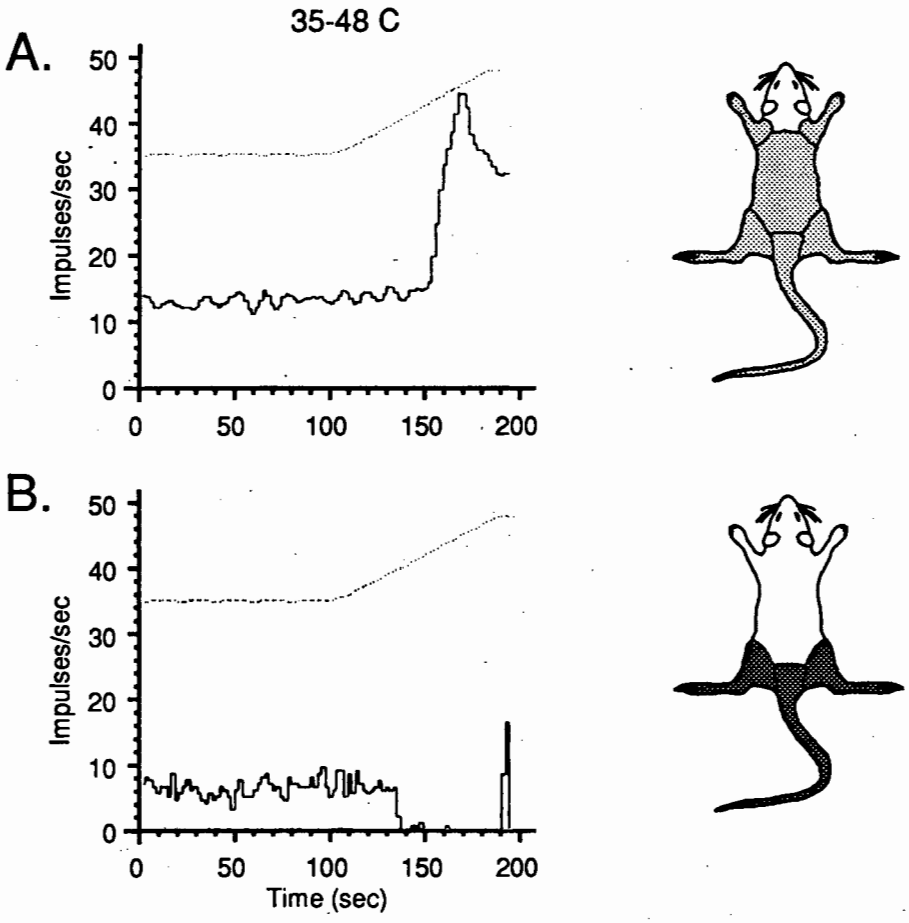

FIGURE 4.2 Responses of 5 representative neurones in the PMRF to a ramp thermal stimulus (0,2°C/s) applied to the glabrous skin on the ventral surface of the hindpaw. The stimulus temperature is represented as a dotted line. The discharge rate of each unit is represented as a histogram of the average number of events per 2 s time bin (solid line). The receptive field for mechanical stimulation and the anatomical location of each unit is shown to the right of each response histogram. A: Unit with background discharge (12,9 spikes/s, ± 1,5 SD) which exhibited an abrupt increase in discharge at threshold (43,4°C). The mean response was 24,1 spikes/s and the maximum difference was 34,1 spikes/s. The peak response was attained before the maximum stimulus temperature (45,9°C), followed by adaptation. B: Unit with background discharge (6,3 spikes/s, ± 1,9 SD) which exhibited an abrupt cessation of activity at 39,7°C. This unit showed a brief burst of activity (maximum rate 17 spikes/s) when the stimulus temperature reached maximum (dT/dt=0).

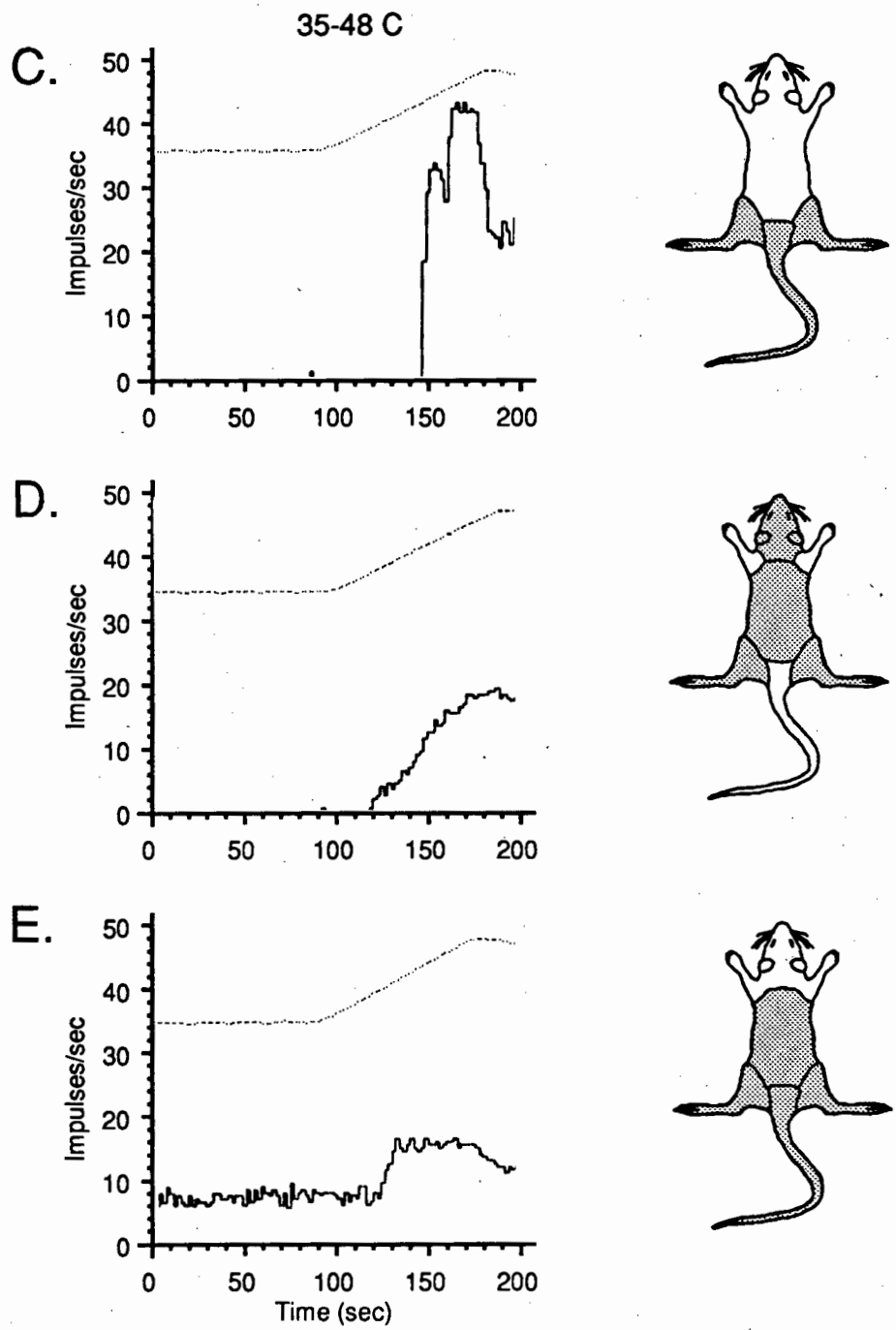

FIGURE 4.2 (cont.) C: Quiescent unit which exhibited an abrupt increase in discharge at 43,1°C (mean response 34,8 spikes/s, maximum discharge rate 43 spikes/s). D: Quiescent unit which exhibited a discharge that was approximately proportional to the stimulus temperature beyond a threshold of 38,3°C (mean response 12,1 spikes/s, maximum discharge rate 20 spikes/s). E: Unit which exhibited a proportional increase in discharge (threshold 40,2°C) followed by a plateau (spontaneous rate 7,3 spikes/s ± 1,4 SD, mean response 7,8 spikes/s, maximum difference 9,7 spikes/s).

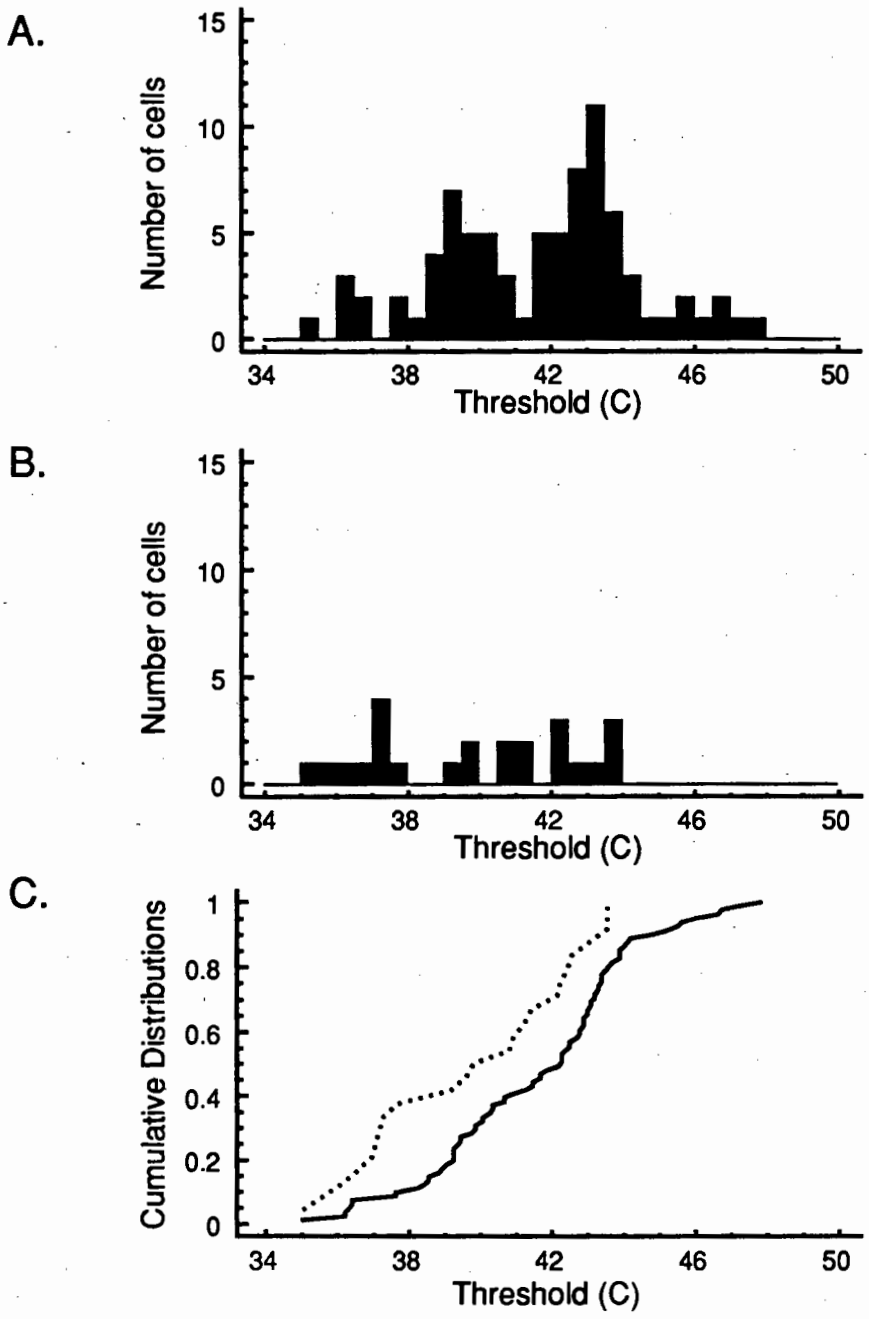

FIGURE 4.3 A: Distribution of thresholds of 82 PMRF units responding to slow ramp thermal stimulation of the ipsilateral hindpaw with increased discharge rates (ON-t cells). The distribution was bimodal, with peaks occurring at 39 and 43°C. B: Distribution of thresholds 24 PMRF units inhibited by thermal ramp stimuli (OFF-t cells). C: Cumulative distribution functions of ON-t (solid line) and OFF-t (dotted line) neurones. The threshold distribution of the ON-t units was shifted significantly towards higher temperatures relative to the threshold distribution of the OFF-t units (Mann Whitney U-test, p=0,01).

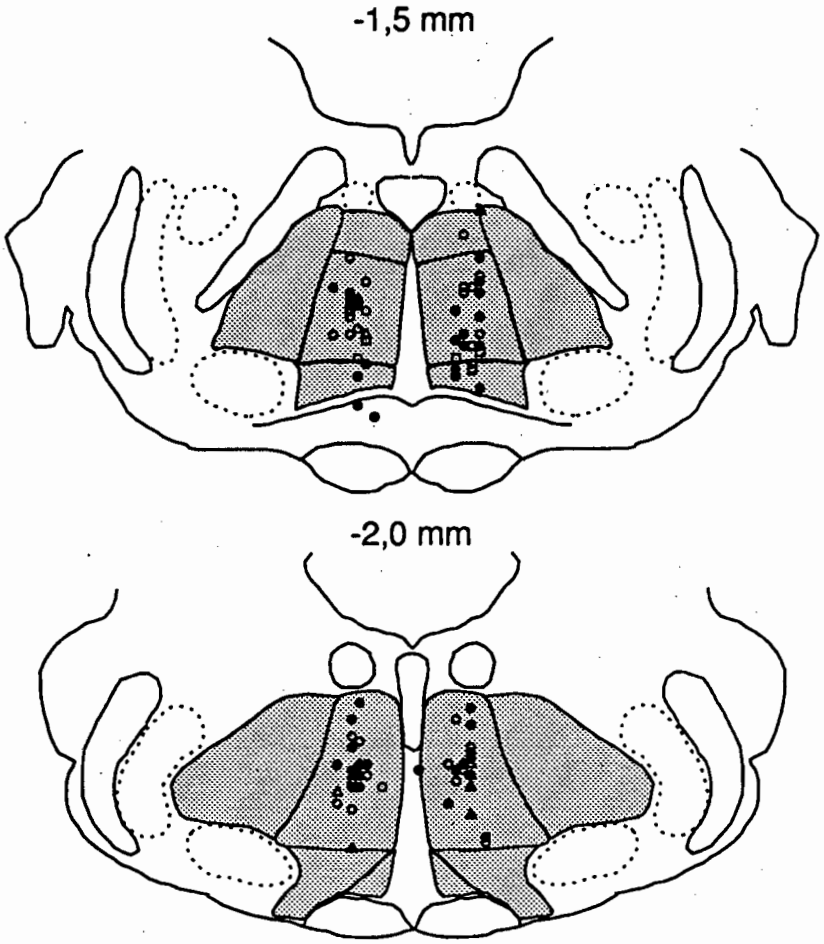

FIGURE 4.4 Anatomical location of PMRF neurones as a function of threshold temperature. Those units with thresholds below 42°C are indicated on the left of each section by closed circles, while those above 42°C are represented on the right of each section as open triangles. No spatial organization with respect to these two threshold groups is apparent.

4.3.2.2 Magnitude of response

Figure 4.5A shows the distribution of the average change in activity of PMRF neurones to the slow temperature ramp. The change in activity of a given PMRF neurone is expressed as the mean firing rate from the onset of the change in discharge rate to the end of the ramp, minus the mean spontaneous firing rate (see Section 4.2.2). The distribution of the maximum differences in discharge rate following the onset of the ramp is shown in Figure 4.5B. The latter is a measure of the dynamic response of the neurones. The distributions of both the average responses (Figure 4.5A) and the maximum differences (Figure 4.5B) were not significantly different from Gaussian distributions (p=0,18 and p=0,06, respectively). The mean of the average response rates was 5,9 spikes/s (±11,0, SD), and the range was -28,24 to 40,14 spikes/s. The mean of the maximum responses was 9,3 spikes/s (±16,1, SD), with a range from -46,4 to 65 spikes/s. There was a highly significant positive correlation between the average responses of individual neurones and their maximum responses (Figure 4.5C). The coefficient of correlation (r) was 0,978, and the slope was 1,43 (p<0,0001).

4.3.2.3 Time course of response

The time taken from the threshold of response to the maximum difference in firing rate was taken as a measure of the speed of response. The distribution of times to response maxima is shown in Figure 4.6. This distribution was skewed towards the right (skewness = +0,708). The mean time taken to reach maximum response was 30,8 s, and the mode was 22 s.

An early attempt to classify the responses of PMRF neurones to cutaneous thermal stimuli into "switch" and "proportional" types (Farham and Douglas, 1985) was probably oversimplistic. A switch response was defined as one which attained more than two-thirds of its maximum response within 10 s of threshold; the remaining responses were termed proportional. The 10 s cut-off point was clearly arbitrary. This arbitrariness is not removed if a distinction is made between "peaked" and "monotonic" responses (no whimsical time-to-2/3-maximum cut-off point). Since the duration of the temperature ramp (the cutaneous stimulus) was only 100 s, all responses with times to maximum greater than 100 s were truncated. The firing rate in these cases therefore rose steadily from threshold to the end of the ramp, giving the appearance of "monotonic", rather than "peaked" responses.

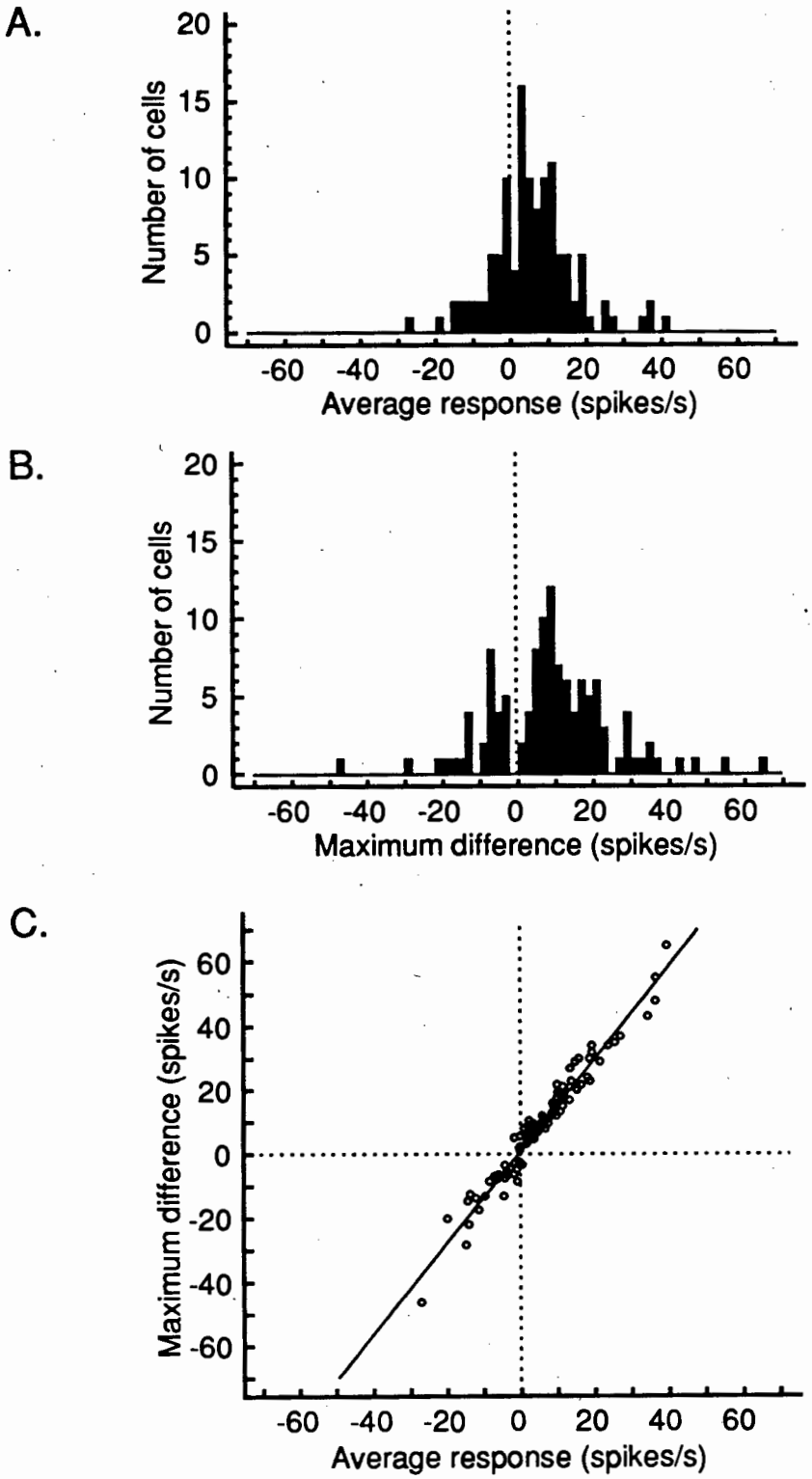

FIGURE 4.5 A: Distribution of average response magnitudes of 117 PMRF units to ramp thermal stimulation of the ipsilateral hindpaw. The distribution was Gaussian (mean 5,9 ± 11,0 spikes/s). B: Distribution of maximum changes in activity of the same PMRF neurones (Gaussian distribution, mean 9,3 ± 16,1 spikes/s). C: Comparison of the average and maximum response magnitudes of these PMRF units to ipsilateral thermal stimuli. These two response measures were significantly correlated ($p<0,0001$).

Forty-four of 106 thermoresponsive PMRF neurones (42%) had responses that were still increasing (ON-t cells) or decreasing (OFF-t cells) at the end of the temperature ramp (i.e. true "monotonic" responses plus truncated "peaked" responses; Figure 4.2D). The remaining neurones showed either a clear maximum with a fall-off in the responses before the end of the ramp (25%; Figure 4.2A and C), or reached a plateau which was maintained to the end of the ramp (33%; Figure 4.2E). All of these response types were observed in both spontaneously active and quiescent neurones.

Many of the neurones in all 3 groups showed dramatic decreases in response beyond the maximum temperature, and/or distinct oscillations in discharge rate, which coincided with small oscillations in the stimulus temperature (approximately 0,5°C peak-to-peak; see Figure 4.15D).

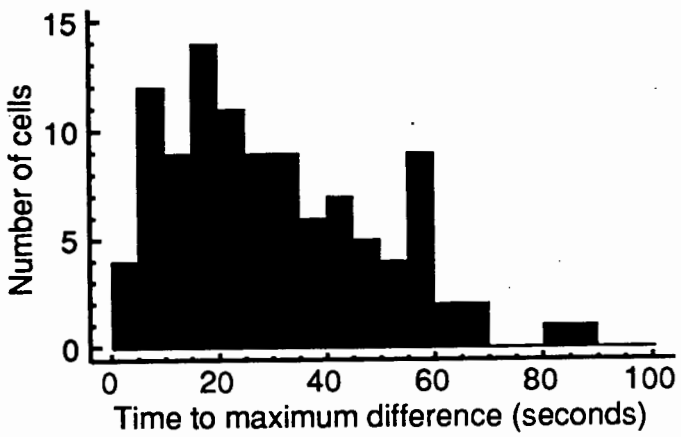

FIGURE 4.6 Distribution of time taken from response threshold to maximum (ON-t units) or minimum (OFF-t units) discharge rates in thermoresponsive PMRF units. The mode occurred at 22 s.

4.3.2.4 Repeated ipsilateral heat stimuli

The responses to repeated ipsilateral slow ramp stimuli were studied in 36 neurones. In these experiments, the thermal stimulator was removed from the stimulation site, cooled, and re-attached to the same site on the ipsilateral hindpaw. The second ramp stimulus was begun 10 minutes after the first, or in some cases 10 minutes after a contralateral stimulus (Section 4.3.2.5). The responses to ipsilateral stimulation were studied at further 10 minute intervals for periods of 30 to 60 minutes in 25 neurones. Figures 4.7 and 4.8 show two representative, and two unusual, unit responses to repeated ipsilateral thermal stimuli, respectively. The responses of individual neurones were generally stable and repeatable with respect to their polarity (ON-t or OFF-t), magnitude and time-course. The spontaneous discharge rates of the majority of neurones returned to their pre-stimulus levels between thermal stimuli ($r=0,838$, slope=0,78, 34 d.f., $p<0,0001$; Figure 4.9A).

The threshold temperatures of the majority of cells showed large variability with time. Non-parametric correlation analysis was performed on the threshold temperatures at which cells responded to a first and second slow ramp stimulus. Only those cells which responded on both occasions could be included in the analysis. The Spearman rank correlation coefficient (r_S) between the threshold temperatures of the first and second ipsilateral stimuli was 0,051 ($n=33$, $p=0,77$; Figure 4.9B).

In contrast to the poor correlation between threshold temperatures, the magnitudes of the responses to the first and second stimuli were highly significantly correlated. The slope of the regression between the average responses to repeated ipsilateral stimulation was 0,55 ($r=0,811$, 34 d.f., $p<0,0001$; Figure 4.9C), while that of the maximum responses was 0,65 ($r=0,851$, 34 d.f., $p<0,0001$; Figure 4.9D).

Two cells exhibited reversal of the polarity of their responses to successive stimuli (Figure 4.8B). In these cases, the direction of the responses appeared to depend on the spontaneous discharge rate of the cell in the control period preceding each stimulus.

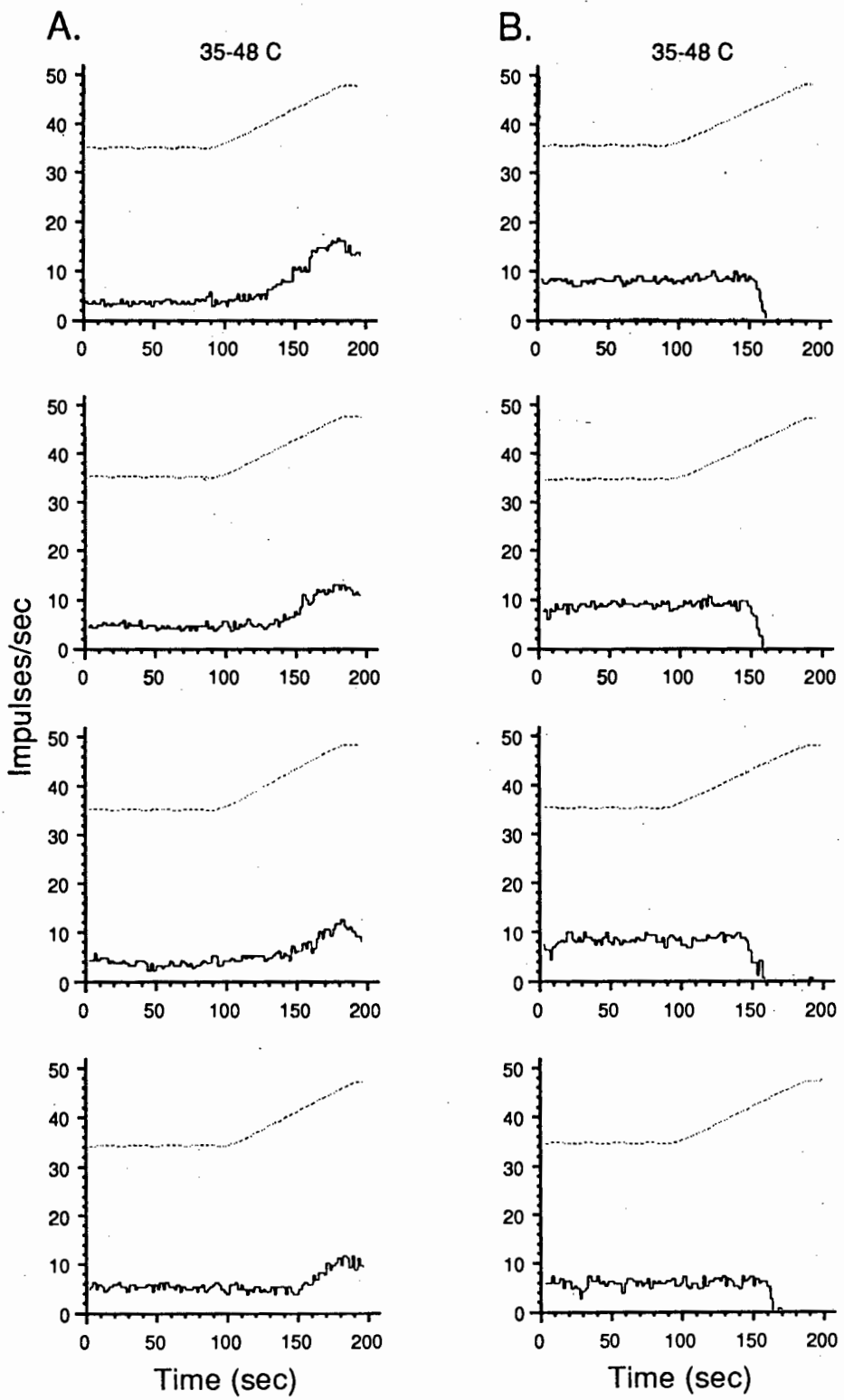

FIGURE 4.7 Responses of 2 representative PMRF units to repeated thermal stimulation of the glabrous skin on the ipsilateral hindpaw. A: ON-t unit. B: OFF-t unit. In both cases, the spontaneous rate and the polarity and magnitude of response were relatively consistent. The threshold increased marginally with successive stimuli in A, but was approximately constant in B.

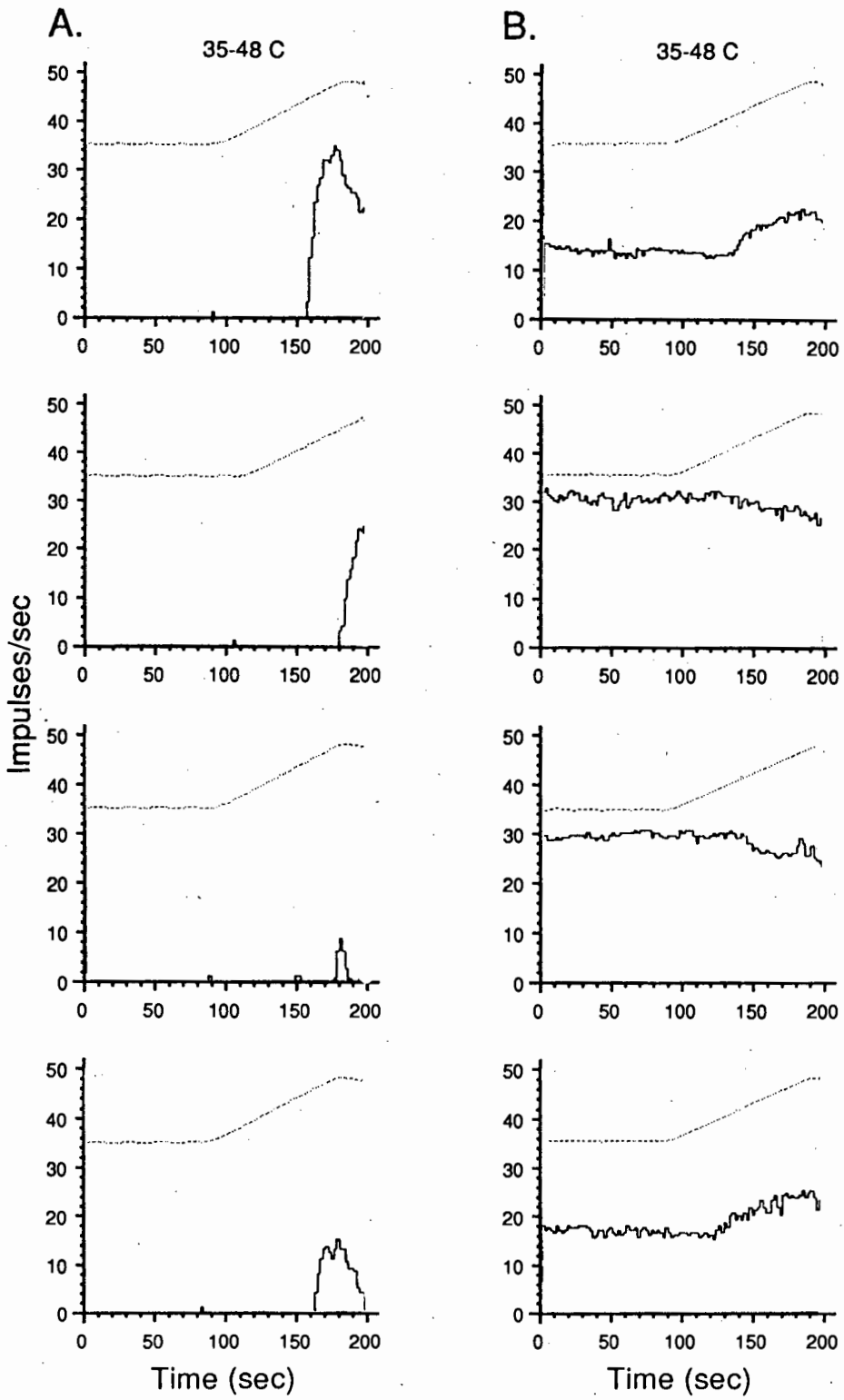

FIGURE 4.8 Two unusual responses of PMRF neurones to repeated ipsilateral thermal ramp stimuli. A: Neurone showing no spontaneous discharge, and highly variable threshold and magnitude responses to successive stimuli. B: Neurone with spontaneous discharge that varied between 2 levels (approximately 18 and 30 spikes/s, respectively). The polarity of response of this unit varied as a function of the spontaneous rate. However, the threshold did not noticeably change.

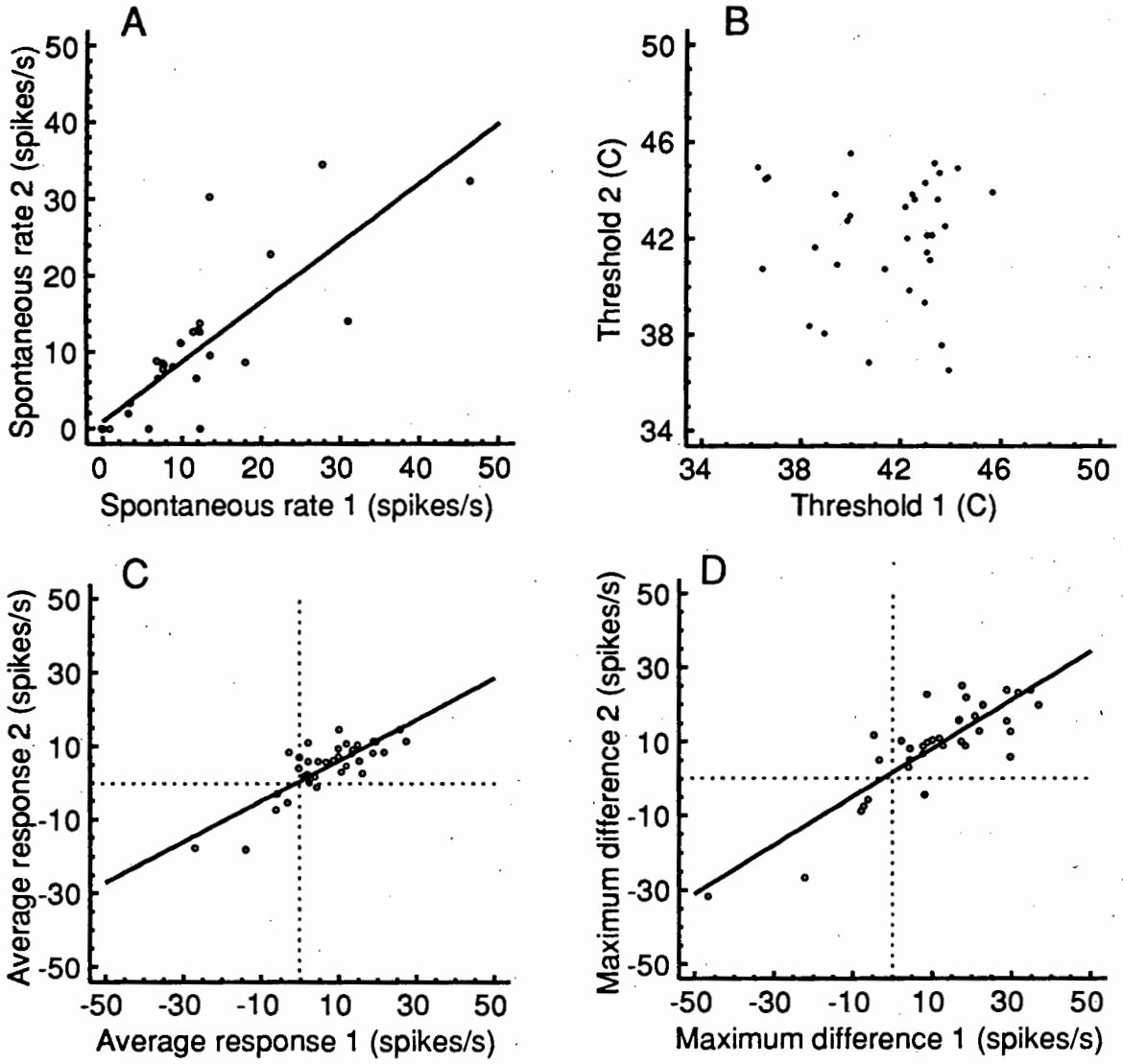

FIGURE 4.9 A: Comparison of spontaneous discharge rates of these units recorded during the control periods preceding each of the first two thermal stimuli. The spontaneous rates generally returned to their original levels between thermal stimuli ($p<0,0001$). B: Comparison of thresholds of 35 units in the PMRF responsive to repeated thermal stimulation of the ipsilateral hindpaw. These thresholds were not correlated ($p>0,05$). C: Comparison of average responses of 35 PMRF units responsive to repeated ipsilateral thermal stimulation (slope of regression=0,55, $p<0,0001$). D: Comparison of maximum responses of these units (slope=0,65, $p<0,0001$).

4.3.2.5 Spatial convergence: responses to ipsi- and contralateral stimuli

Forty-eight neurones were tested with both an ipsilateral and a contralateral thermal ramp stimulus. Representative responses examples are illustrated in Figure 4.10. The ipsilateral experiment was always performed first, followed 10 minutes later by the contralateral experiment. Thirty-seven (77%) of these units exhibited the same response polarity (ON-t or OFF-t) to both stimuli, while two units (4%) responded with opposite polarity to the two stimuli. Three cells (6%) responded only to stimulation of the ipsilateral hindpaw, while 5 cells (10%) responded only to contralateral stimulation. One neurone did not respond to either stimulus.

The distribution of threshold temperatures to contralateral stimulation is shown in Figure 4.11A. Thresholds were not randomly distributed over the entire stimulus range (Chi-Square=16,63, 5 d.f., p=0,005): seventy percent of the thresholds clustered between 38 and 44°C. The distribution of thresholds to contralateral stimulation did not differ significantly from those to ipsilateral heat stimuli (Mann-Whitney U-test, n_1=106, n_2=46, Z= -0,148, p=0,88).

The threshold temperatures of PMRF neurones to ipsi- and contralateral thermal stimulation were subjected to non-parametric correlation analysis. As in the repeated ipsilateral comparisons (Section 4.3.2.4), only those neurones which responded to both stimuli could be included in the analysis. The Spearman's rank correlation coefficient (r) was 0,392 (p=0,013; Figure 4.11B). The statistical significance of this result is questionable. If it had been possible to include the 7 data points for cells which responded to one side, but not to the other, the correlation would have been very poor indeed.

There was a highly significant positive correlation between the average response to stimulation of the ipsilateral and contralateral hindpaws (r=0,824, 47 d.f., p<0,0001; Figure 4.12A). The slope of the regression line was less than one (0,69), indicating that there was a greater response, on average, to ipsilateral than to contralateral stimulation. The maximum responses were similarly highly correlated (r=0,867, slope=0,74, 47 d.f., p<0,0001; Figure 4.12B).

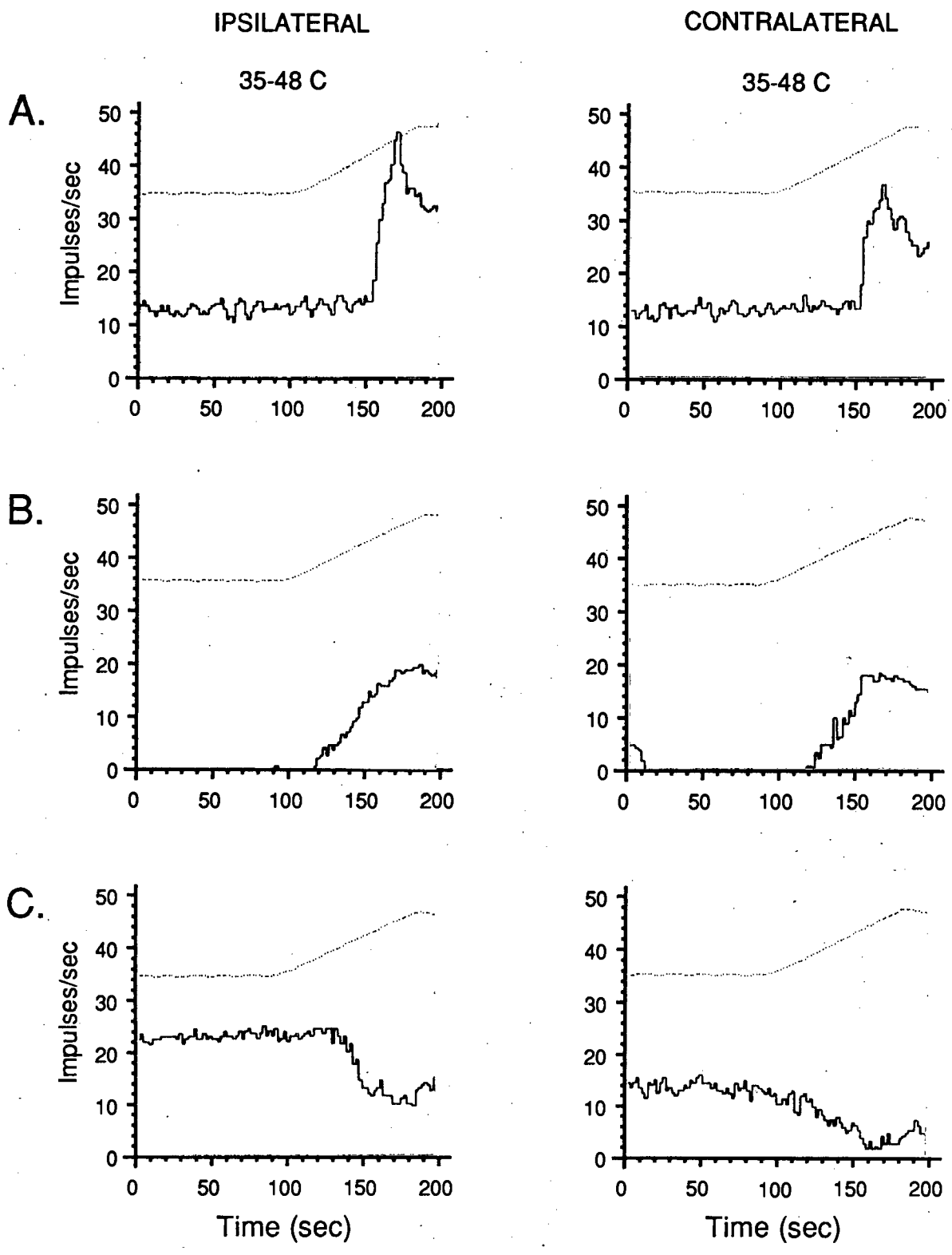

FIGURE 4.10 Responses of PMRF neurones to ipsilateral and contralateral thermal ramp stimulation. A: Neurone with steady spontaneous discharge exhibiting abrupt increases in firing rate above threshold, with marked adaptation. B: Quiescent neurone exhibiting proportional increases in discharge above threshold. There is some evidence that the firing rate reaches a plateau with contralateral stimulation. C: Inhibitory responses in a neurone with relatively high spontaneous discharge. The units illustrated in A and B are the same as those shown in Figure 4.2A and D.

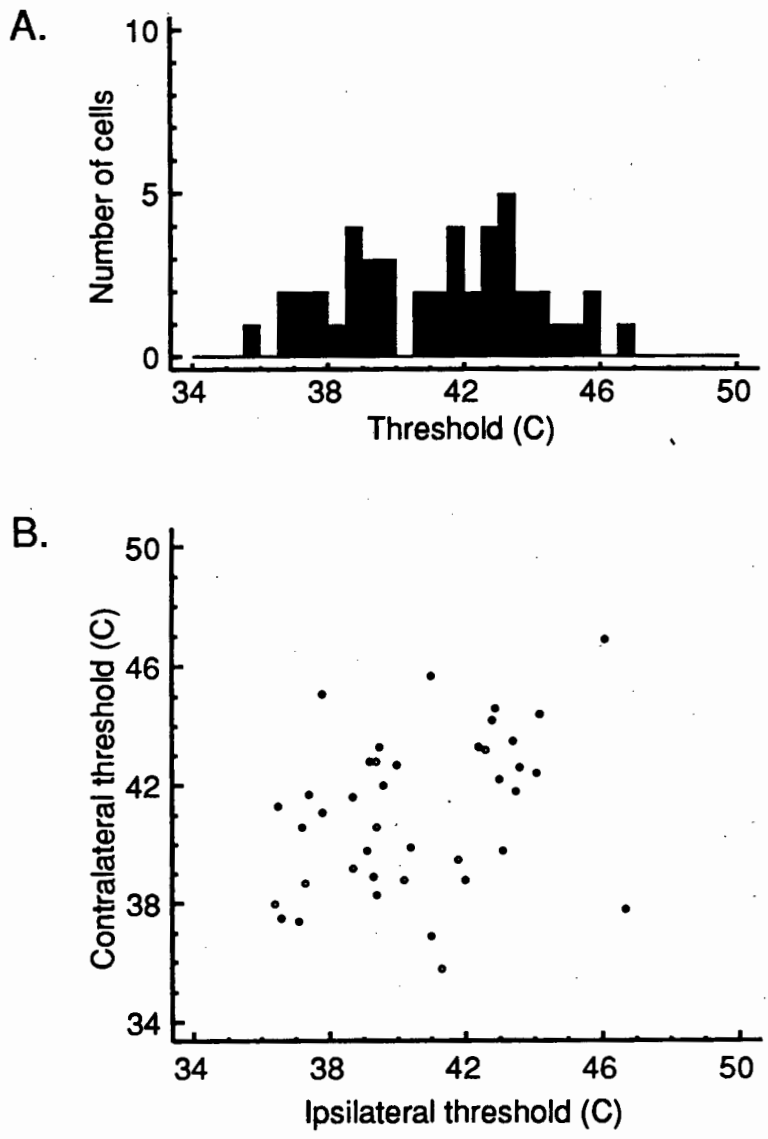

FIGURE 4.11 A: Distribution of thresholds of 44 PMRF units which were responsive to thermal ramp stimulation of the contralateral hindpaw. B: Comparison of ipsilateral and contralateral thresholds of 40 units in the PMRF responsive to thermal stimulation of both the hindpaws.

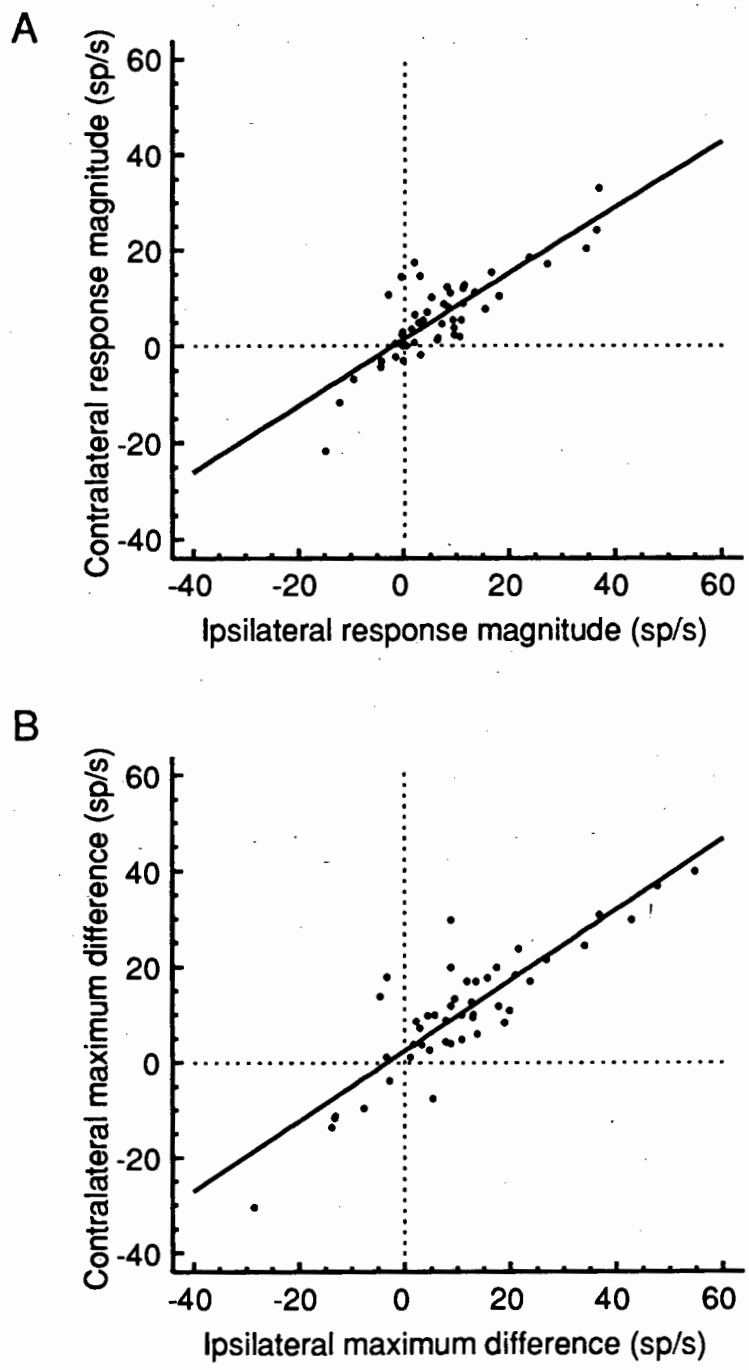

FIGURE 4.12 Comparison of the average (A) and maximum (B) response magnitudes of 48 PMRF units to thermal stimulation of the ipsi- and contralateral hindpaws. These were both strongly correlated ($p<0,0001$). The slopes of the regression lines were 0,69 and 0,74, respectively, indicating that there was a greater response, on average, to ipsilateral than to contralateral stimulation.

4.3.2.6 Variable gradient ramp stimuli

Twelve PMRF neurones were subjected to thermal ramps of varying steepness. Each ramp started at 35°C, and terminated at 48°C. Gradients of 0,2, 0,3, 0,5, 1 and 2°C/s were used. These were presented in random order. The inter-stimulus interval was 3 to 5 minutes in all cases. Not all cells were tested with all 5 ramp gradients (Figure 4.13).

The variations in threshold temperature in response to the different ramps are shown in Figure 4.14A. Neurones exhibiting high thresholds to slow ramps showed very little change in their thresholds with increased ramp gradients (see Figure 4.13A). On the other hand, the thresholds of 3 neurones showed marked sensitivity to the steepness of the ramp gradient over most of the range tested. The thresholds of 2 of these neurones were below 40°C at all rates up to, and including, 1°C/s.

Since the stimulus duration differed for each of the ramp gradients in this series, the maximum differences in firing rates, rather than the average differences, were used as the measure of the response magnitude. Figure 4.14B illustrates that there was no relationship between the ramp gradient and the maximum differences in firing rate of the cells.

Of the 12 cells in this series, 5 appeared to switch between 2 (and occasionally 3) spontaneous discharge rates from one ramp to the next (Figure 4.13C). In these instances, the absolute firing rate at the temperature plateau tended to be more reproducible than the stimulus-evoked maximum change in firing rate.

One cell (Figure 4.13B) exhibited unmistakable sensitivity to the ramp gradient, in that the rise to maximum response was almost directly proportional to the temperature. This neurone was also unusual in that it showed a biphasic response during the temperature ramp, with excitation following a transient inhibitory phase. In the remaining cells, the rate of increase or decrease in neuronal discharge was independent of the ramp gradient.

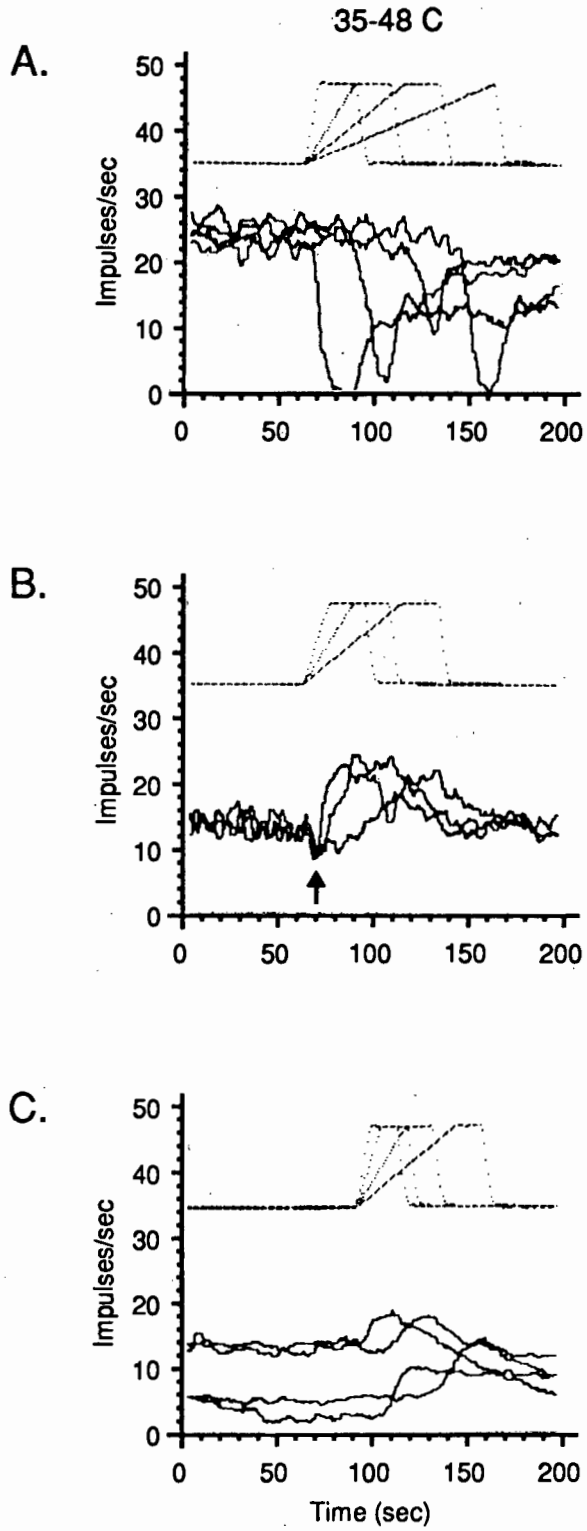

FIGURE 4.13 Responses of 3 representative PMRF neurones to variable thermal ramp gradients. The stimuli were presented in random order. A: High threshold (greater than 43°C) neurone exhibiting inhibitory responses. The response magnitude varied markedly to the different stimuli, but was not systematically related to the thermal ramp gradient. B: Low threshold (less than 40°C) neurone whose response varied as a function of the thermal ramp gradient. This neurone also exhibited transient inhibition (arrow) before the excitatory response. The response magnitude was relatively constant. C: Excitatory neurone whose spontaneous discharge rate appeared to switch between two levels. The change in discharge rate in response to each stimulus was approximately constant.

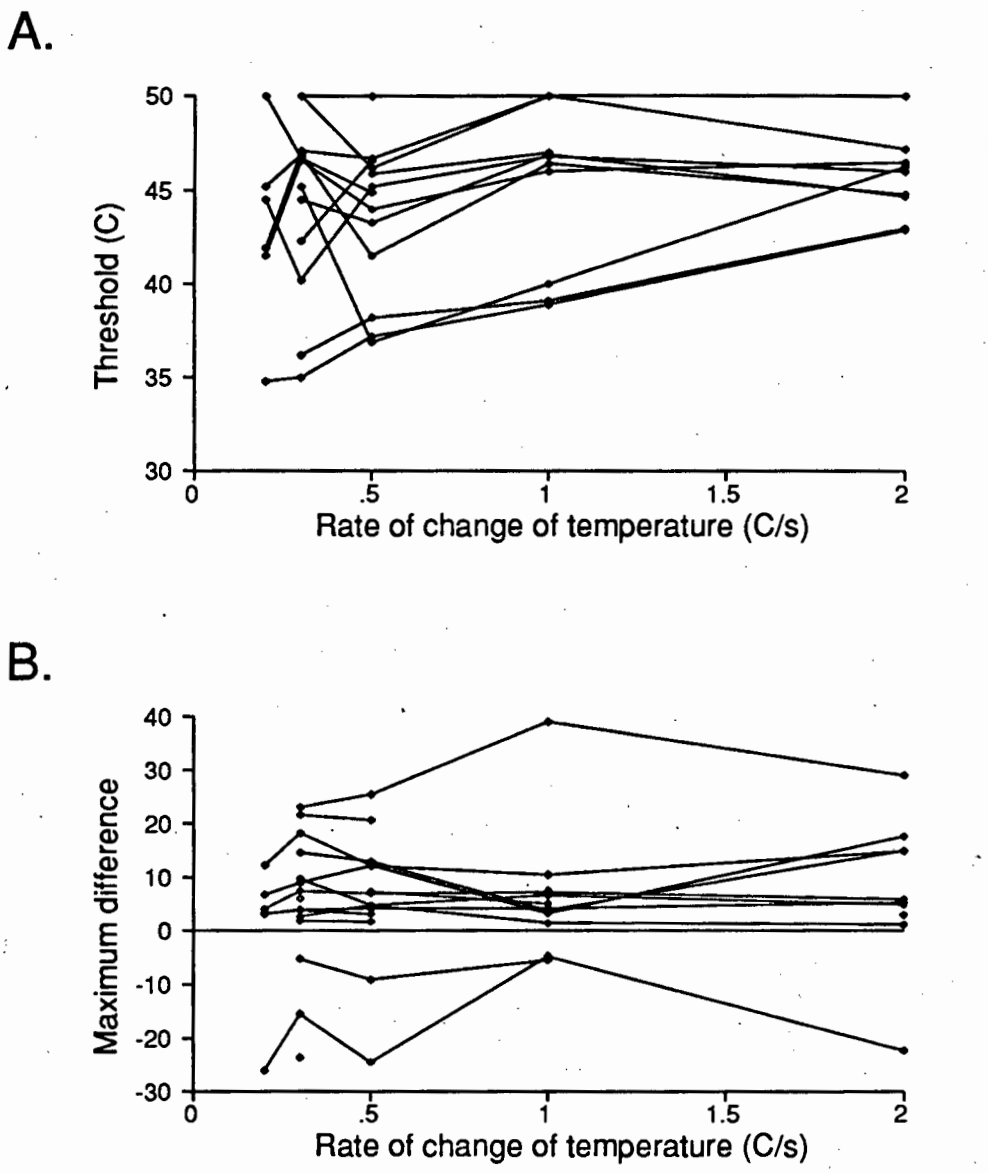

FIGURE 4.14 A: Relationship between threshold temperature and rate of change of stimulus temperature. Three units showed some measure of coding of the rate of temperature increase by their thresholds, while the remainder showed no systematic relationship between these parameters. B: There was no relationship between the maximum difference in discharge and the rate of thermal gradients. The majority of neurones exhibited the same response magnitude to each stimulus, while others showed dramatic variations in their response magnitudes that were unrelated to the stimulus gradients.

4.3.2.7 Interrupted ramp stimuli

In 16 cells, the slow ramp (0,2°C/s) was interrupted by a plateau at 44°C, lasting for 150 s (Figure 4.15). Five types of response were seen. With the onset of the plateau, the firing rate remained unchanged in 1 cell. In 7 cells, the firing rate peaked at or around the maximum stimulus temperature, and then returned towards baseline (ie showed marked adaptation). One cell began firing for the first time with the onset of the plateau. Three cells showed a biphasic response: an initial adaptation followed by an increase in firing rate. Four cells had not reached threshold by 44°C.

The marked oscillations in the discharge rate during the plateau, shown in Figure 4.15D, were phase-locked with small fluctuations in the stimulus temperature (0,4°C, peak-to-peak). (Similar oscillations were sometimes observed in the first series of slow ramp experiments in neurones whose discharge was observed for at least 10 s after the maximum temperature had been reached.) In the example illustrated in Figure 4.15D, the oscillations were superimposed on a slow increase in firing rate during the plateau.

The second part of the ramp (from 44 to 48°C) followed the plateau in 14 of the 16 cells. The 4 cells which had not responded to the 44°C plateau, all started firing during this phase of the experiment; 8 cells increased their responses; 1 cell continued firing at the same rate; and 1 cell was inhibited at the higher temperatures.

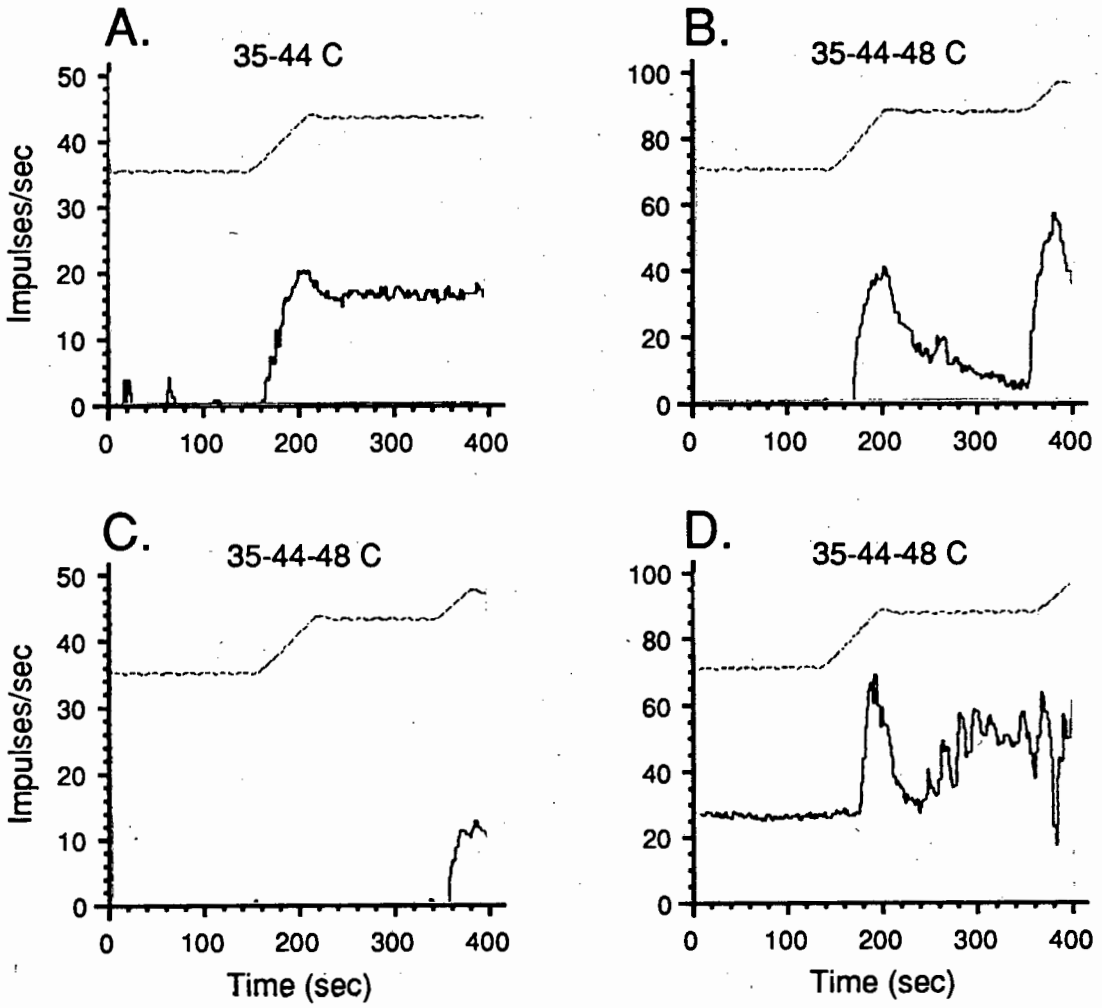

FIGURE 4.15 Responses of PMRF neurones to slow thermal ramps (0,2°C/s) interrupted by a 150 s plateau. (Note: the y-axes of B and D are double those of A and C.) A: Quiescent neurone that responded rapidly to the temperature ramp, showed little adaptation, and maintained an elevated rate of discharge throughout the temperature plateau (42°C). B: Quiescent neurone showing a dramatic response during the stimulus ramp with marked decay (almost to zero) during the temperature plateau. The response to a second thermal ramp to 45°C was larger than the first, and also showed striking adaptation. C: Neurone which did not respond to the first plateau temperature, but only when the temperature was raised above 42°C. D: Neurone showing spontaneous discharge and responding very strongly, with rapid onset and adaptation, during the thermal ramp. There is a second, slower response during the plateau that has superimposed oscillations corresponding to the small (0,5°C) oscillations in the stimulus temperature. This neurone therefore exhibits exquisite (if somewhat unreliable) rate sensitivity.

4.3.3 RESPONSES TO CONSTANT-TEMPERATURE (STEPPED) STIMULI

Thirty-three PMRF neurones were challenged with ascending stepped stimuli starting from baseline (35°C) and going to 40°C, followed by either 43 or 45°C (double steps, Series DS). These temperatures were chosen to correspond to the peaks in the distribution of thresholds in the ramp experiments (see Section 4.3.2.1). These temperatures are regarded as being within the innocuous to noxious range (Chéry-Croze, 1983; Darian-Smith, 1984). The duration of each step was 60 s. Examples of typical responses are shown in Figure 4.16.

Four of the 33 cells in the ascending step series did not respond at all. Of the remaining 29 cells, 8 (28%) responded at both temperatures (6 ON-t, 2 OFF-t cells; Figure 4.16A), while 18 neurones (62%) responded only to the higher temperature (15 ON-t, 3 OFF-t cells; Figures 4.16B and C). There were 3 ON-t (10%) cells which exhibited a marginally greater response to the lower temperature than to the higher.

Twenty-nine neurones were challenged with descending step temperatures starting from 43 or 45°C, and going to 40°C before being returned to baseline. The responses were qualitatively similar to the responses of these neurones to ascending stepped temperature stimuli (Figure 4.16). The majority (59%) showed decreasing responsiveness to the decreasing steps. Two neurones (7%) showed the same response to both steps. Four neurones (14%) remained activated following removal of the stimulus (Figure 4.17A). The remaining 6 cells did not respond to any temperature.

Twenty-three PMRF neurones were tested with both ascending and descending step stimuli. The majority of these neurones behaved in a similar manner to each stimulus sequence: 17 of 23 (74%) neurones responded with the same polarity (14 excited, 3 inhibited), one neurone did not respond to either stimulus, and four neurones responded to one stimulus only. One neurone was unusual in that it responded with opposite polarity to the two stimuli (Figure 4.17B).

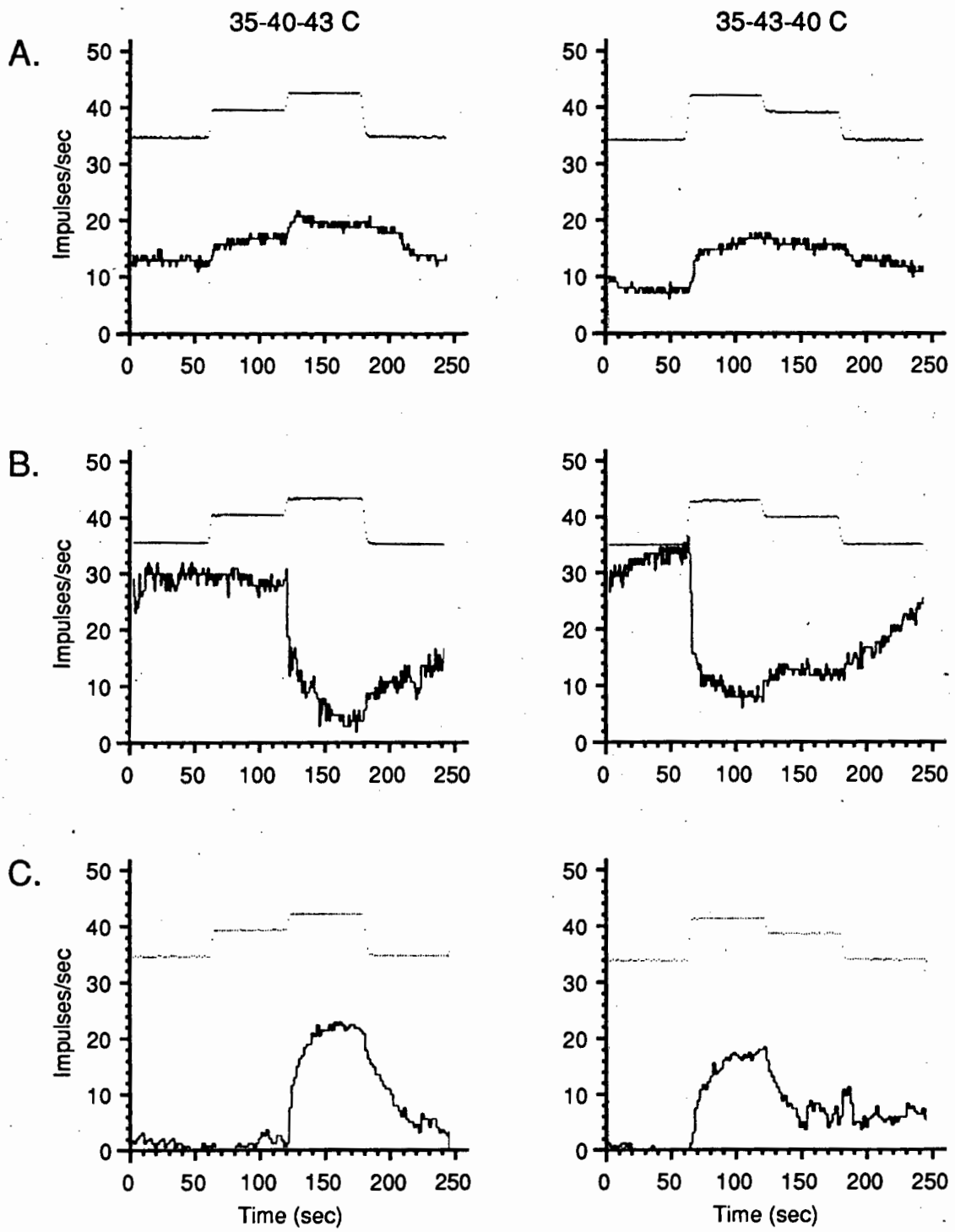

FIGURE 4.16 Responses of PMRF neurones to ascending and descending stepped (2°C/s; 35, 40 and 43°C) thermal stimuli. A: Example of a neurone which showed a small excitatory response to both temperature steps, in the ascending and descending series. B: Neurone exhibiting strong inhibition at noxious temperatures (43°C). Note the effect of adaptation temperature on the response: the cell did not respond when the temperature was raised from 35 to 40°C (left), but remained in a strongly inhibited state when the temperature was decreased from 45 to 40°C, and only reverted towards the baseline firing rate when the temperature was returned to 35°C (right). C: Neurone showing strong excitation only at noxious temperatures (43°C). The response was almost completely reversed when the temperature dropped below 43°C, irrespective of the prior adapting temperature.

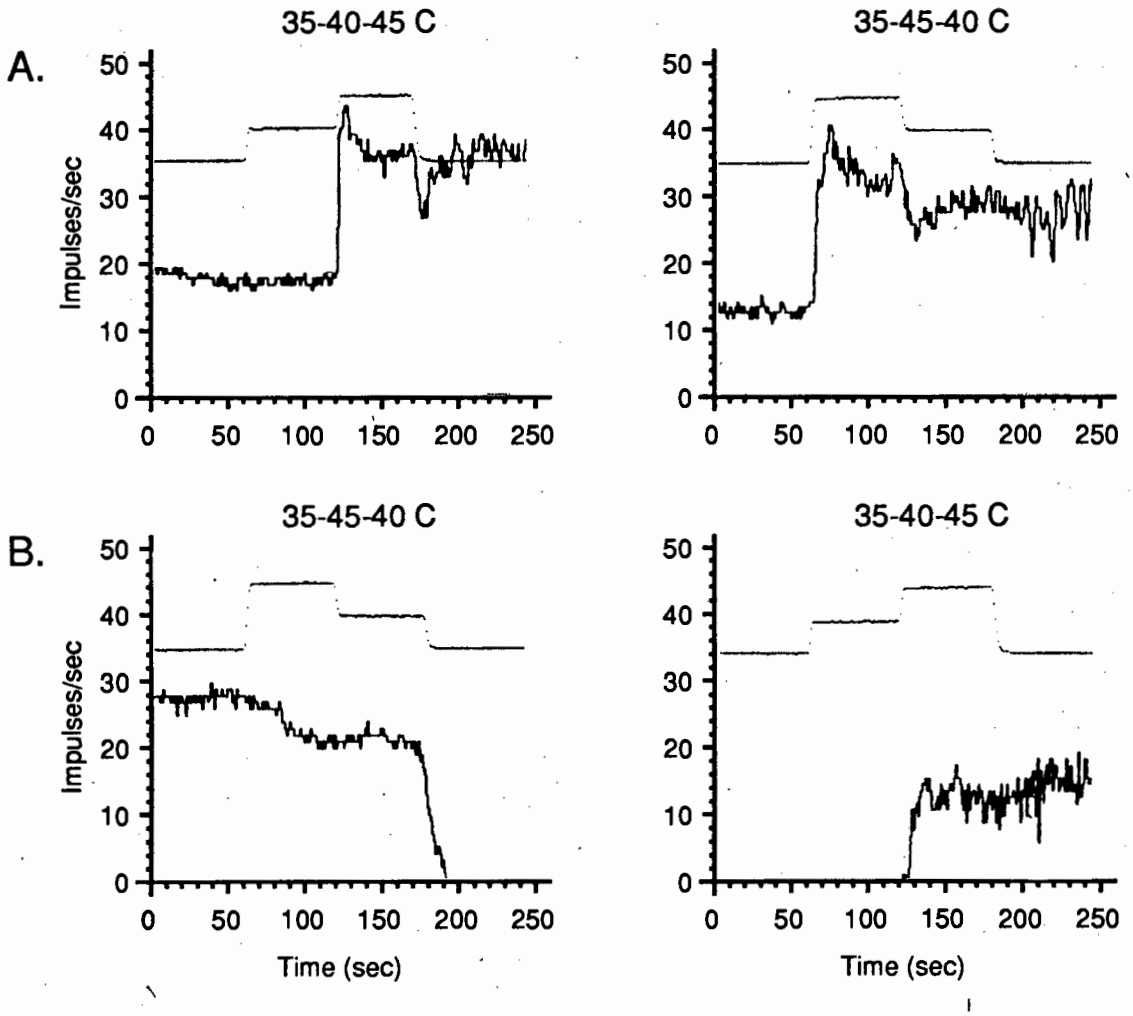

FIGURE 4.17 Two unusual responses of PMRF neurones to stepped thermal stimuli. A: Neurone which exhibited rapid and dramatic responses to noxious temperatures, whose discharge showed transient and incomplete return to baseline discharge and then remained elevated for at least 60 s after removal of the stimulus. B: Neurone which responded with opposite polarity to ascending and descending thermal steps, with complete suppression of spontaneous discharge between stimuli.

In a second series, single steps from baseline to 40, 42, 44, 46 or 48°C were used to stimulate 23 ipsilateral PMRF cells (Series SS). The duration of each step was 30 s, after which the temperature was returned to baseline. The temperature was maintained at 35°C during the interstimulus interval of 3 to 5 minutes. The temperature steps were always presented in ascending order (Figure 4.18).

Not all the cells were subjected to all five step stimuli. Six neurones were taken from 42 to 50°C, thus giving only 17 results for the 40°C stimulus. Three of the cells taken to 46 and/or 48°C developed unstable baseline discharges. Their results for these temperatures, as well as all of the 50°C results, have been discarded. (While the results for the 50°C stimulus conform to the general pattern described below, the results were discarded because there were too few data.)

The percentages of cells responding at each temperature in the double and single step series are shown in Figure 4.19. For comparison, this figure also shows the cumulative distribution of thresholds to slow ramp stimuli. Twenty-one percent of neurones in the single step series responded to stimulus temperatures of 42°C, while 85% of these cells which were still stable at the end of the experiment (n=20) were responsive to 48°C stimuli. (All 6 neurones challenged with 50°C stimuli were responsive.) By interpolation, 50% of the cells responded to a temperature of 45,2°C. This contrasts with the median temperature of 42,1°C in the ramp experiments, and of 40,9°C in the double steps.

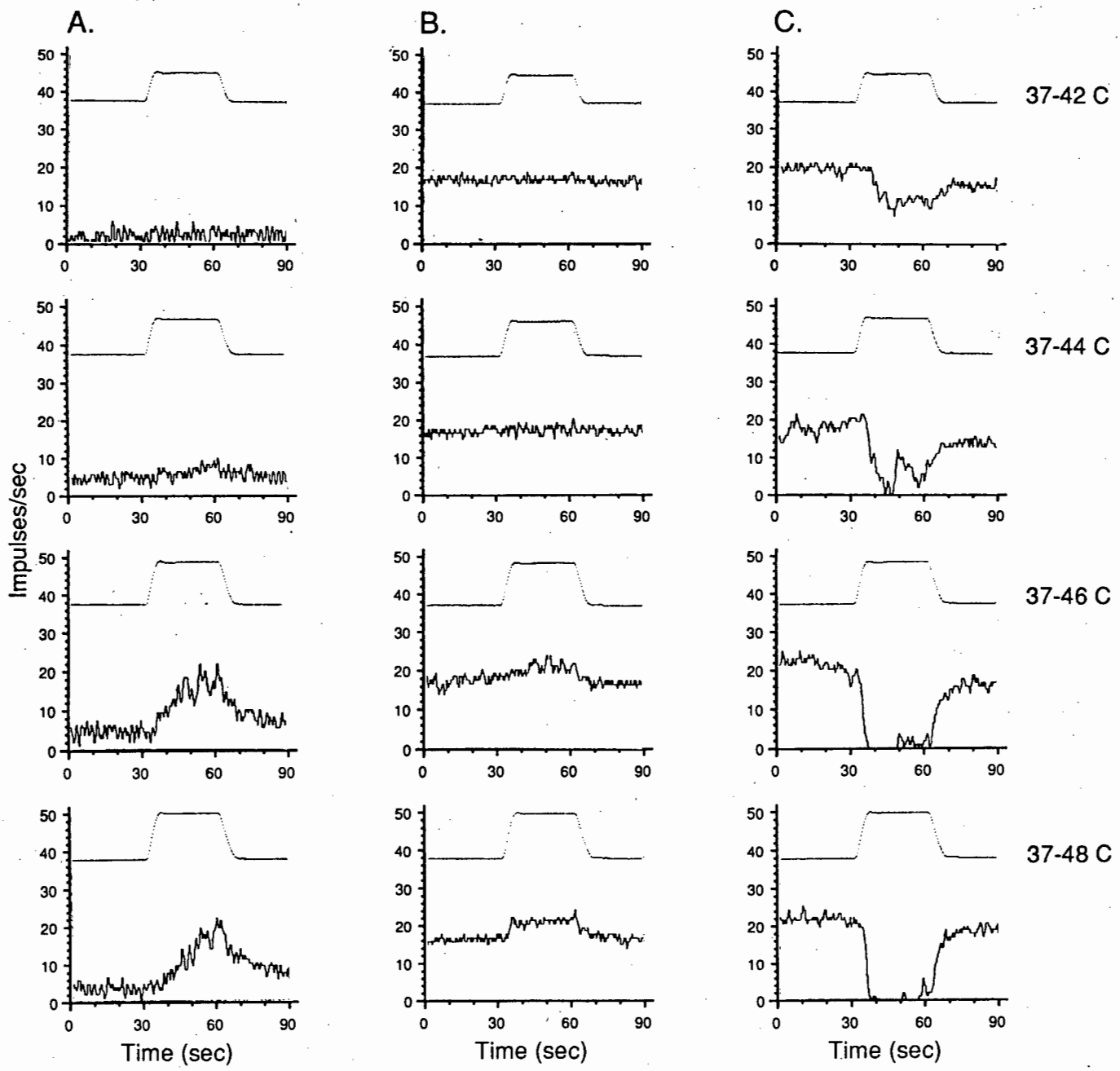

FIGURE 4.18 Responses of 3 representative PMRF neurones to a series of single temperature steps (42, 44, 46 and 48°C, 30 s duration). The steps were presented in ascending order. A, B: Excitatory responses (thresholds 44 and 46°C, respectively. C: Inhibitory response (threshold 42°C). Note the increasing (excitatory and inhibitory) responses to increasing temperature in all cases.

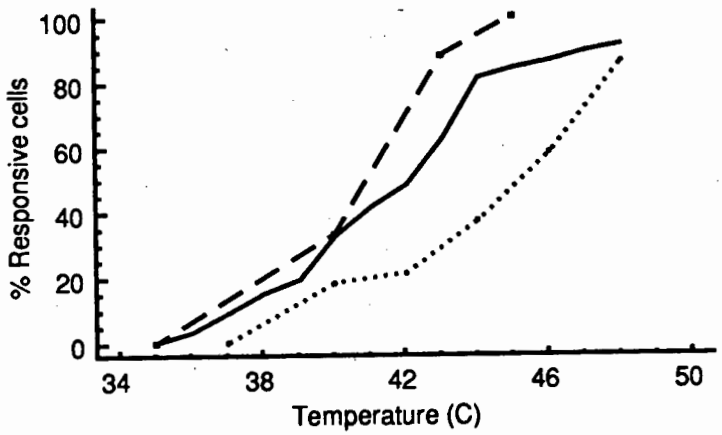

FIGURE 4.19 Percentages of PMRF neurones responding to double step (60 s: broken line), single step (30 s: dotted line), and ramp (0,15°C/s: solid line) thermal stimuli. There is a shift of the distributions towards lower temperatures (i.e. to the left) with increasing duration of the stimulus plateau. Note that almost all neurones were responsive at high temperatures (over 43°C), regardless of the stimulus waveform.

4.3.3.1 Intensity-response relationships

Two quantitative measures were used to examine the intensity-response relationships of PMRF neurones to controlled stepped thermal stimulation of the skin: the average response during thermal stimulation, and the average response following stimulation (post-response). Only the absolute response and post-response magnitudes are reported since there were too few inhibitory responses in these experiments to perform valid statistics on this sub-group.

The distributions of the absolute changes in firing rate from baseline in the ascending double step series are summarized in Figure 4.20. The central boxes cover the middle 50% of data values, between the lower and upper quartiles. The median is plotted as the central line. The "whiskers" extend to those points which lie within 1,5 times the interquartile range. Points outside these values are plotted individually.

One-way analysis of variance showed that the differences between the response magnitudes to the temperature steps were highly significant ($F=17,865$; 3, 95 d.f.; $p<0,0001$). The post-ANOVA multiple range analysis clearly distinguishes two groups: the responses to 35 and 40°C, and the responses to 43 or 45°C ($p<0,05$; Table 4.2). Thus,

PMRF neurones appear capable of distinguishing between innocuous and noxious cutaneous temperatures.

Figure 4.21 summarizes the distributions of the absolute changes in average firing rate from baseline in the single step series. The differences in firing rates for the steps to 40, 42, 44 and 46°C were not statistically significant ($p>0,05$), whereas the responses to 48°C were significantly different from the rest (ANOVA $F=8,376$; 4, 99 d.f.; $p<0,0001$; post-ANOVA multiple range analysis; see Table 4.3).

Most PMRF neurones showed significant after-responses to the thermal stimuli applied in these experiments (see Figures 4.16 to 4.18). Discharge remained elevated above baseline (in ON-t cells), or suppressed (in OFF-t cells), long after removal of the stimulus, and, presumably, beyond the arrival of the afferent inputs giving rise to the PMRF responses. The majority of cells in the both the double step and single step series returned to their pre-stimulus firing rates within 3 to 5 minutes after removal of the stimulus. Detailed records of the post-stimulus responses were made only during the first 60 s (double step series) or 30 s (single step series). (Recordings for the next step stimulus were begun 3-5 minutes later.) In the single step series, there was a significant positive correlation between the discharge rates during the stimulus and the 30 s post-stimulus periods ($r=0,72$, 108 d.f., $p<0,0001$; Figure 4.22). The regression line had a slope of 0,63, indicating that the mean response during the 30 s post-stimulus period was approximately 2/3 that in stimulus period.

When the mean firing rate during the 30 s after removal of the stimulus was incorporated as a covariate in the analysis of the single step data, 3 subgroups were distinguishable at the 95% confidence level. The first group comprised the responses to 40-44°C; the second group overlapped the first, comprising the responses to 42-46°C stimuli; the responses to the 48°C stimuli were in a group of their own (Table 4.3).

The single step stimuli were repeated in 9 PMRF cells. The responses to the second series of steps did not differ significantly from those in the first series. The average response to the second series was highly correlated with that to the first ($r=0,80$, slope=1,07, 44 d.f., $p<0,0001$).

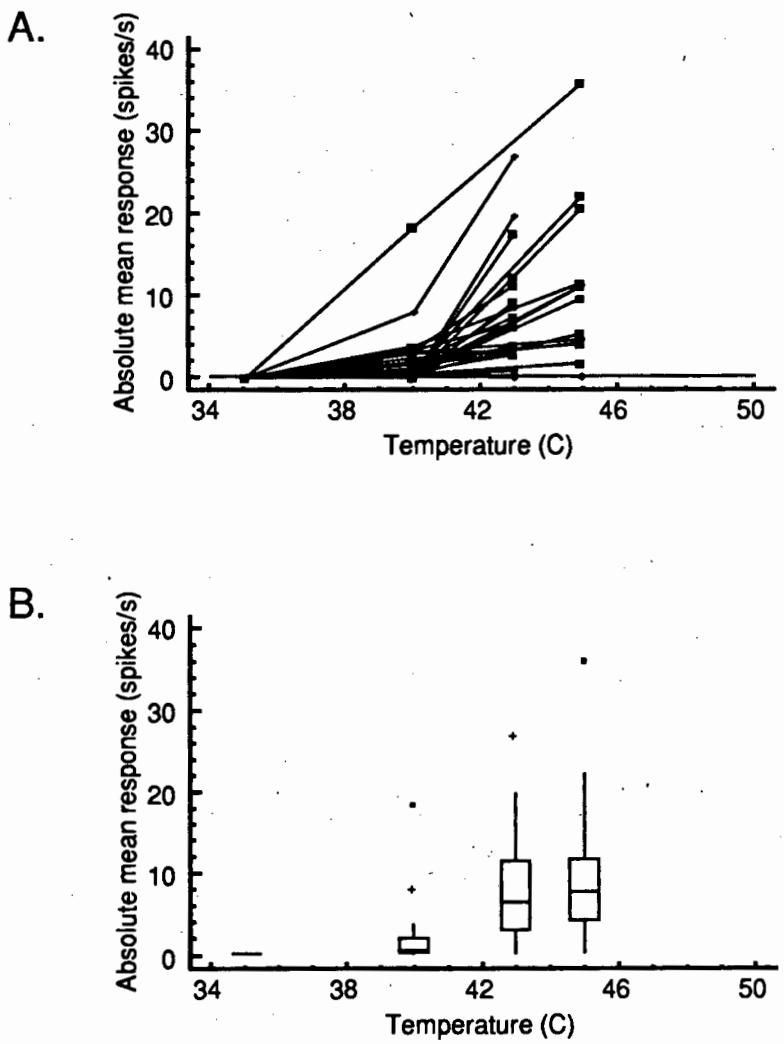

FIGURE 4.20 Intensity-response relationships of PMRF neurones: double step series (35-40-43/45°C). A: The average number of spikes from the onset of the step to the end of each temperature plateau is plotted for each neurone against the intensity of these stimuli. At least two neurones in this sample showed strong linear or accelerating response functions to these stimuli. B: Box-and-whisker plot summarizing the distribution of magnitude responses to each temperature. The responses to innocuous (35/40°C) and noxious (43/45°C) temperatures were significantly different (Post-ANOVA multiple range test, $p<0,05$; see Table 4.2).

TABLE 4.2 Post-ANOVA multiple range analysis of intensity-response functions of PMRF neurones to cutaneous thermal step stimuli (double step series).

Temperature (°C)	Count	Average response	Homogeneous Groups
35	33	0,00	*
40	33	1,77	*
43	19	7,58	*
45	14	10,28	*

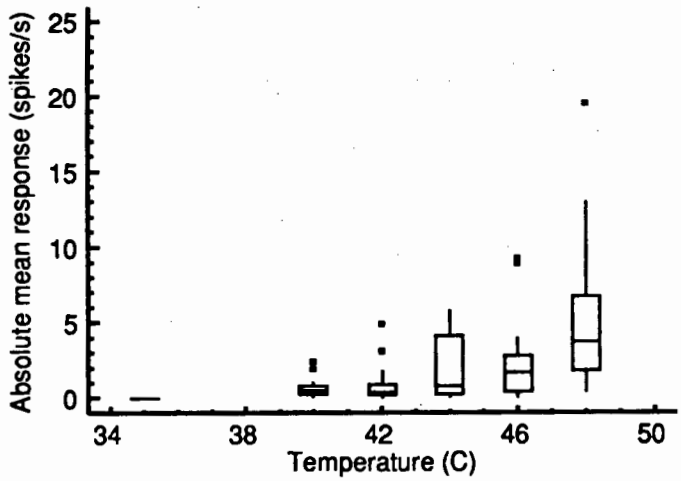

FIGURE 4.21 Intensity-response relationships of PMRF neurones: single step series (40, 42, 44, 46 and 48℃). The box-and-whisker plot summarizes the distribution of magnitude responses to each temperature. Only the responses to 48℃ were significantly different from the other temperatures (Post-ANOVA multiple range test, p<0,05; see Table 4.3).

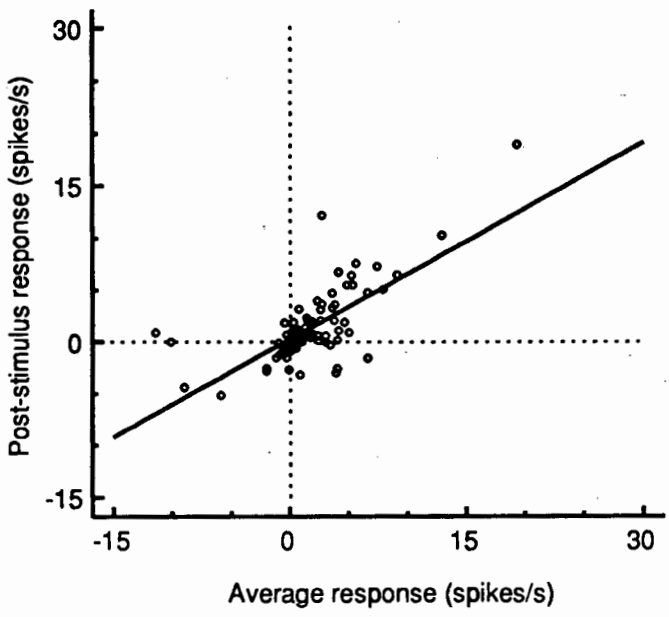

FIGURE 4.22 Correlation between the response and post-stimulus response in 23 PMRF neurones (single step series). There was a significant positive correlation between these two parameters (r=0,72, 108 d.f., p<0,0001). The slope of the regression was 0,63. Incorporation of the post-stimulus response as a covariate in the analysis of the stimulus-response data marginally increased the resolution of temperature discrimination by these cells (Table 4.3).

TABLE 4.3 Post-ANOVA multiple range analysis of intensity-response functions of PMRF neurones to cutaneous thermal step stimuli (single step series), excluding and including the post-stimulus response.

Temperature (°C)	Count	Average response (spikes/s)	Homogeneous Groups (excl. post-stim.)	Homogeneous groups (incl. post-stim.)
40	17	0,64	*	*
42	23	0,86	*	* *
44	23	1,88	*	* *
46	21	2,21	*	*
48	20	4,97	*	*

4.3.3.2 Time course of response

The responses to step stimuli all had substantial latencies to the onset of the stimulus. The latencies of all cells challenged with ascending thermal step stimuli are shown in Figures 4.23 and 4.24. The median latency of the pooled population of cells to all heating stimuli was 4 s (range 0 to 50 s).

After the latent period, 70% of PMRF neurones exhibited a rapid change in firing rate, which slowed to a plateau (Figures 4.16B and C). The remaining cells (30%) attained a peak (or minimum) discharge rate followed by adaptation at a new static firing rate (Figures 4.16A and 4.17A).

Removal of the stimulus (or its reduction in the descending step series), usually resulted in a diminution of the response. This began after a short latent period (mode 1-2 s, range 0-35 s). The latency to removal (or reduction) of the stimulus is significantly shorter than the latency to the onset of the stimulus (Mann-Whitney U-test: ascending steps, n_1=25, n_2=21, Z=2,30, p=0,022; descending steps, n_1=23, n_2=17, Z=2,68, p=0,007; single steps, n_1=47, n_2=41, Z=7,21, p<0,0001).

The firing rate of 6 neurones in double step series behaved anomalously to the removal of the stimulus during the first 60 s of recovery. In 2 of these cells, the response was exaggerated (the difference in firing rate from baseline increased further), while in 4 cells the firing rate remained unchanged during the post-stimulus observation period.

In those cells which showed an immediate response-decay on removal of the stimulus, the return towards baseline was generally more rapid in the early part of the observation period than later on. The average decay of the response was slower than the onset of the

response during heating of the skin: over 60% of the cells had not returned to baseline by the end of the 30 or 60 s post-stimulus period, whereas they had all reached the maximum observed response within the 30 or 60 s stimulus period. Few cells (8 of 56, 14%) overshot the baseline within the post-stimulus observation period (30 or 60 s).

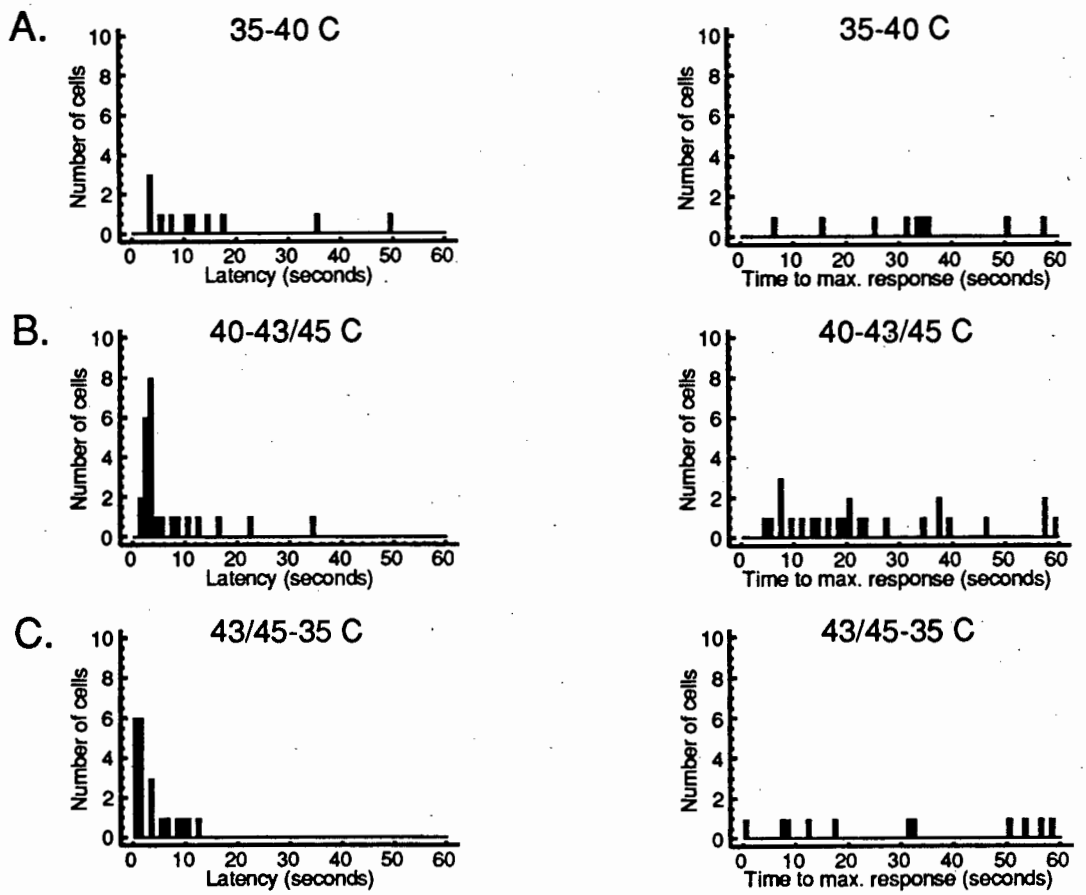

FIGURE 4.23 Latency to onset of response (left) and time to maximum response (right) in the ascending double step series. The latencies to heating (A and B) are significantly longer than those to removal of the stimulus (C; p=0,022).

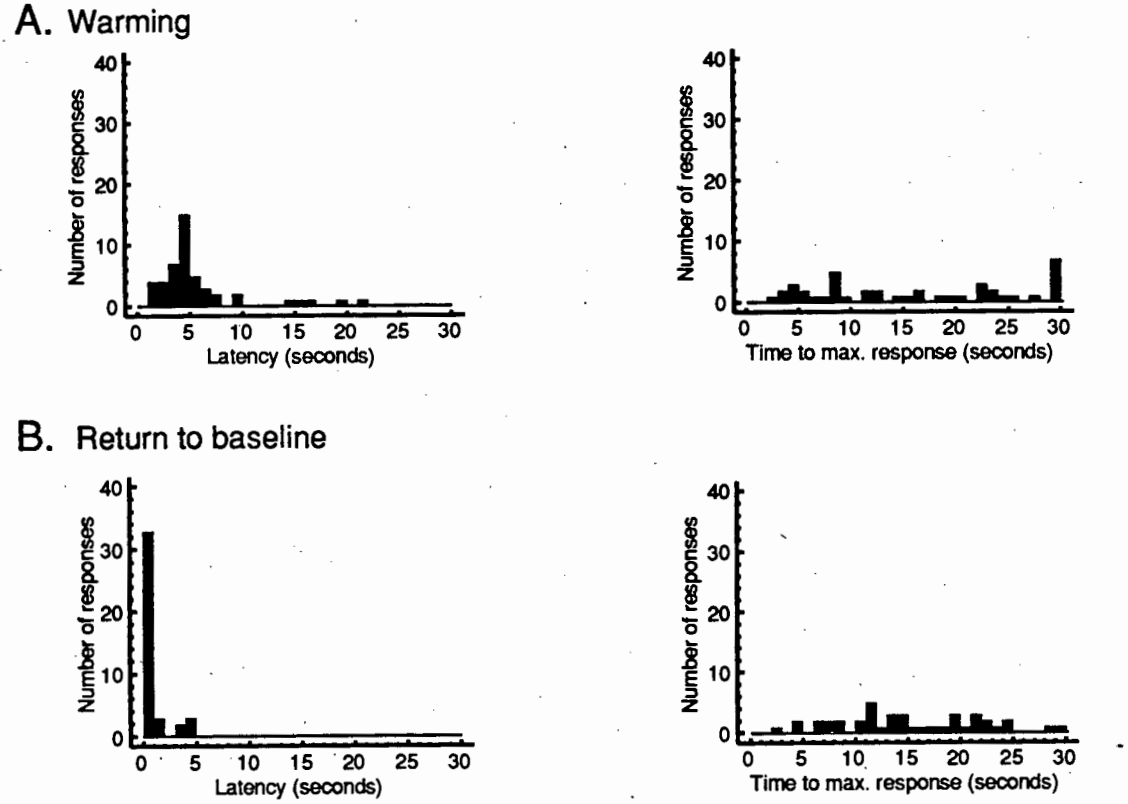

FIGURE 4.24 Latency to onset of response (left) and time to maximum response (responses) of all single step thermal stimuli. The mode of the latencies to warming occurred at 4 s, while that to removal of the stimulus occurred within 1 s ($p<0,0001$).

4.3.4 RESPONSES TO LOW FREQUENCY SINE WAVE THERMAL STIMULI

Twenty-six PMRF cells were driven by sine wave thermal stimuli to the ipsilateral hindpaw. The amplitude of all the sine wave stimuli was 9°C (36-45°C peak-to-peak). Three wavelengths were used: 50, 100 and 200 s (0,02, 0,01 and 0,005 Hz). All of the cells were tested with the 50 s wavelength, while 7 cells were also tested with the longer wavelengths.

Eighty-five percent of PMRF neurones (22 of 26) responded to the 50 s sine wave stimulus. Of the 22 responsive neurones, 16 (73%) increased their action potential discharge rates during the warming phase of the sine wave (ON-t), and 6 (27%) were inhibited during the warming phase (OFF-t). No cells exhibited a non-oscillatory change in firing rate to the sine wave stimulus. Representative responses of PMRF neurones to sine wave thermal stimuli are shown in Figure 4.25A.

All of the individual responses to the 50 s sine wave exhibited a saw-toothed pattern of discharge. The upstroke of the ON-t cells was always steeper than the return phase. The onset of the response (beginning of the upstroke) occurred, on average, at 42,1 °C (±1,8, SD), representing a "phase shift" of +2,11 (±0,62, SD) radians with respect to the stimulus. The downstroke of the response in ON-t cells was more gradual than the upstroke. The downstroke started at 44,0 °C (±1,0, SD), representing a "phase shift" of +0,37 (±0,34, SD) radians, and generally returned to baseline only just before the beginning of the next upstroke. The upstroke therefore lasted, on average, 1,40 radians, and the downstroke 4,88 radians.

The OFF-t cells showed very similar patterns to the ON-t cells, except that the response curves were inverted (Figure 4.25B).

Two cells showed changing maximum and/or minimum discharge rates to successive cycles of the sine wave (see Figure 4.25C). This response pattern was reproducible in each cell.

The peak-to-peak amplitude of the responses to sine wave thermal stimuli varied between 5,2 spikes/s and 40 spikes/s. The average response amplitude of the ON-t cells was 15,2 spikes/s (±8,4, SD), while that of the OFF-t cells was 18,3 spikes/s (±9,8, SD). The average minimum and maximum discharge rates of all responsive neurones, as well as the phase at which the maxima and minima occurred, are shown in Figure 4.26.

The 7 cells which were challenged with the 50, 100, and 200 s wavelength stimuli, exhibited the same response polarity to each stimulus. The maximum and minimum discharge rates, as well as the phase relationships to the stimulus, were unaffected by the stimulus wavelength (Figure 4.27).

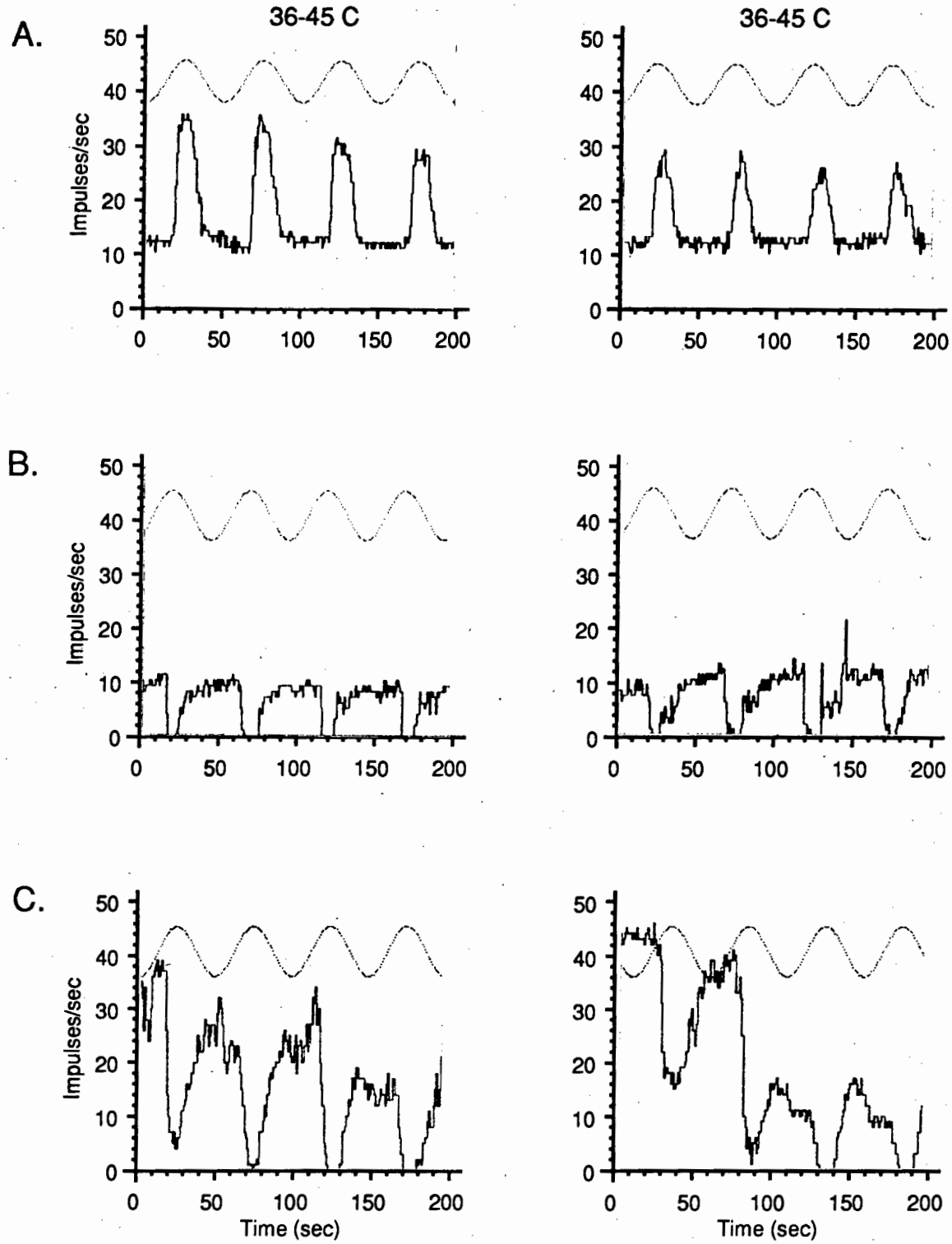

FIGURE 4.25 Representative responses of PMRF neurones to sine wave thermal stimuli (50 s wavelength). A: Neurone responding with increased discharge rates during the warming phase of the sine wave, and decaying to a steady background discharge between responses (ON-t cell). This particular neurone showed a small decrease in the maximum response to successive stimuli. B: Neurone exhibiting decreased firing rates during the warming phase of the sine wave (OFF-t cell). The discharge returned to a steady background rate during the cooling phase, although some sign of breakthrough excitation started appearing towards the end of the second observation period (right). C: OFF-t cell showing decay of background discharge with successive sine wave thermal stimuli. The spontaneous rate returned to its original level between the two periods of stimulation (approximately 10 minutes). A similar pattern occurred in the second observation period.

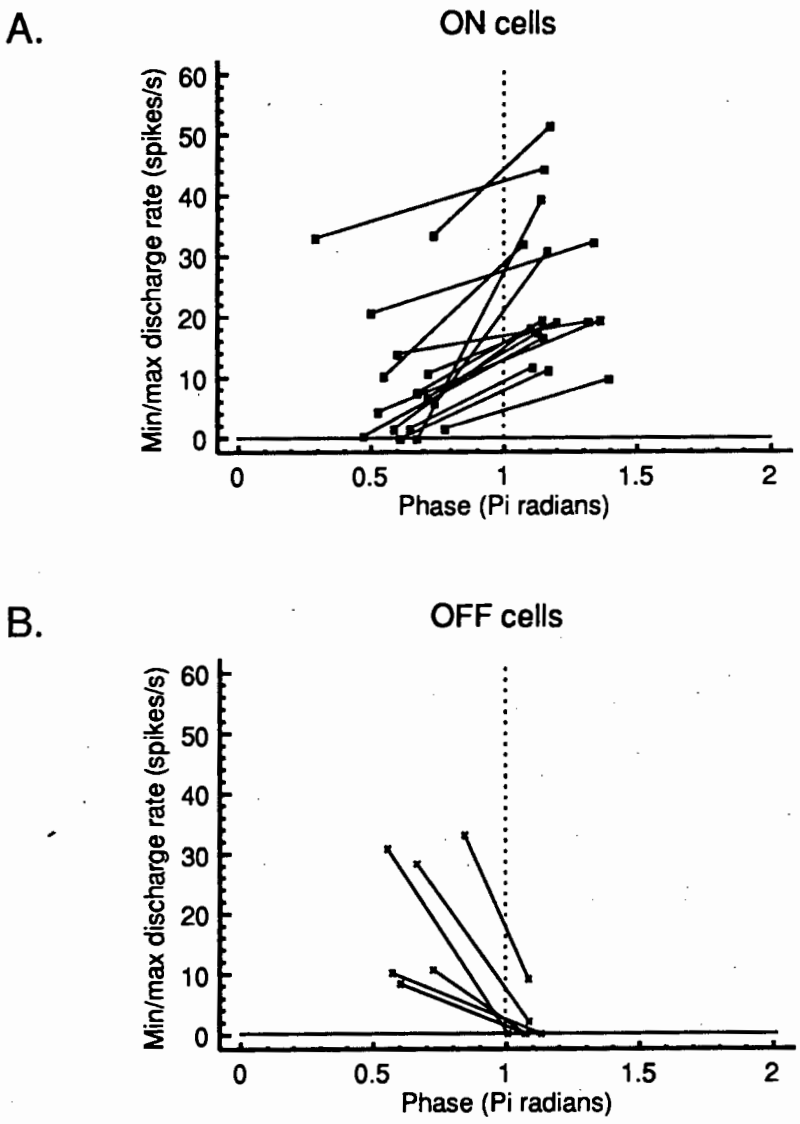

FIGURE 4.26 Average minimum and maximum discharge rates and phase relationships of responses to sine wave thermal stimuli (λ=50 s).

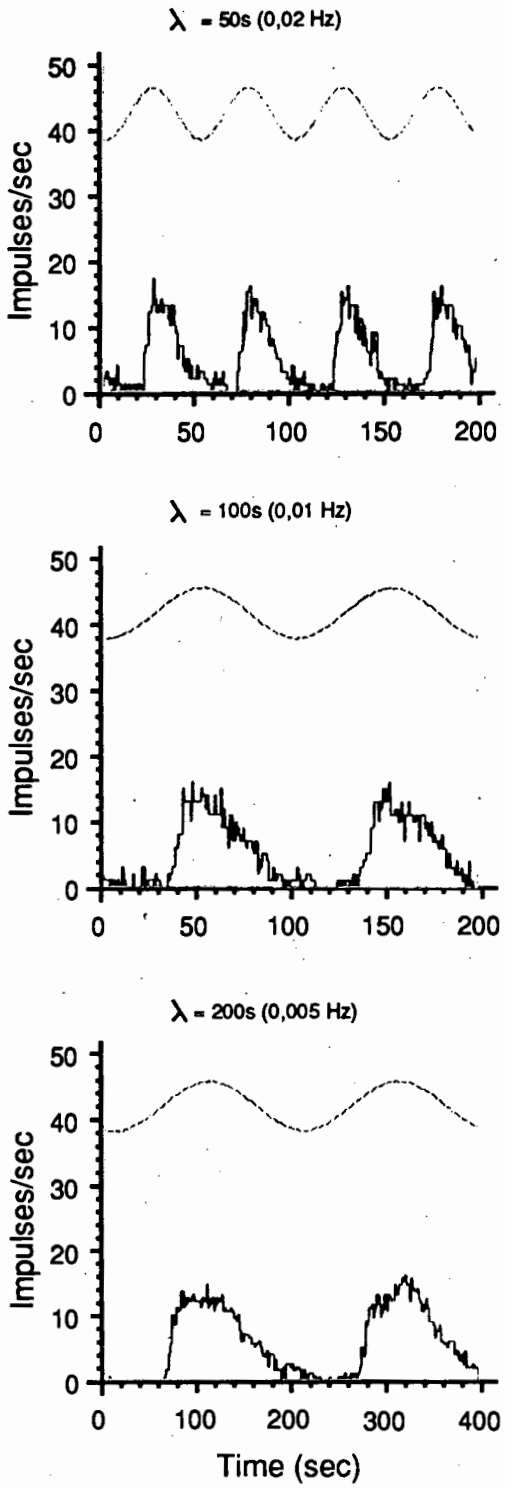

FIGURE 4.27 Representative PMRF neuronal response to increasing wavelength thermal stimuli (λ=50, 100 and 200 s). The stimulus wavelength had no effect on the size and shape of the response.

4.4 DISCUSSION

4.4.1 GENERAL

The results show that the great majority (86%) of mechanosensitive PMRF neurones are also responsive to cutaneous thermal stimuli. Approximately 80% of thermoresponsive neurones were excited by skin heating (ON-t cells). The remainder decreased their discharge rates in response to cutaneous heat stimuli (OFF-t cells). Their response thresholds were in both the warm range (less than 42°C) and in the noxious range (greater than 42°C), strongly suggesting that the polymodality of PMRF neurones includes the sense of pain.

The responses to repeated stimuli applied either to the ipsi- or to the contralateral hindpaw, correlated one with the other, with respect to both polarity and response magnitude.

Despite their lack of ability to discriminate between stimuli of different modalities or in different locations, many PMRF neurones appear capable of tracking the intensity of thermal stimuli to some extent. Some cells tracked the rate of change of stimulus, some followed the absolute stimulus intensity, and others appeared to do both.

4.4.2 REPRODUCIBILITY OF RESULTS

4.4.2.1 Reproducibility in the same cell

The Peltier thermal stimulator could be actively cooled, allowing repeated stimulation without removal of the device between stimuli. In more than 98% of cells examined in this way, a qualitatively identical response was obtained: the pattern and polarity of the responses were highly reproducible. On average, the magnitudes of the response tended to be the same during both trials: the slope of the correlation between first and second single step trials was 1,07, although there was individual variability of the mean firing rates between trials (r=0,80; Section 4.3.3.1). The responses to the sine wave stimuli were similarly reproducible (Section 4.3.4).

The few cells which were exceptions to the rule, all exhibited changes in their baseline discharge rates between successive stimuli (Figure 4.25). When changes in baseline discharge rate occurred in the variable gradient experiments, they were also associated with substantial changes in the response patterns (Figure 4.13C).

In the slow ramp experiments, the stimulator was removed from the stimulation site between successive stimuli. Identical results were obtained whether the stimulator was re-attached to the same site or to the contralateral hindpaw. The response magnitudes to successive stimuli were highly correlated one with the other, all having r-values in excess of 0,81 (Figures 4.9 and 4.12). The only measure that was not repeatable, either on the ipsilateral or contralateral limb, was the threshold temperature (Figures 4.9 and 4.11).

In a separate study (Francis, 1987), the responses of PMRF cells to thermal stimulation of glabrous skin on the hindpaw and hairy skin on the abdomen were also highly correlated with respect to polarity and response magnitude. The threshold temperatures to stimulation of the two skin types were, again, poorly correlated.

This study has therefore shown, for the first time, that the great majority of PMRF neurones respond in a highly stereotypic manner to repeated cutaneous thermal stimuli, at least in the short term (up to 60 minutes). This stereotypy of response occurred over very large receptive fields extending across the midline and incorporating at least the hindpaws and part of the trunk. Furthermore, the responses did not vary as a function of skin type.

This stereotypy could be due to the precision with which the stimulus was delivered by means of the thermal pad, even when the pad had to be removed and re-attached. On the other hand, these cells might always respond in exactly the same manner, irrespective of where or how a suprathreshold stimulus is applied. Individual cells were never challenged with stimuli of completely different waveform (for example, step and sine waves). However, they were subjected to different intensities of the same waveform. This included differences in rate of change of stimulus, as well as differences in stimulus magnitude. The results showed that PMRF cells exhibit at least some measure of stimulus coding (Section 4.4.3.4). I therefore ascribe the reproducibility of my results largely to the degree to which the PMRF (and the neural system in which it is embedded) could be controlled via the thermal pad. This, however, does not imply that the configuration of afferent input to the spinal cord was as precisely controlled as was the

pad temperature. Indeed, when the pad is removed and re-applied, it is unlikely that the number, type and degree of stimulation of the receptors remains constant. This is particularly likely to be true when the pad is moved from the paw to the abdomen (Francis, 1987), as the densities of touch, temperature and pain receptors differ markedly in different regions of the body (Hensel, 1974, 1981; Darian-Smith, 1984; Mountcastle, 1984; Perl, 1984)).

These results are clearly specific to the present experimental parameters. The animals were all anaesthetized with urethane, and changes in extraneous stimulation were kept to a minimum. No cell was studied repeatedly on different days, or in different behavioural states.

4.4.2.2 Inter-cell variability of results

The stereotypy of individual cells does not extend to inter-cell response types. Very few cells shared identical responses to a given stimulus type. The similarities between cells were largely confined to their polymodality (76% correspondence), and to a lesser extent their polarity of response (68% correspondence). Their magnitudes of response and threshold temperatures showed very little cross-neurone correspondence. Generally, the pattern of response could be classified into two or more categories.

The inter-cell variability of thermal responses of PMRF neurones may be due to differential sensitivity of individual units to cutaneous thermal stimulation, to inter-animal variability, or to the inevitable differences in environmental conditions during different experiments. The latter include local factors (thermal conductivity of the skin, intensity and amount of previous stimulation, including habituation and microtrauma), stimulus-dependent factors (pressure of the thermal pad on the skin, area of application, and the tactile stimuli produced by the adhesive tape used to affix the pad to the stimulation site), or general factors (hypercapnia of the urethane anaesthetic, hour and date of measurement, and simultaneous stimuli, such as auditory and postural sensations or pain from the surgical wound).

The noise from these extraneous variables was kept to a minimum by using the same anaesthetic (urethane), in the same dose (1,25 g/kg body mass), only in adult, virgin, female, Long-Evans rats weighing 280 to 350 g. All animals had free access to food and water up to the time of the anaesthetic. All surgical procedures were performed in the early morning, and the experiments carried out during the subsequent 7-8 hours. No

experiments were carried out at night, when these animals are naturally most active. The body temperature was monitored, and maintained at 37,5 ± 0,5°C by means of a thermal mattress. All the rats lay on their abdomens, in as quiet an environment as possible. Their eyes were invariably closed during the entire experiment. The adapting temperature of the stimulus pad was always 35°C. Using thermal stimulation made it possible to deliver identical stimuli from one experiment to the next, even over periods of days or months.

4.4.2.3 Variability in threshold determination

The most variable of all the response parameters was the threshold temperature. There was no correlation between the threshold temperatures to repeated ipsilateral stimulation (r=0,05), or between the thresholds to ipsi- and contralateral stimuli (r=0,39: Sections 4.3.2.4 and 4.3.2.5).

The major sources of error in the estimation of the thermal thresholds of PMRF neurones are presumably due to differences between the temperature of the stimulator surface and the effective temperature at the receptors. It is not practical to quantify the thermal resistive-capacitative properties of the stimulator-skin-receptor complex. However, for thermal stimuli greater than the normal skin temperature (approximately 31°C), the series resistive elements between the stimulator and the cutaneous thermal receptors would cause the stimulator to be at a higher temperature than the receptors. This would result in the measured threshold being an overestimate of the effective receptor temperature.

The temperature lag due to thermal equilibration effects is also expected to contribute to overestimation of the thresholds. The time constant for this equilibration in the footpad of the cat is about 1 s (Beck et al., 1974). Thus, for the slow ramp stimuli, which had a positive ramp of approximately 0,15°C/s, the PMRF thresholds are likely to have been overestimated by a temperature difference attributable to a latency of about 3 time-constants. Thus, the error from this source might be in the order of 0,45°C. However, variations in the skin conductivity through factors such as dryness of the epidermis or its compression by the thermal stimulator, would introduce further unquantifiable variability of the threshold.

Both sources of error contribute to an overestimation of the thresholds. The distribution of thresholds to slow temperature ramps (Figure 4.3) is therefore expected to be

displaced towards higher temperatures than the effective value at the receptors. However, from an operational point of view it is the surface temperature of an object (or stimulus) which is relevant to the evaluation of an animal's behaviour. Therefore, either the stimulator temperature or the skin surface temperature is the appropriate measure for evaluating PMRF responses. The slow rise time of the ramp (0,15°C/s) during threshold estimations, the high thermal conductivity of the aluminium stimulator and the capacity of the heat source suggest that the temperature of the stimulator surface was a good estimate of the temperature of the surface of the skin under the stimulator. This was confirmed by interposing a reference thermocouple between the skin and the thermal stimulator probe. The reference thermocouple tracked the stimulator temperature exactly.

The low correlation between thresholds to repeated stimuli might not be due to experimental error, but could be an expression of the fundamental physiology of PMRF cells. This possibility is explored below (Section 4.4.3.2).

4.4.3 PHYSIOLOGICAL VARIABILITY OF THE THERMAL RESPONSES OF PMRF NEURONES

4.4.3.1 Polymodality of the PMRF responses

Only 14% of the mechanosensitive PMRF neurones observed in this study were unaffected by the thermal stimuli employed. It is possible that even these neurones were responsive to skin heating, but not adequately stimulated in these experiments. The thresholds of these neurones might have been above the maximum stimulus temperature of 48°C. Temperatures higher than 48°C tend to cause tissue damage, and would therefore have limited the number of repeated stimuli that could be applied to a given animal. Alternatively, the thermal receptive fields of these cells might have excluded the hindpaws.

The extensive thermal responsiveness of PMRF neurones reported here contrasts with the findings of Casey (1969) who was unable to elicit thermal responses from cat medial bulboreticular units with radiant heating of the skin to 50-60°C. On the other hand, thermoresponsive neurones have been detected in midline medullary neurones (Young and Dawson, 1987), and in regions of the brainstem more caudal (Burton, 1968) and

more rostral (Eickhoff et al., 1978) to that investigated in the present study, in rodents and carnivores. The thermal response characteristics of each of those groups of neurones differed considerably from the characteristics of the PMRF neurones reported here. Young and Dawson (1987) studied the responses of rat medial medullary neurones to changes in total-body-surface temperature. These neurones were located in a region extending beyond the reported boundaries of serotonergic neurones constituting the raphe nuclei. Twenty-five percent of these neurones were warm responsive, showing increased activity between 20 and 40°C, with their maximum static discharge rates occurring at 35°C. These neurones were inhibited by temperatures of 45°C, as well as by noxious tail squeezing. A further 20% of Young and Dawson's sample were cold responsive, exhibiting a bell-shaped response curve below 30°C with maximum discharge at 5°C. The cold responsive neurones were excited by noxious tail pinch stimuli. Burton (1968) reported that approximately 65% of units in cat bulbar reticular formation which responded to noxious mechanical stimuli applied to the facial region, also responded to noxious thermal stimuli (thresholds 43 to 62°C). None of these units responded to innocuous thermal stimuli. Eickhoff et al. (1978) studied units in the medial mesencephalon and rostral pons of rats that responded to innocuous and/or noxious mechanical stimulation. About half of those also responded only to noxious levels of radiant heat (thresholds greater than 42°C).

These reports all contrast with the high percentage of thermal responsiveness and the wider range of thresholds (36 to 48°C, Figure 4.3) observed in the PMRF in this study. These differences may be a reflection of the different anatomical, and therefore functional, distributions of these neuronal populations. The PMRF cells of the current study have never previously been tested for thermal responsiveness. Alternatively, the observed differences between my results and those of previous studies of reticular formation cells may be due, at least partially, to differences in experimental design. Radiant heat, for instance, is likely to be perceived as a pure (unimodal) stimulus if the skin is not heated to temperatures above approximately 42°C. Above the pain threshold, however, radiant heat presumably becomes a mixed (multimodal) stimulus. All heat stimuli in this study were unavoidably multimodal, even in the neutral to warm temperature range, since a contact thermal stimulator was used. The difference in the proportion of responsive neurones between this study and those of Burton (1968) and Eickhoff et al. (1978) might therefore be due to differences in the combination of stimulus modalities. If this interpretation is correct, then this suggests that PMRF cells respond

primarily to the multimodal nature of a stimulus, rather than simply responding to the temperature component of the stimulus.

There was a high correspondence between the response polarity to mechanical stimuli and the subsequent response to thermal stimulation (Table 4.1). Eighty-two percent of neurones excited by mechanical stimulation were also excited by heating the skin; 76% of neurones inhibited by mechanical inputs were similarly inhibited by increases in cutaneous temperature. The design of the study meant that cells which did not respond to mechanical stimulation were not systematically tested for thermal sensitivity, hence it cannot be asserted that non-reactivity to one modality tends to be carried over to another sensory modality.

In early experiments, the cutaneous thermal sensitivity was tested in 10 PMRF neurones that were unresponsive to mechanical stimuli (Table 4.1). Two of these neurones did not respond to thermal ramp stimuli. Of the remainder, 7 were excited and 1 inhibited by skin heating. The thermal responses of this very small sample of mechanically insensitive neurones are thus qualitatively similar to those of the remainder of the PMRF sample. These figures do not accurately indicate the probability of encountering exclusively temperature sensitive neurones in this region of the brain however. As explained above, the present study is biased towards mechanosensitive PMRF neurones. In addition, these mechanically insensitive neurones were not exhaustively tested for convergence of other sensory modalities. Thus, it is conceivable that a population of exclusively thermoresponsive neurones exists in the PMRF. However, this is unlikely since very few such cells have been found anywhere in the central nervous system. Most reports of temperature-related activity in the spinal cord (Wall, 1960; Price and Browe, 1973; Iggo, 1974; Zimmermann and Handwerker, 1974; Burton, 1975; Price et al., 1978; Surmeier et al., 1988), brainstem (Rowe and Sessle, 1972; Oliveras et al., 1989), thalamus (Martin and Manning, 1971; Chung et al, 1986) and cortex (Kriesman and Zimmermann, 1973) have shown a predominance of neurones with temperature sensitivity plus tactile sensitivity. Unimodal thermal activation of central neurones has generally been limited to oral, perioral (Polous and Benjamin, 1968), and scrotal regions (Hellon and Misra, 1973a, 1973b; Hellon et al., 1973).

4.4.3.2 Bimodal distribution of threshold responses

Despite the poor reproducibility of the threshold responses of PMRF neurones (Section 4.4.2.3), the distribution of the thresholds of these neurones to slow ramp thermal stimuli

was consistently bimodal, pertaining to the data obtained from repeated ipsilateral stimulation (Figure 4.3) and from ipsi- versus contralateral stimulation (Figure 4.11). The bimodality persisted even when all the threshold data were pooled (Figure 4.28A). This suggests that when a given cell was driven from a slightly different receptive field (the stimulator having been removed and re-attached, either to the same or to the opposite hindpaw), its threshold either remained almost unchanged, or exhibited a quantum change corresponding to the difference between the innocuous and noxious temperatures. Indeed, when the absolute differences in threshold temperatures from two experiments on the same cell are plotted as in Figure 4.28B, there is a suggestion of 2, or possibly 3 peaks, at 0-1℃, 3-4℃ and at 7-8℃. The peak at 3-4℃ corresponds exactly to the difference between the peaks of the bimodal threshold distributions (Figures 4.3, 4.11 and 4.28A). Those cells with very large changes in threshold (7-8℃) are enigmatic. These latter cells had thresholds (at about 36℃ and 45℃) at the extremes of the range in successive tests.

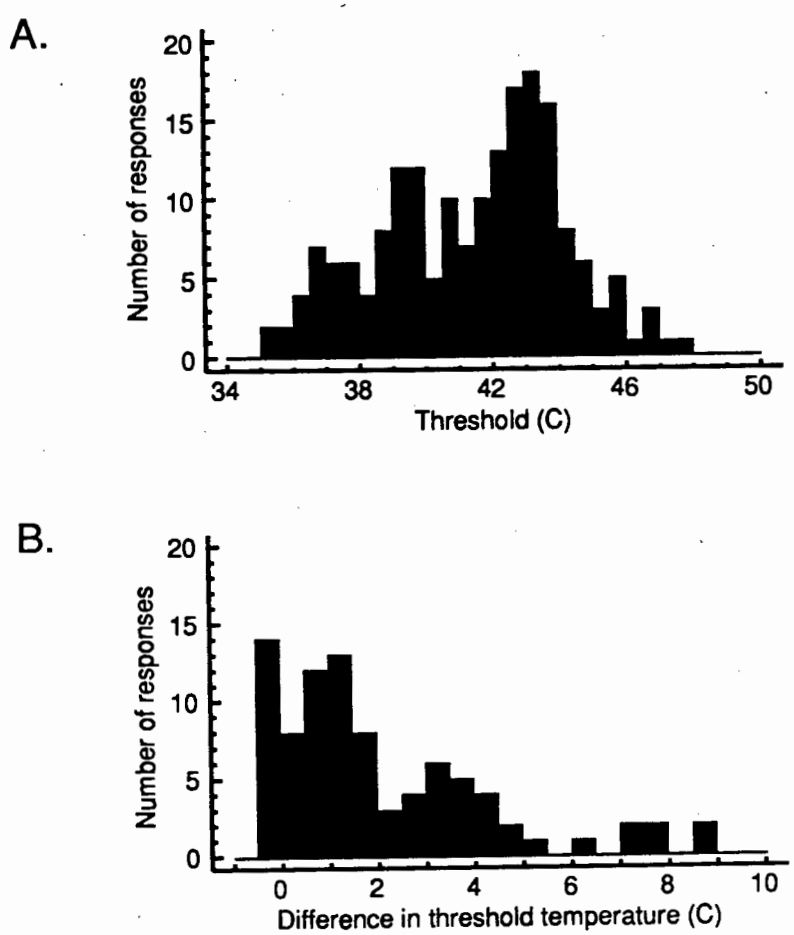

FIGURE 4.28 A: Distribution of pooled thresholds from all ipsilateral and contralateral thermal ramp stimuli. B: Absolute differences in threshold temperatures between successive ipsilateral or ipsi- versus contralateral thermal ramps. The two major peaks occur at 0-1℃ and 3-4℃.

Since the peaks of the threshold distributions of PMRF neurones occur at around 39°C and 43°C, which conform to the maximum discharge ranges for warm and noxious cutaneous thermoreceptors respectively (Iggo, 1969; LaMotte and Campbell, 1978), it is likely that the thermal input to individual PMRF cells is derived from both types of receptors. While the output of some of these cells is probably determined by both inputs together, others appear capable of switching emphasis, as evident in Figure 4.28B. Thus, in addition to responding to mechanical and thermal stimulation, PMRF neurones appear to receive input from the different types of thermal receptors. More importantly, however, these cells appear capable of selective suppression of some of these multiple inputs.

Switching behaviour was also seen in the spontaneous discharge rates of PMRF cells (Figures 4.8B, 4.13C and 4.17C), which was sometimes accompanied by a switch from an excitatory to an inhibitory response, or vice versa, to identical thermal stimuli (Figures 4.8B and 4.17B).

The source of the switching behaviour of PMRF neurones is not known. The switch could be determined by factors intrinsic to individual PMRF cells, or could be driven by extrinsic factors. Both the intrinsic and extrinsic factors could be influenced by cyclical changes in responsiveness, related possibly to the time of day. On the other hand, switching might occur as a result of a change in the total sensory input either to the individual cell, or to the sensorium as a whole.

4.4.3.3 Intensity coding by PMRF neurones

Individual PMRF neurones appear to encode the intensity of cutaneous thermal stimuli by increasing or decreasing their activity. Thus, individual neurones showed increased or decreased discharge rates in relation to the stimulus temperature (Figures 4.20 and 4.21). Furthermore, PMRF neurones responded to repeated stimuli with approximately the same magnitude of change in their discharge rates (Figures 4.9 and 4.12). However, the magnitude response of the majority of these neurones was small (see Figures 4.5, 4.9, 4.12, 4.14, 4.20, 4.21 and 4.26)

Approximately 10% of thermoresponsive neurones cells did not show intensity coding of the driving stimulus. These cells showed very weak responses to warm stimuli, and did not distinguish innocuous from noxious input. All of the remaining responsive cells

exhibited a greater absolute change in discharge rate in response to the higher temperatures.

Maximal activity would presumably have reached an asymptote at higher temperatures, but these were avoided to prevent irreversible skin damage. While responses occurred in many neurones following innocuous temperatures (range 36-42°C), the steepest portions of the response function appeared above 42°C. Linear and accelerating response functions were observed. These responses were all repeatable for individual neurones.

Large changes in firing rate are not necessarily modality specific. For example, polymodal neurones in the spinothalamic system fire at extremely high levels (maximum 300 Hz) both to noxious thermal stimulation, and to repetitive innocuous stimulation of the same area (Price, 1986). Thus, stimuli do not need to be noxious to produce maximal discharge rates elsewhere in the sensory system. This suggests that what might superficially appear to be intensity coding in the PMRF cells, is something else. Since noxious thermal stimulation was required to produce the highest changes in discharge rate, these cells could simply be responding to the summation of stimulus modalities produced by the increasing skin temperature. Increasing temperature is known to stimulate warm, then hot, then noxious receptors. In addition, there is the possibility that tactile changes occurred with increasing temperature as a result of sweating and alterations in the mechanical properties of keratin.

Whether the change in discharge of PMRF neurones in response to increasing thermal stimulation is due to summation of modalities, or to genuine intensity coding, the generally modest responsiveness of these cells, compared to other thermosensitive neurones in the CNS, remains enigmatic. If these cells are primarily responsive to the combination of sensory modalities, then greater changes in firing rate than those observed here might be expected if the animal were subjected to a larger number of simultaneous stimuli. No information to confirm or reject this assertion is currently available.

If PMRF cells encode the intensity of individual stimuli, then their resolution, based on their average and maximum responses, seems surprisingly poor. Thus, while most PMRF neurones are able to distinguish innocuous from noxious stimuli, few appear capable of clearly encoding stimulus intensity within the noxious range (above 43°C). A few neurones exhibited powerful accelerating functions, and may therefore be involved

in sensory-discriminative aspects of nociception. However, linear or monotonic stimulus-response relationships do not imply that the PMRF is necessarily involved in this aspect of pain. Neurones in the PMRF possess very extensive cutaneous receptive fields and heterosensory inputs, and are therefore likely to be involved in other aspects of nociception such as arousal and/or stress responses. Obtaining a monotonic relationship between the heat intensity and neuronal responses does not exclude this possibility.

4.4.3.4 Temporal features of PMRF thermal responses

Although a few PMRF cells responded to cutaneous thermal step stimuli within 1 s, the average latency was 4 s, with some as long as 50 s. This could be due to one or more of the following: poor thermal conductivity of the skin; long loop pathways to the brainstem; slow conduction velocity of input fibres; and/or polysynapsis. Time to reach threshold is probably not a factor, since step stimuli (3°C/s) were used to measure latency.

Poor thermal conductivity of the skin is unlikely to account for latencies of the magnitude observed, since the response to removal of the stimulus often occurred within 360 ms (Figure 4.24B). Furthermore, the 0,4°C oscillations in stimulus temperature during the slow ramp experiments were faithfully tracked and amplified by some PMRF cells (Figures 4.2 and 4.15), which indicates undamped, and therefore exquisite, transmission between the stimulator pad and the cutaneous receptors. On the other hand, both the short latency following stimulus removal and the oscillations of PMRF discharge occurred only at high temperature. It is therefore possible that the conductivity of the skin at high temperature was influenced by autonomic and/or physical effects, while at neutral temperature the conductivity contributed substantially to the long latency.

The conduction velocity of the cat unmyelinated fibres is approximately 0,8 m/s (LaMotte and Campbell, 1978). Thus, it would require a path of at least 3 metres, in an animal not more than 25 cm from nose to tail, to account for a latency of 4 s if thermal impulses were conducted entirely along C-fibres. In fact, thermal information is carried in peripheral nerves along Aδ as well as C-fibres (Darian-Smith, 1980; Sumino and Dubner, 1981; Lynn, 1984; Pertovaara et al., 1984; Spray, 1986).

It would appear, therefore, that polysynapsis is probably the major contributor to the observed long latencies of PMRF neurones. Since the PMRF receives major sensory input direct from the spinal cord (see Chapter 2), much of this polysynapsis is likely to occur within the PMRF itself. This would imply that the PMRF must be involved in considerable processing of sensory information, and that at least some of the cells with the longest latencies in this study were involved in higher order sensory processing. If, on the other hand, these cells were driven by higher centres, then they might merely have been performing output functions.

In addition to the long latencies, the majority of PMRF cells also exhibited slow changes in discharge rate in response to square wave stimuli, before reaching a plateau. Very few cells showed dynamic overshoot with adaptation to sustained stimuli. Furthermore, most PMRF cells showed marked afterdischarge following removal of the stimulus. Thus, the responses of PMRF cells were not merely phase-shifted with respect to the stimulus, or to the presumptive cutaneous receptor response. This implies, therefore, that these cells either received highly processed inputs (via polysynaptic routes), or that they themselves were capable of major transformations of the incoming information. The large variability of the time course of responses of these neurones, which included cells with short latencies and distinct dynamic and static phases, could be due to cells situated on different processing pathways, or occupying different positions within a single processing hierarchy.

The responses to sine wave stimuli show similar patterns. Again, the response was not merely phase-shifted, but exhibited a long latency during the warming phase (which is probably a threshold phenomenon), with a prompt response to the cooling phase of the stimulus (Figure 4.25).

There was little evidence in these experiments of PMRF cells becoming hyper- or de-sensitized to repeated thermal stimuli. This contrasts with the marked hypersensitization of peripheral C fibres and of spinal cord neurones by repeated noxious stimuli, leading to decreased temperature thresholds in C fibres (Bessou and Perl, 1969), and decreased response magnitudes in the spinal cord (Burton, 1975).

The temporal features of PMRF discharge provide evidence that these neurones are not involved in classical sensory discrimination.

4.4.3.5 Spatial features of PMRF thermal response

The thermal receptive fields of the great majority of PMRF neurones were large, incorporating at least both hindlimbs (Figure 4.2) as well as the hairy skin of the abdomen (Francis, 1987). The extensive receptive field sizes of the PMRF neurones provides evidence against them having a role in stimulus location.

The correlation between ipsilateral and contralateral thermal response patterns suggests that there is selective convergence of thermal input on individual PMRF neurones. This convergence could occur at either the spinal or brainstem level. Fields et al. (1970, 1975) reported that although there was considerable spatial and modal convergence of somatosensory input at the level of the spinoreticular neurones, the majority of those neurones received information only from the ipsilateral side of the body (however, see Maunz et al., 1978). The authors did not examine the thermal responses of the spinoreticular neurones. However, if it is supposed that thermal input is likely to be handled in a manner similar to other somatosensory input, then the large fraction of bilateral PMRF thermal receptive fields observed here was probably due to convergence at the PMRF level rather than at the spinal level. The spatial convergence of somatosensory input at the PMRF level is also implied by the bilateral distribution of the spinoreticular projections: about two-thirds of spinoreticular neurones project to the ipsilateral nucleus gigantocellularis, while the remainder project to the contralateral nucleus gigantocellularis (Fields et al., 1975).

The functional significance of spatial and modal convergence on PMRF neurones is not known. The large redundancy in the receptive fields and the lack of anatomical organization of PMRF neurones provides further support for the notion that these cells are unlikely to subserve sensory-discriminative functions (Bowsher, 1976; Casey, 1980). Since a large fraction of the PMRF neurones exhibited abrupt (switch-like) responses to both innocuous and noxious thermal input over a large receptive field, I propose that the PMRF neurones function as stimulus detectors, rather than as fine discriminators of sensory type or location (Farham and Douglas, 1985).

Chapter 5

CONCLUDING DISCUSSION

The electrophysiological data presented in this study show that a given PMRF neurone can be activated by several types of cutaneous input, including weak and nociceptive levels of thermal and mechanical stimuli. The somatic receptive fields of PMRF cells are large, sometimes extending over the entire body surface. Thus, a large proportion of PMRF neurones possess multisensory and multisegmental inputs.

The thresholds of some of the PMRF neurones in this study were very low. These responded to light brushing of the fur or small increments in temperature (less than 1°C above the adapting temperature of 35°C). On the other hand, the great majority of PMRF neurones responded exclusively or preferentially to peripheral noxious thermal stimuli. These high threshold neurones generally exhibited asymptotic discharge patterns (with no dynamic overshoot - i.e. preferentially responded to the static component of the response) and/or marked afterdischarges (i.e. extension of the response beyond the duration of the stimulus). These properties are characteristic of nociceptive coding in the CNS (Price, 1986). However, this does not necessarily mean that nociception is the primary function of PMRF neurones.

Highly convergent neurones such as those found in the PMRF are relatively common in the spinal cord. Here they have been classed as common carriers (Wall, 1960), trigger cells (Melzack and Wall, 1965), wide dynamic range cells (Mendell, 1966), lamina V type (Wall, 1967), class 2 cells (Iggo, 1974), polymodal cells (Zimmermann, 1977), or multireceptive cells (see Brown and Réthelyi, 1981). This cell type is concentrated mainly in spinal cord lamina V (Wall, 1967), which has direct ascending projections to, and descending afferents from, nucleus gigantocellularis in the PMRF (Chapter 2). These convergent neurones in the cord usually have excitatory or inhibitory receptive fields larger than those of specifically nociceptive neurones, but are still compatible with some measure of spatial localization (Willis, 1986). In the spinal cord, noxious stimuli alter the firing rates of the majority of convergent neurones, no matter where the stimulus is applied (LeBars et al., 1986). Similarly, in this study 90% of PMRF neurones responded to

noxious stimuli applied to either hindlimb. Furthermore, 86% exhibited modal convergence from touch-pressure and cutaneous heat stimuli.

The multimodal responsiveness of PMRF neurones is compatible with their anatomical characteristics as described in Chapter 2. First, the input to these cells is derived from a variety of sources including the spinoreticular, spinothalamic and vestibular systems. Second, there is abundant interconnection between PMRF cells, with richly branching collaterals. Finally, most axons of these cells project beyond the boundaries of the PMRF to such structures as the centre median nucleus, locus coeruleus, tectum, periaqueductal gray, cerebellum, and laminae V, VII and VIII in the spinal cord. These spatially distributed, non-topographical but nevertheless highly organized afferent inputs, interconnections and outputs suggest extensive possibilities for integration of somatic and other sensory information by PMRF cells.

The pattern of centrally activated neurones could be a critical factor in distinguishing between different qualities of somatic sensations (Erickson, 1968, 1975). Thus, the PMRF may distinguish between innocuous or noxious, mechanical or thermal stimuli by the different proportions or combinations of low threshold, high threshold and wide range neurones that are activated by each of these modalities. Different somatic sensations may also be represented, at least in part, by different spatial arrangements of centrally activated neurones. Most neurones in the spinal dorsal horn have larger receptive fields than those of the primary afferents (Price, 1986). The receptive fields of PMRF neurones are even larger than those of their ascending afferent inputs, sometimes extending over the entire body surface. In addition, the total number of PMRF neurones activated by noxious heat is considerably larger than that activated by innocuous temperatures (Chapter 4). Thus, it is likely that the total number of activated PMRF neurones may contribute to the discrimination between innocuous and noxious thermal inputs.

Frequency coding is the most elementary and self-evident temporal factor in sensory coding. Some neurones in the dorsal horn and trigeminal nucleus have stimulus intensity-response relationships that closely resemble those of the primary afferents converging on them, showing positively accelerating frequency responses to cutaneous thermal stimuli of 45-51°C (Price et al., 1976; Price and Dubner, 1977). These first- and second-order neuronal responses are also similar to the psychophysical responses to temperature in this range (Price et al., 1976, 1978, 1980, 1983; LaMotte and Campbell, 1978; Hoffman et al. 1981). In contrast, while many PMRF neurones exhibited monotonic

increases (or decreases) in their discharge rates between 43-49°C, their responses are unlike those of ascending afferents or the reported psychophysical responses to these temperatures. In particular, the small magnitude response of the majority of PMRF neurones strongly suggest that these neurones are not participating in classical sensory discrimination.

The majority of PMRF neurones responded to a thermal step stimulus with a slow increase or decrease to a new static discharge rate (temporal summation) which was maintained with little or no adaptation for the duration of the stimulus. Many PMRF neurones also showed marked afterdischarge for periods of up to 5 minutes after removal of the thermal stimulus. While some cells responded with high fidelity to low frequency temperature oscillations above 42°C, small, rapid changes in temperature generally had very little effect on their discharge (personal observations). These temporal features provide further support for the suggestion that PMRF neurones are not suited to sensory-discriminative functions, since their response times to cutaneous thermal stimuli are far too long. These slow responses might be involved in other functions such as second pain, attention selecting mechanisms, arousal and emotional responses. It is unlikely that these very slow responses are related to the withdrawal and other emergency reflexes associated with noxious stimuli. This was not investigated in these anaesthetized animals.

It was suggested in Chapter 4 that PMRF neurones might function as non-specific stimulus detectors, rather than as fine discriminators of sensory type or location. The long, highly variable latencies of these cells suggests that there may be recruitment of these neurones in response to stimuli of long duration. The variation in latencies, according to this view, is then not a function of the physiology of the individual cells, but their rank in the recruitment series. If this is so, then this population of cells would be integrating stimulus severity with respect to time. A mildly noxious stimulus of long duration might therefore be perceived as more painful than an intensely noxious stimulus of very short duration. The assumption being made here is that the perceived stimulus intensity is a function of the number of activated cells.

It is possible that individual PMRF cells are also capable of integrating the severity of noxious stimuli with respect to time. The time to reach the maximum response to step stimuli was exceedingly long (Section 4.3.3.2). Thus, the longer the duration of the stimulus, the greater the change in firing rate of individual neurones, up to 1 minute.

Unlike the population response (recruitment), this rapidly reaches saturation. The maximum latent period recorded was 50 s in a stimulus of 60 s. It is thus possible that the small number of cells that did not respond to these stimuli had latencies exceeding 60 s, and were therefore not unresponsive to cutaneous heat. Assuming that this interpretation is correct, then recruitment provides a greater scope for integration of sensory information with respect to time than do the slow responses of individual cells.

If one of the functions of the population of PMRF cells is to integrate incoming sensory information with respect to time by recruitment of cells, then the responses of individual cells to identical stimuli need not be consistent. Individual cells can be recruited early or late (and thus display variable latencies to the same stimulus) without necessarily disturbing the overall pattern.

There have been a number of studies indicating that "across neurone" population responses may be operative in the spinal cord (Surmeier et al., 1988), thalamus (Chung et al., 1986), olfactory (Haberly, 1985) and gustatory systems (Smith et al., 1983a, 1983b; Maes, 1984; Maes and Erickson, 1984; Faurion, 1987), and others. Faurion (1987) likens this population response of neurones to a screen containing as many lights as there are neurones in a particular population. In one model, each lamp is lit or not depending on whether the neurone it represents is responsive to the applied stimulus or not. The resulting global pattern of lit and unlit spots may be different for each different stimulus, although a great number of individual lamps (neurones) may be common to several patterns. In a second model, the lamps do not represent all-or-none functions, but emit light of variable intensity. Different global patterns in this model emerge from the relative intensities of the light spots, which are nearly all lit in most cases. This is a more useful model than the first, in that it is able to account for the spontaneous activity of PMRF neurones as well as their inhibitory responses. These models thus provide an alternative explanation for the variability in the responses of PMRF neurones to identical cutaneous stimuli, in which the time course of the responses (and therefore their integrative function) are ignored. However, it is still the global pattern of activity that conveys the relevant information.

While the PMRF has the requisite anatomical features for sensory coding by population responses, testing the applicability of such "across-neurone" models to this region has not been done. The PMRF is far removed from the sensory receptors, and has a complex structure that is not easy to analyze. Furthermore, to verify these models, simultaneous

recordings are required from numerous PMRF cells, preferably in conscious animals. Thus, the behaviour of these cells in assemblies remains unknown. Nevertheless, development of such models in parallel with circuit analysis might serve to provide a useful framework for understanding sensory coding by this region. This, in turn, may provide clues about the operation of other "association areas" in the CNS that have strong spatially distributed connections.

The basic assumption throughout this thesis has been that PMRF neurones are performing primarily sensory functions. However, none of the data are incompatible with the view that they form part of the output limb of reflex activity. Thus, they might be involved in the somatic or autonomic responses to sensory stimulation. They could be concerned with arousal and the emotions, or with memory and associative functions. On the other hand, these possibilities do not provide any parsimonious insights into the puzzling variations of PMRF neuronal responses that are such a prominent feature of this study.

REFERENCES

Albe-Fessard, D., Berkley, K. J., Kruger, L., Ralston, H. J., and Willis, W. D. (1985). Diencephalic mechanisms of pain sensation. Brain Res. Rev. 9: 217-296.

Albe-Fessard, D., Levante, A., and Lamour, Y. (1974). Origin of spinothalamic and spinoreticular pathways in cats and monkeys. Adv. Neurol. 4: 157-166.

Amassian, V. E., and DeVito, R. V. (1954). Unit activity in reticular formation and nearby structures. J. Neurophysiol. 17: 575-603.

Ammons, W. S. (1987). Characteristics of spinoreticular and spinothalamic neurons with renal input. J. Neurophysiol. 58: 480-495.

Anderson, K. V., and Pearl, G. S. (1975). Long term increases in nociceptive thresholds following lesions in feline nucleus reticularis gigantocellularis. First World Congress on Pain (IASP) Abstr.

Andrezik, J. A., and Beitz, A. J. (1985). Reticular formation, central gray and related tegmental nuclei. In: G. Paxinos, ed. The rat nervous system. Vol. 2. Hindbrain and spinal cord. Sydney: Academic; pp. 1-28.

Barbaro, N. M., Heinricher, M. M., and Fields, H. L. (1986). Putative pain modulating neurons in the rostral ventral medulla: reflex-related activity predicts effects of morphine. Brain Res. 366: 203-210.

Basbaum, A. I., and Fields, H. L. (1978). Endogenous pain control mechanisms: review and hypothesis. Ann. Neurol. 4: 451-462.

Basbaum, A. I., and Fields, H. L. (1980). Pain control: a new role for the medullary reticular formation. In: J. A. Hobson and M. A. B. Brazier, eds. The reticular formation revisited. Specifying function for a nonspecific system. New York: Raven; pp. 329-348.

Beck, P. W., Handwerker, H. O., and Zimmerman, M. (1974). Nervous outflow from the cat's foot during noxious radiant heat stimulation. Brain Res. 67: 373-386.

Bell, C., Sierra, G., Buendia, N., and Segundo, J. P. (1964). Sensory properties of neurons in the mesencephalic reticular formation. J. Neurophysiol. 27: 961-987.

Benjamin, R. M. (1970). Single neurons in the rat medulla responsive to nociceptive stimulation. Brain Res. 24: 525-529.

Besson, J. M., Catchlove, R. H. F., Feltz, P., and LeBars, D. (1974). Further evidence for postsynaptic inhibition on lamina V dorsal interneurons. Brain Res. 66: 531-536.

Bessou, P., and Perl, E. R. (1969). Response of cutaneous sensory units with unmyelinated fibres to noxious stimuli. J. Neurophysiol. 32: 1025-1043.

Blair, R. W. (1985). Noxious cardiac input onto neurons in medullary reticular formation. Brain Res. 326: 335-346.

Blair, R. W. (1987). Responses of feline medial medullary reticulospinal neurons to cardiac input. J. Neurophysiol. 58: 1149-1167.

Blair, R. W., Ammons, W. S., and Foreman, R. D. (1984). Responses of thoracic spinothalamic and spinoreticular cells to coronary artery occlusion. J. Neurophysiol. 51: 636-648.

Bowker, R. M., Westlund, K. N., and Coulter, J. D. (1982). Organization of descending serotonergic projections to the spinal cord. In: H. G. J. M. Kuypers and G. F. Martin, eds. Progress in brain research: Descending pathways to the spinal cord. New York: Elsevier; pp. 239-265.

Bowsher, D. (1970). Place and modality analysis in caudal reticular formation. J. Physiol. Lond. 209: 473-486.

Bowsher, D. (1976). Role of the reticular formation in responses to noxious stimulation. Pain 2: 361-378.

Bowsher, D., Mallart, A., Petit, D., and Albe-Fessard, D. (1968). A bulbar relay to the centre median. J. Neurophysiol. 31: 288-300.

Brodal, A. (1957). The reticular formation of the brain stem; anatomical aspects and functional correlations. London: Oliver and Boyd.

Brodal, A. (1981). The reticular formation and some related nuclei. In: Neurological anatomy in relation to clinical medicine. 3rd ed. New York: Oxford University Press; pp. 394-447.

Brown, A. G., and Réthelyi, M., eds. (1981). Spinal cord sensation - sensory processing in the dorsal horn. Edinburgh: Scottish Academic.

Burton, H. (1968). Somatic sensory properties of caudal bulbar reticular neurons in the cat (Felis domestica). Brain Res. 11: 357-372.

Burton, H. (1975). Responses of spinal cord neurons to systematic changes in hindlimb skin temperatures in cats and primates. J. Neurophysiol. 38: 1060-1079.

Casey, K. L. (1969). Somatic stimuli, spinal pathways, and size of cutaneous fibres influencing unit activity in the medial medullary reticular formation. Exp. Neurol. 25: 35-56.

Casey, K. L. (1971a). Responses of bulboreticular units to somatic stimuli eliciting escape behavior in the cat. Int. J. Neurosci. 2: 15-28.

Casey, K. L. (1971b). Escape elicited by bulboreticular stimulation in the cat. Int. J. Neurosci. 2: 29-34.

Casey, K. L. (1980). Reticular formation and pain: toward a unifying concept. In: J. J. Bonica, ed. Pain. New York: Raven; pp. 93-105.

Casey, K. L., Keene, J. J., and Morrow, T. J. (1974). Bulboreticular and medial thalamic unit activity in relation to aversive behavior and pain. Adv. Neurol. 4: 197-205.

Chaouch, A., Menétrey, D., Binder, D., and Besson, J. M. (1983). Neurons at the origin of the medial component of the bulbopontine spinoreticular tract in the rat: an anatomical study using horseradish peroxidase retrograde transport. J. Comp. Neurol. 214: 309-320.

Chéry-Croze, S. (1983). Painful sensation induced by a thermal cutaneous stimulus. Pain 17: 109-137.

Christensen, B. N., and Perl, E. R. (1970). Spinal neurons specifically excited by noxious or thermal stimuli: marginal zone of the dorsal horn. J. Neurophysiol. 33: 293-307.

Chung, J. M., Lee, K. H., Surmeier, D. J., Sorkin, L. S., Kim, J., and Willis, W. D. (1986). Response characteristics of neurons in the ventral posterior lateral nucleus of the monkey thalamus. J. Neurophysiol. 56: 370-390.

Cohen, A. M. L., and Henn, V. (1972). Unit activity in the pontine reticular formation associated with eye movement. Brain Res. 46: 403-410.

Cronin, M. J., and Baker, M. A. (1977). Thermosensitive midbrain neurons in the cat. Brain Res. 128: 461-472.

Darian-Smith, I. (1980). Thermoreceptive fibres innervating the palm and fingers: differentiating small changes in skin temperature. Adv. Physiol. Sci. 16: 229-239.

Darian-Smith, I. (1984). Thermal sensibility. In: I. Darian-Smith, ed. Handbook of physiology. Section 1: The nervous system. Volume III. Sensory processes. Bethesda, Md.: American Physiological Society; pp. 879-913.

Douglas, R. J. (1984). The temporal structure of the action potential discharge of the medial pontomedullary reticular formation neurones. PhD. Thesis. University of Cape Town.

Edwards, D. L., Johnston, K. M., Poletti, C. E., and Foote, W. E. (1987). Morphology of pontomedullary raphe and reticular formation neurons in the brainstem of the cat: an intracellular HRP study. J. Comp. Neurol. 256: 257-273.

Eickhoff, R., Handwerker, H. O., McQueen, D. S., and Schick, E. (1978). Noxious and tactile input to medial structures of midbrain and pons in the rat. Pain 5: 99-113.

Erickson, R. P. (1968). Stimulus coding in topographic and non-topographic afferent modalities: on the significance of the activity of individual sensory neurons. Psychol. Rev. 75: 447-465.

Erickson, R. P. (1975). Parallel "population" neural coding in feature extraction. In: G. Werner, ed. Feature extraction by neurons and behavior. Cambridge, Mass.: MIT Press; pp. 155-169.

Farham, C. J., and Douglas, R. J. (1985). The response of neurons of the medial pontomedullary reticular formation of rats to peripheral thermal stimuli. Brain Res. 336: 107-115.

Faurion, A. (1987). Physiology of the sweet taste. In: D. Ottoson, ed. Progress in sensory physiology. Vol. 8. Berlin: Springer-Verlag; pp. 129-201.

Fields, H. L., and Basbaum, A. I. (1989). Endogenous pain control mechanisms. In: P. D. Wall and R. Melzack, eds. Textbook of pain. 2nd ed. Edinburgh: Churchill Livingstone; pp. 206-217.

Fields, H. L., Clanton, C. H., and Anderson, S. D. (1977). Somatosensory properties of spinoreticular neurons in the cat. Brain Res. 120: 49-66.

Fields, H. L., Partridge, L. D., and Winter, D. L. (1970). Somatic and visceral receptive field properties of fibres in the ventral quadrant white matter of the cat spinal cord. J. Neurophysiol. 33: 827-837.

Fields, H. L., Wagner, G. M., and Anderson, S. D. (1975). Some properties of spinal neurons projecting to the medial brainstem reticular formation. Exp. Neurol. 47: 118-134.

Fox, J. E., and Wolstencroft, J. H. (1976). The reduced responsiveness of neurones in nucleus reticularis gigantocellularis following their excitation by peripheral nerve stimulation. J. Physiol. Lond. 258: 687-704.

Francis, P. (1987). A comparative study of the responses of pontomedullary reticular formation neurones to therma stimulation of glabrous and hairy skin. B.Sc. (Hons.) Thesis. University of Cape Town.

Gallager, D. W., and Pert, A. (1978). Afferents to brainstem nuclei (brain stem raphe, nucleus reticularis pontis caudalis and nucleus gigantocellularis) in the rat as demonstrated by microiontophoretically applied horseradish peroxidase. Brain Res. 144: 257-275.

Giesler, G. J., Yezierski, R. P., Gerhart, K. D., and Willis, W. D. (1981). Spinothalamic tract neurons that project to medial and/or lateral thalamic nuclei: evidence for a physiologically novel population of spinal cord neurons. J. Neurophysiol. 46: 1285-1308.

Goldman, P. L., Collins, W. F., Taub, A., and Fitzmartin, J. (1972). Evoked bulbar reticular unit activity following delta fibre stimulation of peripheral somatosensory nerve in cat. Exp. Neurol. 37: 597-606.

Graybiel, A. M. (1977). Direct and indirect preoculomotor pathways of the brainstem: an autoradiographic study of the pontine reticular formation in the cat. J. Comp. Neurol. 175: 37-78.

Grillner, S., and Lund, S. (1968). The origin of a descending pathway with monosynaptic action on flexor motoneurons. Acta. Physiol. Scand. 74: 274-284.

Groves, P. M., Miller, S. W., Parker, M. V., and Rebec, G. V. (1973). Organization by sensory modality in the reticular formation of the rat. Brain Res. 54: 207-224.

Guilbaud, G., Besson, J. M., Oliveras, J. L., and Wyon-Maillard, M. C. (1973). Modifications of the firing rate of bulbar reticular units (nucleus gigantocellularis) after intra-arterial injection of bradykinin into the limbs. Brain Res. 63: 131-140.

Haber, L. H., Martin, R. F., Chatt, A. B., and Willis, W. D. (1978). Effects of stimulation in nucleus reticularis gigantocellularis on the activity of spinothalamic tract neurons in the monkey. Brain Res. 153: 163-168.

Haber, L. H., Martin, R. F., Chung, J. M., and Willis, W. D. (1980). Inhibition and excitation of primate spino-thalamic tract neurons by stimulation in the region of nucleus reticularis gigantocellularis. J. Neurophysiol. 43: 1578-1593.

Haber, L. H., Moore, B. D., and Willis, W. D. (1982). Electrophysiological response properties of spinoreticular neurons in the monkey. J. Comp. Neurol. 207: 75-84.

Haberly, L. B. (1985). Neuronal circuitry in olfactory cortex: Anatomy and functional implications. Chem. Senses 10: 219-238.

Halpern, B. P., and Halverson, J. D. (1974). Modification of escape from noxious stimuli after bulbar reticular formation lesions. Behav. Biol. 11: 215-229.

Hellon, R. F., and Misra, N. K. (1973a). Neurones in the dorsal horn of the rat responding to scrotal skin temperature changes. J. Physiol. Lond. 232: 375-388.

Hellon, R. F., and Misra, N. K. (1973b). Neurones in the ventrobasal complex of the rat thalamus responding to scrotal skin temperature changes. J. Physiol. Lond. 232: 389-399.

Hellon, R. F., Misra, N. K., and Provins, K. A. (1973). Neurones in the somatosensory cortex responding to scrotal skin temperature changes. J. Physiol. Lond. 232: 401-411

Henry, J. L., and Calaresu, F. R. (1974). Excitatory and inhibitory inputs from medullary nuclei projecting to spinal cardioacceleratory neurons in the cat. Exp. Brain Res. 20: 485-504.

Hensel, H. (1974). Thermoreceptors. Ann. Rev. Physiol. 36: 233-249.

Hensel, H. (1981). Thermoreception and temperature regulation. Monographs of the Physiological Society, No. 38. London: Academic.

Hobson, J. A. (1980). Toward a cellular neurophysiology of the reticular formation: Conceptual and methodological milestones. In: J. A. Hobson and M. A. B. Brazier, eds. The reticular formation revisited: Specifying function for a nonspecific system. New York: Raven; pp. 7-29.

Hobson, J. A., and Brazier, M. A. B., eds. (1980). The reticular formation revisited: Specifying function for a nonspecific system. New York: Raven.

Hobson, J. A., McCarley, R. W., Pivik, T., and Freeman, R. (1974). Selective firing by cat pontine brain stem neurones in desynchronized sleep. J. Neurophysiol. 37: 497-511.

Hobson, J. A., and Scheibel, A. B., eds. (1980). The brainstem core: sensorimotor integration and behavioral state control. Neurosci. Res. Prog. Bull. 18: 1-173.

Hobson, J. A., and Steriade, M. (1986). Neuronal basis of behavioral state control. In: F. E. Bloom, ed. Handbook of physiology. Section 1: The nervous system. Volume IV. Intrinsic regulatory systems of the brain. Bethesda, Md.: American Physiological Society; pp. 701-827.

Hoffman, D. S., Dubner, R., Hayes, R. L., and Medlin, T. P. (1981). Neuronal activity in medullary dorsal horn of awake monkeys trained in a thermal discrimination task. 1. Responses to innocuous and noxious thermal stimuli. J. Neurophysiol. 46: 409-427.

Hökfelt, T., Skirboll, L., Dalsgaard, C., Johansson, O., Lundberg, J. M., Norell, G., and Jansco, G. (1982). Peptide neurons in the spinal cord with special reference to descending systems. In: B. Sjölund and A. Björklund, eds. Brainstem control of spinal mechanisms. New York: Elsevier; pp. 89-117.

Holstege, J. C., and Kuypers, H. G. J. M. (1987). Brainstem projections to spinal motoneurons: an update. Neurosci. 23: 809-821.

Hornby, J. B., and Rose, J. D. (1976). Responses of caudal brainstem neurons to vaginal and somatosensory stimulation in the rat and evidence of genital nociceptive interactions. Exp. Neurol. 51: 363-376.

Huisman, A. M., Kuypers, H. G. J. M., and Verburgh, C. A. (1981). Quantitative differences in collateralization of the descending spinal pathways from red nucleus and other brainstem cell groups in rats as demonstrated with the multiple flourescent retrograde tracer technique. Brain Res. 209: 271-286.

Iggo, A. (1969). Cutaneous thermoreceptors in primates and sub-primates. J. Physiol. Lond. 200: 403-430.

Iggo, A. (1974). Activation of cutaneous nociceptors and their action on dorsal horn neurons. Adv. Neurol. 4: 1-9.

Ito, M., Udo, M., and Mano, N. (1970). Long inhibitory and excitatory pathways converging onto cat reticular and Dieters' neurons and their relevance to reticulofigal axons. J. Neurophysiol. 33: 210-226.

Jasper, H. H., Procter, L. D., Knighton, R. S., Noshay, W. S., and Costello, R. T., eds. (1958). Reticular formation of the brain. Boston, Ma.: Little Brown.

Kawamura, K., Brodal, A., and Hoddevik, G. (1974). The projection of the superior colliculus onto the reticular formation of the brain stem. An experimental anatomical study in the cat. Exp. Brain Res. 19: 1-19.

Keene, J. J., and Casey, K. L. (1970). Excitatory connection from lateral hypothalamic self-stimulation sites to escape sites in medullary reticular formation. Exp. Neurol. 28: 155-166.

Keene, J. J., and Casey, K. L. (1973). Rewarding and aversive brain stimulation: Opposite effects on medial thalamic units. Physiol. Behav. 10: 283-287.

Kellaway, L. A., and Douglas, R. J. (1985). Caudal projections of the reticulospinal neurones mapped by combined electrophysiological and retrograde horseradish peroxidase techniques. S. A. J. Sci. 81: 139-140.

Keller, E. L. (1974). Participation of medial pontine reticular formation in eye movement generation in monkey. J. Neurophysiol. 37: 316-332.

Kevetter, G. A., Haber, L. H., Yezierski, R. P., Chung, J. M., Martin, R. F., and Willis, W. D. (1982). Cells of origin of the spinoreticular tract in the monkey. J. Comp. Neurol. 207: 61-74.

Kevetter, G. A., and Willis, W. D. (1982). Spinothalamic cells in the rat lumbar cord with collaterals to the medullary reticular formation. Brain Res. 238: 181-185.

Kevetter, G. A., and Willis, W. D. (1983). Collaterals of spinothalamic cells in the rat. J. Comp. Neurol. 215: 453-464.

Kevetter, G. A., and Willis, W. D. (1984). Collateralization in the spinothalamic tract: new methodology to support or deny phylogenetic theories. Brain Res. Rev. 7: 1-14.

Kow, L. M., and Pfaff, D. W. (1982). Responses of medullary reticulospinal and other reticular neurons to somatosensory and brainstem stimulation in anesthetized or freely-moving ovariectomized rats with or without estrogen treatment. Exp. Brain Res. 47: 191-202.

Kriesman, N. R., and Zimmermann, I. D. (1973). Representation of information about skin temperature in the discharge of single cortical neurons. Brain Res. 55: 343-353.

Kuraishi, Y., Sugimoto, M., Hamada, T., Kayanoki, Y., and Takagi, H. (1984). Noxious stimuli and met-enkephalin release from nucleus reticularis gigantocellularis. Brain Res. Bull. 12: 123-127.

Kuypers, H. G. J. M. (1958a). An anatomical analysis of cortico-bulbar connexions to the pons and lower brain stem in the cat. J. Anat. Lond. 92: 198-218.

Kuypers, H. G. J. M. (1958b). Some projections from the peri-central cortex to the pons and lower brain stem in monkey and chimpanzee. J. Comp. Neurol. 110: 221-255.

Kuypers, H. G. J. M. (1982). A new look at the organization of the motor system. In: H. G. J. M. Kuypers and G. F. Martin, eds. Progress in brain research: Descending pathways to the spinal cord. New York: Elsevier; pp. 381-403.

Kuypers, H. G. J. M. (1985). The anatomical and functional organization of the motor system. In: M. Swash and C. Kennard, eds. Scientific basis of clinical neurology. Edinburgh: Churchill Livingstone.

Ladpli, R., and Brodal, A. (1968). Experimental studies of commissural and reticular formation projections from the vestibular nuclei in the cat. Brain Res. 8: 65-96.

LaMotte, R. H., and Campbell, J. N. (1978). Comparison of responses of warm and nociceptive C-fibre afferents in monkey with human judgements of thermal pain. J. Neurophysiol. 41: 509-528.

Langhorst, P., Schulz, B., Schulz, G., and Lambertz, M. (1983). Reticular formation of the lower brainstem. A common system for cardiorespiratory and somatomotor functions: discharge patterns of neighboring neurons influenced by cardiovascular and respiratory afferents. J. Auton. Nerv. Sys. 9: 411-432.

LeBars, D., Dickenson, A. H., Besson, J. M., and Villanueva, L. (1986). Aspects of sensory processing through convergent neurons. In: T. L. Yaksh, ed. Spinal afferent processing. New York: Plenum; pp. 467-504.

LeBlanc, H. J., and Gatipon, G. B. (1974). Medial bulboreticular response to peripherally applied noxious stimuli. Exp. Neurol. 42: 264-273.

Lee, H. K., Chai, C. Y., Chung, P. M., and Chen, C. C. (1977). Medullary unit responses to changes in local and hypothalamic temperatures in the cat. Brain Res. Bull. 2: 375-380.

Liebeskind, J. C., Guilbaud, G., Besson, J. M., and Oliveras, J. L. (1973). Analgesia from electrical stimulation of the periaqueductal gray matter in the cat: behavioral observations and inhibitory effects on spinal cord interneurons. Brain Res. 50: 441-446.

Loewy, A. D., Wallach, J. H., and McKellar, S. (1981). Efferent connections of the ventral medulla oblongata. Brain Res. Rev. 3: 63-80.

Lynn, B. (1984). Effect of neonatal treatment with capsaicin on the numbers and properties of cutaneous afferent units from the hairy skin of the rat. Brain Res. 322: 255-260.

MacGregor, R. J., Prieto-Diaz, R., Miller, S. W., and Groves, P. M. (1973). Statistical properties of neurones in the rat mesencephalic reticular formation. Brain Res. 64: 167-187.

Maes, F. W. (1984). A neural coding model for sensory intensity discrimination, to be applied to gustation. J. Comp. Physiol. A 155: 263-270.

Maes, F. W., and Erickson, R. P. (1984). Gustatory intensity discrimination in rat NTS: a tool for the evaluation of neural coding theories. J. Comp. Physiol. A 155: 271-282.

Magni, F., and Willis, W. D. (1963). Identification of reticular formation neurons by intracellular recording. Arch. Ital. Biol. 101: 681-702.

Martin, G. F., Cabana, T., DiTirro, F. J., Ho, R. H., and Humbertson, A. O. (1982). Raphe spinal projections in the North American opossum. Evidence for connectional heterogeneity. J. Comp. Neurol. 196: 67-84.

Martin, G. F., Humbertson, A. O., Laxson, L. C., Panneton, W. M., and Tschismadia, I. (1979). Spinal projections from the mesencephalic and pontine reticular formation in the North American opossum: A study using axonal transport techniques. J. Comp. Neurol. 187: 373-400.

Martin, G. F., and Waltzer, R. (1984). Spinal projections of the gigantocellular reticular formation in the rat. Evidence for differential projections to laminae I, II and IX. Soc. Neurosci. Abst. 10: 29.

Martin, G. F., Waltzer, R., and Vertes, R. P. (1985). Major projections of the reticular formation. In: G. Paxinos, ed. The rat nervous system. Vol. 2. Hindbrain and spinal cord. Sydney: Academic; pp. 29-42.

Martin, H. F., and Manning, J. W. (1971). Thalamic "warming" and "cooling" units responding to cutaneous stimulation. Brain Res. 27: 377-381.

Maunz, R. A., Pitts, N. G., and Peterson, B. W. (1978). Cat spinoreticular neurons: locations, responses and changes in responses during repetitive stimulation. Brain Res. 148: 365-379.

Mayer, D. J., and Price, D. D. (1976). Central nervous system mechanisms of analgesia. Pain 2: 379-404.

McCall, R. B., and Aghajanian, G. K. (1979). Serotonergic facilitation of facial motoneuron excitation. Brain Res. 169: 11-27.

McCreery, D. B., Bloedel, J. R., and Hames, E. G. (1979). Effects of stimulating in raphe nuclei and in reticular formation on response of spinothalamic neurons to mechanical stimuli. J. Neurophysiol. 42: 166-182.

Melzack, R., and Wall, P. D. (1965). Pain mechanisms: A new theory. Science 150: 971-979.

Mendell, L. M. (1966). Physiological properties of unmeyelinated fiber projections to the spinal cord. Exp. Neurol. 16: 316-332.

Menétrey, D., Chaouch, A., and Besson, J. M. (1980). Location and properties of dorsal horn neurons at origin of spinoreticular tract in lumbar enlargement of the rat. J. Neurophysiol. 44: 862-877.

Morhland, J. S., and Gebhart, G. F. (1980). Effects of focal electrical stimulation and morphine microinjection in the periaqueductal gray of the rat mesencephalon and neuronal activity in the medullary reticular formation. Brain Res. 201: 23-37.

Moruzzi, G., and Magoun, H. W. (1949). Brain stem reticular formation and activation of the EEG. Electroencephalogr. Clin. Neurophysiol. 1: 455-473.

Mountcastle, V. B. (1984). Central nervous mechanisms in mechanoreceptive sensibility. In: I. Darian-Smith, ed. Handbook of physiology. Section 1: The nervous system. Volume III. Sensory processes. Bethesda, Md.: American Physiological Society; pp. 789-878.

Muschaweck, L. G., and Loevner, D. (1978). Analysis of neuronal spike trains: survey of the stochastic techniques and implementation of the cumulative-sums statistic for the evaluation of spontaneous and driven activity. Int. J. Neurosci. 8: 51-60.

Nauta, W. J. H., and Kuypers, H. G. J. M. (1958). Some ascending pathways in the brainstem reticular formation. In: H. H. Jasper, L. D. Procter, R. S. Knighton, W. S. Noshay and R. T. Costello, eds. Reticular formation of the brain. Boston, Ma.: Little Brown; pp. 13-30.

Newman, D. B., and Kiddy, K. M. (1981). A comparison of the nucleus reticularis gigantocellularis (Rgc) and nucleus reticularis magnocellularis (Rmc) in the rat. A Nissl, Golgi and HRP study. Anat. Rec. 199: 182A.

Oliveras, J. L., Hosobuchi, Y., Redjemi, F., Guilbaud, G., and Besson, J. M. (1977). Opiate antagonist, naloxone, strongly reduces analgesia induced by stimulation of a raphe nucleus (centralis inferior). Brain Res. 120: 221-229.

Oliveras, J. L., Vos, B., Martin, G., and Montagne, J. (1989). Electrophysiological properties of ventromedial medulla neurons in response to noxious and non-noxious stimuli in the awake, freely moving rat: a single-unit study. Brain Res. 486: 1-14.

Pavlasek, J., Gokin, A. P., and Duda, P. (1977). Visceral pain: responses of reticular formation neurons to gallbladder distension. J. Physiol. Paris 57: 307-321.

Pearl, G. S., and Anderson, K. V. (1978). Response patterns of cells in the feline caudal nucleus reticularis gigantocellularis after noxious trigeminal and spinal stimulation. Exp. Neurol. 58: 231-241.

Pearl, G. S., and Anderson, K. V. (1980). Interactions between nucleus centrum medianum and gigantocellular nociceptive neurons. Brain Res. Bull. 5: 203-206.

Pepler, J. H., Farham, C. J., and Douglas, R. J. (1985). An inexpensive programmable stimulator for the study of thermal sensation. J. Neurosci. Meth. 15: 131-140.

Perl, E. R. (1984). Pain and nociception. In: I. Darian-Smith, ed. Handbook of physiology. Section 1: The nervous system. Volume III. Sensory processes. Bethesda, Md.: American Physiological Society; pp. 915-975.

Pertovaara, A., Reinikainen, K., and Hari, R. (1984). The activation of unmyelinated or myelinated afferent fibres by brief infrared laser pulses varies with skin type. Brain Res. 307: 341-343.

Peschanski, M., and Besson, J. M. (1984). A spino-reticulo-thalamic pathway in the rat: an anatomical study with reference to pain transmission. Neurosci. 12: 165-178.

Peterson, B. W. (1979). Reticulospinal projections to spinal motor nuclei. Ann. Rev. Physiol. 41: 127-140.

Peterson, B. W. (1980). Participation of pontomedullary reticular formation neurons in specific motor activity. Chairman's overview of part III. In: J. A. Hobson and M. A. B. Brazier, eds. The reticular formation revisited. Specifying function for a nonspecific system. New York: Raven; pp. 171-192.

Peterson, B. W., and Abzug, C. (1975). Properties of projections from vestibular nuclei to medial reticular formation in the cat. J. Neurophysiol. 38: 1421-1435.

Peterson, B. W., Filion, M., Felpel, L. P., and Abzug, G. (1975b). Responses of medial reticular neurons to stimulation of the vestibular nerve. Exp. Brain Res. 22: 335-350.

Peterson, B. W., Maunz, R. A., Pitts, N. G., and Mackel, R. G. (1975a). Patterns of projection and branching of reticulospinal neurons. Exp. Brain Res. 23: 333-351.

Peterson, B. W., Pitts, N. G., and Fukushima, K. (1979). Reticulospinal connections with limb and axial motoneurons. Exp. Brain Res. 36: 1-20

Peterson, B. W., Pitts, N. G., Fukushima, K., and Mackel, R. G. (1978). Reticulospinal excitation and inhibition of neck motoneurons. Exp. Brain Res. 32: 471-489.

Pompeiano, O., and Barnes, C. D. (1971). Responses of brain stem reticular neurons to muscle vibration in the decerebrate cat. J. Neurophysiol. 34: 709-724.

Poulos, D. A., and Benjamin, R. M. (1968). Response of thalamic neurons to thermal stimulation of the tongue. J. Neurophysiol. 31: 28-43.

Price, D. D. (1986). The question of how the dorsal horn encodes sensory information. In: T. L. Yaksh, ed. Spinal afferent processing. New York: Plenum; pp. 445-466.

Price, D. D., Barrell, J. J., and Gracely, R. H. A. (1980). A psychological analysis of experiential factors that selectively influence the affective dimension of pain. Pain 8: 137-150.

Price, D. D., and Browe, A. C. (1973). Responses of spinal cord neurons to graded noxious and non-noxious stimuli. Brain Res. 64: 425-429.

Price, D. D., and Dubner, R. (1977). Neurons that subserve the sensory-discriminative aspects of pain. Pain 3: 307-338.

Price, D. D., Dubner, R., and Hu, J. W. (1976). Trigeminothalamic neurons in nucleus caudalis responsive to tactile, thermal, and nociceptive stimulation of monkey's face. J. Neurophysiol. 39: 936-953.

Price, D. D., Hayes, R. L., Ruda, M., and Dubner, R. (1978). Spatial and temporal transformations of input to spinothalamic tract neurons and their relation to somatic sensations. J. Neurophysiol. 41: 933-947.

Price, D. D., and Mayer, D. J. (1974). Physiological laminar organization of the dorsal horn of Macaca mulatta. Brain Res. 79: 321-325.

Price, D. D., McGrath, P. A., Rafii, A., and Buckingham, B. (1983). The validation of visual analogue scales as ratio scale measures for chronic and experimental pain. Pain 17: 45-56.

Robertson, R. T., and Feiner, A. R. (1982). Diencephalic projections from the pontine reticular formation: Autoradiographic studies in the cat. Brain Res. 239: 3-16.

Rose, J. D. (1975a). Response properties and anatomical organization of pontine and medullary units responsive to vaginal stimulation in the cat. Brain Res. 97: 79-93.

Rose, J. D. (1975b). Responses of midbrain neurons to genital and somatosensory stimulation in estrous and anestrous rats. Exp. Neurol. 49: 639-652.

Rose, J. D. (1978). Midbrain and pontine unit responses to lordosis-controlling forms of somatosensory stimuli in the female golden hamster. Exp. Neurol. 60: 499-508.

Rose, J. D., and Michael, R. P. (1978). Facilitation by estradiol of midbrain and pontine unit responses to vaginal and somatosensory stimulation in the squirrel monkey (Siamiri sciureus). Exp. Neurol. 58: 46-58.

Rossi, G. F., and Brodal, A. (1956). Corticofugal fibres to the brain stem reticular formation. an experimental study in the cat. J. Anat. Lond. 90: 42-62.

Rowe, M. J., and Sessle, B. J. (1972). Responses of small myelinated 'warm' fibres to noxious heat applied to the monkey's face. Brain Res. 42: 367-384.

Scheibel, A. B. (1984). The brainstem reticular core and sensory function. In: I. Darian-Smith, ed. Handbook of physiology. Section 1: The nervous system. Volume III. Sensory processes. Bethesda, Md.: American Physiological Society.; pp. 213-256.

Scheibel, M. E., and Scheibel, A. B. (1958). Structural substrates for integrative patterns in the brain stem reticular core. In: H. H. Jasper, L. D. Procter, R. S. Knighton, W. C. Noshay and R. T. Costello, eds. Reticular formation of the brain. Boston, Ma.: Little Brown.

Scheibel, M. E., and Scheibel, A. B. (1965a). The response of reticular units to repetitive stimuli. Arch. Ital. Biol. 103: 279-299.

Scheibel, M. E., and Scheibel, A. B. (1965b). Periodic sensory nonresponsiveness in reticular neurons. Arch. Ital. Biol. 103: 300-316.

Scheibel, M. E., and Scheibel, A. B. (1965c). Activity cycles in neurons of the reticular formation. Recent Adv. Bio. Psych. 8: 283-293.

Scheibel, M. E., Scheibel, A. B., Mollica, A., and Moruzzi, G. (1955). Convergence and interaction of afferent impulses on single units of reticular formation. J. Neurophysiol. 18: 310-331.

Schulz, B., Lambertz, M., Schulz, G., and Langhorst, P. (1983). Reticular formation of the lower brainstem. A common system for cardiorespiratory and somatomotor functions: discharge patterns of neighboring neurons influenced by somatosensory afferents. J. Auton. Nerv. Sys. 9: 433-449.

Segundo, J. P., Takenaka, T., and Encabo, H. (1967). Somatosensory properties of bulbar reticular neurons. J. Neurophysiol. 30: 1221-1238.

Siegel, J. M. (1979). Behavioral functions of the reticular formation. Brain Res. Rev. 1: 69-105.

Siegel, J. M. (1983). A behavioral approach to the analysis of reticular formation unit activity. In: T. E. Robinson, ed. Behavioral approaches to brain research. New York: Oxford University Press; pp. 94-116.

Siegel, J. M., and McGinty, D. J. (1976). Brainstem neurons without spontaneous unit discharge. Science 193: 240-242.

Siegel, J. M., and McGinty, D. J. (1977). Pontine reticular formation neurones: relationship of discharge to motor activity. Science 196: 678-680.

Siegel, J. M., and Tomaszewski, K. S. (1983). Behavioral organization of reticular formation: studies in the unrestrained cat. I. Cells related to axial, limb, eye, and other movements. J. Neurophysiol. 50: 696-716.

Siegel, J. M., Tomaszewski, K. S., and Nienhuis, R. (1986). Behavioral states in the chronic medullary and midpontine cat. Electroencephalogr. Clin. Neurophysiol. 63: 274-288.

Siegel, J. M., Tomaszewski, K. S., and Wheeler, R. L. (1983). Behavioral organization of reticular formation: studies in the restrained cat. II. Cells related to facial movements. J. Neurophysiol. 50: 717-723.

Siegel, S. (1956). Nonparametric statistics for the behavioral sciences. Tokyo: McGraw-Hill Kogakusha.

Sjölund, B., and Björklund, A., eds. (1982). Brainstem control of spinal mechanisms. Amsterdam: Elsevier.

Smith, D. V., Van Buskirk, R. L., Travers, J. B., and Bieber, S. L. (1983a). Gustatory neuron types in hamster brain stem. J. Neurophysiol. 50: 522-540.

Smith, D. B., Van Buskirk, R. L., Travers, J. B., and Bieber, S. L. (1983b). Coding of taste stimuli by hamster brain stem neurones. J. Neurophysiol. 50: 541-558.

Spray, D. C. (1986). Cutaneous temperature receptors. Ann. Rev. Physiol. 48: 625-638.

Sumino, R., and Dubner, R. (1981). Response characteristics of specific thermoreceptive afferents innervating monkey facial skin and their relationship to human thermal sensitivity. Brain Res. Rev. 3: 105-122.

Surmeier, D. J., Honda, C. N., and Willis, W. D. (1988). Natural groupings of primate spinothalamic neurons based on cutaneous stimulation. Physiological and anatomical features. J. Neurophysiol. 59: 833-860.

Takagi, H., Satoh, M., Akaike, A., Shibata, T., Yajima, H., and Ogawa, H. (1978). Analgesia by enkephalins injected into the nucleus reticularis gigantocellularis of rat medulla oblongata. Eur. J. Pharmacol. 49: 113-116.

Takagi, H., Shiosaka, S., Tohyama, M., Senba, E., and Sakanaka, M. (1980). Ascending components of the medial forebrain bundle from the lower brainstem in the rat, with special reference to raphe and catecholamine cell groups. A study by the HRP method. Brain Res. 193: 315-337.

Tohyama, M., Sakai, K., Salvert, D., Touret, M., and Jouvet, M. (1979). Spinal projections from the lower brain stem in the cat as demonstrated by the horseradish peroxidase technique. I. Origins of the reticulospinal tracts and their funicular trajectories. Brain Res. 173: 383-403.

Trevino, D. L., Coulter, J. D., and Willis, W. D. (1973). Location of cells of origin of spinothalamic tract in the lumbar enlargement of the monkey. J. Neurophysiol. 36: 750-761.

Valverde, F. (1961). Reticular formation of the pons and medulla oblongata. A golgi study. J. Comp. Neurol. 116: 71-99.

Valverde, F. (1962). Reticular formation of the albino rat's brain stem. Cytoarchitecture and corticofugal connections. J. Comp. Neurol. 119: 25-53.

Valverde, F. (1966). The pyramidal tract in rodents. A study of its relations with the posterior column nuclei, dorsolateral reticular formation of the medulla oblongata, and cervical spinal cord (Golgi and electron microscopic observations). Z. Zellforsch 71: 297-363.

Vanegas, H., Barbaro, N. M., and Fields, H. L. (1984a). Midbrain stimulation inhibits tail-flick only at currents sufficient to excite rostral medullary neurons. Brain Res. 321: 127-133.

Vanegas, H., Barbaro, N. M., and Fields, H. L. (1984b). Tail-flick related activity in medullospinal neurons. Brain Res. 321: 135-141.

Vertes, R. P. (1977). Selective firing of rat pontine gigantocellular neurons during movement and REM sleep. Brain Res. 128: 146-152.

Vertes, R. P. (1979). Brain stem gigantocellular neurons: patterns of activity during behavior and sleep in the freely moving rat. J. Neurophysiol. 42: 214-228.

Vertes, R. P. (1984a). Brainstem control of the events of REM sleep. Prog. Neurobiol. 22: 241-288.

Vertes, R. P. (1984b). A lectin horseradish peroxidase study of the origin of ascending fibres in the median forebrain bundle of the rat. The lower brainstem. Neurosci. 11: 651-668.

Vertes, R. P. (1984c). A lectin horseradish peroxidase study of the origin of ascending fibres in the median forebrain bundle of the rat. The upper brainstem. Neurosci. 11: 669-690.

Vertes, R. P., and Miller, N. E. (1976). Brain stem neurons that fire selectively to a conditioned stimulus for shock. Brain Res. 103: 229-242.

Vertes, R. P., Waltzer, R., and Martin, G. F. (1984). An autoradiographic study of ascending nucleus gigantocellularis projections in the rat. Soc. Neurosci. Abst. 10: 901.

Walberg, F., Pompeiano, O., Westrum, L. E., and Haughlie-Hansen, E. (1962). Fastigioreticular fibres in the cat. An experimental study with silver methods. J. Comp. Neurol. 119: 187-199.

Wall, P. D. (1960). Cord cells responding to touch, damage and temperature of the skin. J. Neurophysiol. 23: 197-210.

Wall, P. D. (1967). The laminar organization of dorsal horn and effects of descending impulses. J. Physiol. Lond. 188: 403-423.

Waltzer, R. P., and Martin, G. F. (1984). Collateralization of reticulospinal axons from the nucleus gigantocellularis to the cerebellum and diencephalon. A double labelling study in the rat. Brain Res. 293: 153-158.

Willis, W. D. (1986). Ascending somatosensory systems. In: T. L. Yaksh, ed. Spinal afferent processing. New York: Plenum; pp. 243-274.

Willis, W. D. (1989). The origin and destination of pathways involved in pain transmission. In: P. D. Wall and R. Melzack, eds. Textbook of pain. 2nd ed. Edinburgh: Churchill Livingstone; pp. 112-127.

Willis, W. D., and Coggeshall, R. E., eds. (1978). Sensory mechanisms of the spinal cord. New York: Plenum.

Willis, W. D., Haber, L. H., and Martin, R. F. (1977). Inhibition of spinothalamic tract cells and interneurons by brain stem stimulation in the monkey. J. Neurophysiol. 40: 968-981.

Willis, W. D., Trevino, D. L., Coulter, J. D., and Maunz, R. A. (1974). Responses of primate spinothalamic tract neurons to natural stimulation of the hindlimb. J. Neurophysiol. 37: 358-372.

Wilson, V. J., and Yoshida, M. (1969). Comparison of effects of stimulation of Dieters' nucleus and the medial longitudinal fasciculus on neck, forelimb, and hindlimb motoneurons. J. Neurophysiol. 32: 743-758.

Wilson, V. J., Yoshida, M., and Shore, R. H. (1970). Supraspinal monosynaptic excitation and inhibition of thoracic back motoneurons. Exp. Brain Res. 11: 282-295.

Wolstencroft, J. H. (1964). Reticulospinal neurones. J. Physiol. Lond. 174: 91-108.

Young, A. A., and Dawson, N. J. (1987). Static and dynamic response characteristics, receptive fields, and interaction with noxious input of midline medullary thermoresponsive neurons in the rat. J. Neurophysiol. 57: 1925-1936.

Young, D. W., and Gottschaldt, K. M. (1976). Neurons in the rostral mesencephalic reticular formation of the cat responding specifically to noxious mechanical stimulation. Exp. Neurol. 51: 628-636.

Zemlan, F., Behbehani, M. M., and Beckstead, R. M. (1982). Ascending and descending projections from nucleus reticularis magnocellularis and nucleus reticularis gigantocellularis. An autoradiographic and horseradish peroxidase study in the rat. Brain Res. 292: 207-220.

Zemlan, F. P., and Pfaff, D. W. (1979). Topographical organization in medullary reticulospinal systems as demonstrated by the horseradish peroxidase technique. Brain Res. 174: 161-166.

Zimmermann, M. (1977). Encoding in dorsal horn interneurons receiving noxious and nonnoxious afferents. J. Physiol. Paris 73: 221-232.

Zimmerman, M., and Handwerker, H. O. (1974). Total afferent inflow and dorsal horn activity upon radiant heat stimulation to the cat's footpad. Adv. Neurol. 4: 29-33.

APPENDIX

KEY:

HISTOLOGY

Stereotaxic co-ordinates (mm):

AP	Anterior-posterior
L	Lateral
H	Horizontal

MECHANICAL RESPONSES

REGIONS	Number of regions included in the receptive field of a given PMRF neurone
EX or 1	Excitatory response
IN or -1	Inhibitory response
CX	Complex response: both excitation and inhibition
NR or [blank]	No response
HT	High threshold response
WR	Wide range: responsive to both innocuous and noxious stimuli

THERMAL RESPONSES

MEANT*n*	Average temperature in period *n* (double step series)
TEMP	Average temperature (°C, single step series)
TOTSP*n*	Total number of spikes in period *n*
MEANSP*n*	Average number of spikes/s in period *n*
MEANRES	Average response (ramp series; calculated from onset of response to time at maximum temperature)
DMEAN*n*	Average response in period *n*, calculated relative to the mean discharge rate in the control period (i.e. period 1)
MAXSP*n*	Maximum action potential frequency (spikes/s) in period *n*
MINSP*n*	Minimum action potential frequency (spikes/s)
DMAX	Maximum change in firing rate (spikes/s)
THRESH	Threshold temperature (°C)
LATENCY*n*	Latency to onset of response (s)
TPEAK	Time from onset of response to maximum response (s) (ramp stimuli only)
TIMEPK*n*1	Time from onset of stimulus to maximum/minimum discharge (s)
LOCATION	Location of stimulus relative to the position of the recording electrode

TABLE A1: HISTOLOGICAL LOCATION, MECHANICAL RESPONSES AND THERMAL RESPONSE POLARITY - ALL CELLS

	HISTOLOGY			MECHANICAL RESPONSES								
CELL	AP	L	H	TAIL	HIND	TRUNK	FORE	HEAD	REGIONS	ADEQUATE STIMULUS	MECHANICAL POLARITY	THERMAL POLARITY
RA1	-2.0	1.0	-9.4	1	1		1	1	4	HT	EX	EX
RA2	-2.0	1.0	-9.5		1				1	HT	EX	EX
RA3	-1.5	-0.7	-7.8	1	1	1	1		4	WR	EX	EX
RA4	-1.5	0.7	-7.6	1	1				2	HT	EX	EX
RA5	-1.5	-0.7	-7.7		1				1	HT	EX	EX
RA6	-1.5	-0.8	-8.0	1	1	1	1		4	WR	EX	EX
RA7	-1.5	-1.0	-7.5	1	1	1	1		4	WR	EX	EX
RA8	-1.5	-1.0	-8.3	1	1	1	1		4	HT	EX	EX
RA9	-2.0	0.8	-7.1	1	1				2	HT	EX	EX
RA10	-2.0	-0.7	-7.0		1				1	HT	EX	EX
RA11	-1.5	0.8	-8.5	1	1	1	1		4	WR	EX	EX
RA12	-2.0	0.8	-8.1	-1	-1	-1			3	HT	IN	IN
RA13	-1.5	0.8	-7.4	1	1	1	1	1	5	HT	EX	EX
RA14	-2.0	-0.7	-5.0		1				1	HT	EX	NR
RA15	-1.5	0.6	-9.3	1	1	1	1	1	5	HT	EX	EX
RA16	-2.0	-0.8	-6.8	-1	-1			-1	3	HT	IN	NR
RA17	-2.0	-0.5	-8.5	-1	-1	-1			3	HT	IN	IN
RA18	-2.0	0.5	-8.8	1	1	1			3	HT	EX	EX
RA19	-1.5	0.5	-7.9		1	1			2	HT	EX	EX
RA20	-1.5	0.5	-8.4	1	1	1			3	HT	EX	EX
RA21	-2.5	-1.0	-8.1	1	1	1			3	WR	EX	EX
RA22	-1.5	-0.5	-9.7		1				1	HT	EX	EX
RA23	-1.5	0.5	-9.0	1	1	1			3	HT	EX	EX
RA24	-1.5	0.5	-8.7		-1				1	HT	IN	IN
RA25	-1.5	0.5	-8.9	1	1	1			3	WR	EX	EX
RA26	-1.5	0.5	-9.6		-1				1	HT	IN	NR
RA27	-1.5	0.7	-9.3	-1	-1	-1			3	HT	IN	NR
RA28	-1.5	0.7	-8.1	1	1	1			3	HT	EX	EX
RA29	-1.5	0.7	-8.9	-1	-1	-1			3	HT	IN	IN
RA30	-1.5	0.7	-9.3	1	1	1			3	HT	EX	NR
RA31	-1.5	-0.7	-8.7	1	1	1		1	4	HT	EX	EX
RA32	-1.5	-0.7	-9.5	1	1	-1			3	WR	CX	EX
RA33	-2.0	0.8	-7.4	1	1	1			3	WR	EX	EX
RA34	-2.0	0.8	-8.1	1	1	1			3	WR	EX	NR
RA35	-2.0	0.8	-8.5	-1	-1	-1			3	WR	IN	IN
RA36	-1.5	0.7	-8.5	-1	-1	-1			3	HT	IN	IN
RA37	-2.0	0.7	-8.2	1	1				2	HT	EX	EX
RA38	-2.0	0.7	-8.7	1	1				2	HT	EX	NR
RA39	-2.0	-0.8	-8.5	1	1	1		1	4	WR	EX	EX
RA40	-2.0	-0.8	-8.9	1	1	1		1	4	WR	EX	EX
RA41	-2.0	-0.8	-9.6	1	1	1		1	4	HT	EX	IN
RA42	-1.5	-0.7	-7.7	-1	-1			-1	3	HT	IN	IN
RA43	-1.5	0.7	-8.8	1	1				2	HT	EX	EX
RA44	-1.5	0.8	-7.3		1	1			2	WR	EX	EX
RA45	-1.5	0.8	-7.6		1	1		1	3	WR	EX	EX
RA46	-1.5	0.8	-8.6	-1	-1	-1			3	WR	IN	IN
RA47	-1.5	0.8	-9.2	1	1				2	HT	EX	EX
RA48	-1.5	-0.8	-7.8		1	1			2	WR	EX	EX
RA49	-1.5	-0.8	-7.9		1	-1	1		3	WR	CX	IN
RA50	-2.0	0.8	-8.0		1	1			2	WR	EX	EX
RA51	-1.5	-0.6	-7.9	1	1	1	-1		4	WR	CX	EX
RA52	-1.5	-0.6	-9.1	1	1	1		1	4	WR	EX	NR
RA53	-2.0	0.8	-7.4	1	1	-1	1		4	WR	CX	EX
RA54	-2.0	0.8	-7.8	-1	1	1			3	WR	EX	EX
RA55	-1.5	-0.8	-7.0		1	1			2	HT	EX	EX
RA56	-1.5	-0.8	-7.6		1	1			2	HT	EX	EX
RA57	-1.5	0.8	-7.0	1	1	1			3	WR	EX	EX
RA58	-2.0	0.8	-7.9		1	1		1	3	WR	EX	EX
RA59	-1.5	0.8	-8.5	1	1				2	HT	EX	EX
RA60	-2.0	-0.7	-8.3	-1	-1				2	HT	IN	IN
RA61	-1.5	0.7	-8.9	1	1				2	HT	EX	EX
RA62	-2.0	-0.7	-8.1	1	1				2	HT	EX	EX
RA63	-2.0	-0.7	-8.5	1	1			1	3	HT	EX	EX

TABLE A1: HISTOLOGICAL LOCATION, MECHANICAL RESPONSES AND THERMAL RESPONSE POLARITY - ALL CELLS

	HISTOLOGY			MECHANICAL RESPONSES								
CELL	AP	L	H	TAIL	HIND	TRUNK	FORE	HEAD	REGIONS	ADEQUATE STIMULUS	MECHANICAL POLARITY	THERMAL POLARITY
RA64	-1.5	0.8	-8.3	1	1	1		1	4	WR	EX	EX
RA65	-1.5	0.8	-8.6	-1	-1	-1			3	WR	IN	IN
RA66	-1.5	-0.8	-7.2	1	1				2	HT	EX	NR
RA67	-1.5	-0.8	-7.6	1	1				2	HT	EX	EX
RA68	-1.5	-0.8	-7.7	1	1	1		1	4	WR	EX	EX
RA69	-1.5	-0.8	-8.3		1	1		1	3	WR	EX	EX
RA70	-2.5	-0.7	-7.7		1				1	HT	EX	EX
RA71	-3.0	-0.7	-8.3	1	1				2	HT	EX	EX
RA72	-2.5	0.6	-8.4		1				1	HT	EX	EX
RA73	-1.5	-0.7	-9.0	1	1	1			3	WR	EX	EX
RA74	-2.0	0.1	-8.2	1	1				2	HT	EX	EX
RA75	-1.5	0.8	-8.0		-1	-1			2	HT	IN	EX
RA76	-2.0	-0.4	-8.5	1	1	1			3	WR	EX	EX
RA77	-1.5	0.6	-6.6	1	1			1	3	HT	EX	EX
RA78	-1.5	0.6	-8.5		1				1	HT	EX	EX
RA79	-1.5	-0.7	-8.2	1	1				2	HT	EX	EX
RA80	-2.0	0.7	-8.1	-1	-1				2	HT	IN	IN
RA81	-2.0	-0.7	-8.5	1	1	1	1	1	5	HT	EX	EX
RA82	-1.5	0.6	-7.6		1	1			2	WR	EX	EX
RA83	-1.5	0.6	-8.3	1	1		1		3	HT	EX	EX
RA84	-1.5	0.6	-8.3		1	1	1	1	4	WR	EX	EX
RA85	-1.5	-0.6	-7.4		1				1	HT	EX	EX
RA86	-2.0	-0.8	-8.4	-1	-1				2	HT	IN	IN
RA87	-1.5	-0.6	-8.8	1	1			1	3	HT	EX	EX
RA88	-1.5	-0.8	-8.3	1	1				2	HT	EX	EX
RA89	-1.5	-0.6	-8.3	-1	-1				2	HT	IN	IN
RA90	-1.5	0.7	-7.5		1				1	HT	EX	EX
RA91	-1.5	0.7	-8.5		1				1	HT	EX	EX
RA92	-2.5	-1.0	-8.6	-1	-1				2	HT	IN	IN
RA93	-2.5	-1.0	-8.8		1		1	1	3	HT	EX	EX
RA94	-2.0	0.5	-8.1		-1				1	HT	IN	EX
RA95	-2.5	0.6	-8.2		1				1	HT	EX	EX
RA96	-1.5	0.6	-7.5		1				1	HT	EX	EX
RA97	-1.5	-0.8	-7.7	1	1				2	HT	EX	EX
RA98	-2.0	0.6	-7.3		1				1	HT	EX	EX
RA99	-1.5	0.8	-6.2	-1	-1				2	HT	IN	IN
RA100	-1.5	0.8	-6.8		1				1	HT	EX	NR
RA101	-1.5	-0.6	-8.4		1				1	HT	EX	IN
RA102	-2.0	-0.6	-8.1	1	1	1	1	1	5	WR	EX	EX
RA103	-2.0	-0.6	-8.3	1	1	1			3	WR	EX	EX
RA104	-2.0	0.8	-8.3		-1				1	HT	IN	IN
RA105	-2.0	-0.7	-8.1	-1	-1		-1		3	HT	IN	IN
RA106	-2.0	0.8	-7.1		1			1	2	HT	EX	EX
RA107	-2.0	0.8	-8.0		1				1	HT	EX	EX
RA108	-2.0	0.8	-9.0	-1	-1				2	HT	IN	IN
RA109	-2.0	-0.8	-7.3	1	1	1			3	WR	EX	EX
RA110	-2.0	0.8	-8.3		1		1	1	3	HT	EX	EX
RA111	-2.0	0.8	-7.4	1	1				2	HT	EX	EX
RA112	-2.5	-0.8	-7.6		1				1	HT	EX	EX
RA113	-2.0	0.7	-8.1	1	1				2	HT	EX	EX
RA114	-2.0	0.7	-8.2		1				1	HT	EX	EX
RA115	-2.5	-0.8	-7.8	1	1	1			3	HT	EX	EX
RA116	-2.0	-0.8	-8.3	-1	-1				2	HT	IN	IN
RA117	-2.5	-0.8	-8.2		1				1	HT	EX	EX

TABLE A1: HISTOLOGICAL LOCATION, MECHANICAL RESPONSES AND THERMAL RESPONSE POLARITY - ALL CELLS

	HISTOLOGY			MECHANICAL RESPONSES								
CELL	AP	L	H	TAIL	HIND	TRUNK	FORE	HEAD	REGIONS	ADEQUATE STIMULUS	MECHANICAL POLARITY	THERMAL POLARITY
VR1	-2.0	0.6	-7.5	-1	-1		-1	-1	4	HT	IN	EX
VR2	-2.0	0.6	-7.9	-1	-1				2	HT	IN	EX
VR3	-2.5	0.6	-8.1	1	1		1	1	4	HT	EX	EX
VR4	-2.0	0.6	-7.6	1	1	1	1	1	5	WR	EX	EX
VR5	-2.0	0.6	-8.1	1	1	1			3	WR	EX	EX
VR6	-2.0	-0.4	-6.6		1				1	HT	EX	NR
VR7	-2.0	-1.0	-8.4		-1				1	HT	IN	IN
VR8	-2.0	-1.0	-8.9		1				1	HT	EX	EX
VR9	-1.5	0.7	-8.0	1	1	-1			3	WR	CX	NR
VR10	-2.0	0.7	-7.0	1	1				2	HT	EX	EX
VR11	-2.5	0.6	-7.8		1				1	HT	EX	EX
VR12	-2.0	1.0	-8.1	1	1			1	3	HT	EX	NR
VR13	-2.0	0.4	-7.4		1				1	HT	EX	EX
VR14	-2.0	0.4	-8.0	1	1	1		1	4	WR	EX	EX
VR15	-2.5	0.7	-7.0	1	1			1	3	HT	EX	EX
VR16	-2.0	-0.8	-7.7		-1				1	HT	IN	IN
DS1	-2.0	-0.7	-6.7		1				1	HT	EX	EX
DS2	-2.0	0.7	-7.7		1				1	HT	EX	NR
DS3	-2.0	0.7	-8.3		1				1	HT	EX	NR
DS4	-2.0	0.8	-6.8	1	1	1			3	WR	EX	EX
DS5	-2.0	0.8	-7.5	1	1				2	HT	EX	EX
DS6	-2.0	-0.8	-6.6	1	1				2	HT	EX	EX
DS7	-2.0	0.8	-8.0		1				1	HT	EX	EX
DS8	-2.0	-0.8	-6.3		1				1	HT	EX	EX
DS9	-2.0	-0.8	-6.8		1				1	HT	EX	EX
DS10	-2.0	0.7	-8.9	1	1	-1			3	WR	CX	IN
DS11	-2.5	-0.7	-6.8	1	1	1	1		4	WR	EX	EX
DS12	-2.5	-0.7	-8.5		1				1	HT	EX	EX
DS13	-2.0	0.6	-7.0	1	1				2	HT	EX	NR
DS14	-2.0	0.6	-8.7		1				1	HT	EX	EX
DS15	-2.0	-0.8	-7.9	1	1	1			3	WR	EX	EX
DS16	-2.0	0.8	-7.1	1	1				2	HT	EX	NR
DS17	-2.0	0.8	-7.9		1	1			2	WR	EX	EX
DS18	-2.5	-0.7	-8.9		-1				1	HT	IN	NR
DS19	-2.5	-0.7	-9.3		-1	-1	-1		3	HT	IN	NR
DS20	-2.0	0.8	-8.0	1	1				2	HT	EX	EX
DS21	-1.5	-0.8	-8.1		-1		-1		2	HT	IN	IN
DS22	-2.0	0.8	-7.4		1				1	HT	EX	NR
DS23	-2.0	0.8	-9.0		-1				1	HT	IN	IN
DS24	-2.0	0.8	-7.2		1				1	HT	EX	EX
DS25	-2.5	0.8	-8.2		1				1	HT	EX	EX
DS26	-2.5	-0.7	-8.8	1	1				2	HT	EX	EX
DS27	-2.5	-0.7	-8.2		1				1	HT	EX	IN
DS28	-2.0	-0.7	-8.5		1				1	HT	EX	IN
DS29	-2.0	-0.7	-8.7	1	1				2	HT	EX	EX
DS30	-2.0	0.5	-8.7		1				1	HT	EX	EX
DS31	-2.0	0.8	-8.4	1	1	1			3	WR	EX	EX
DS32	-2.0	-0.8	-7.4	1	1	1			3	WR	EX	EX
DS33	-1.5	0.9	-8.0		1				1	HT	EX	NR
DS34	-1.5	0.9	-8.2		1	1			2	WR	EX	EX
DS35	-2.0	0.9	-7.1	1	1	1			3	WR	EX	EX
DS36	-1.5	0.8	-7.5		1				1	HT	EX	IN
DS37	-1.5	0.8	-7.7	1	1	1	1	1	5	WR	EX	NR
DS38	-1.5	0.8	-8.5	1	1			1	3	HT	EX	EX
DS39	-1.5	0.8	-7.2	-1	-1	-1	-1	-1	5	WR	IN	IN

TABLE A1: HISTOLOGICAL LOCATION, MECHANICAL RESPONSES AND THERMAL RESPONSE POLARITY - ALL CELLS

	HISTOLOGY			MECHANICAL RESPONSES								
CELL	AP	L	H	TAIL	HIND	TRUNK	FORE	HEAD	REGIONS	ADEQUATE STIMULUS	MECHANICAL POLARITY	THERMAL POLARITY
SS1	-2.0	-0.8	-8.9		1	1			2	WR	EX	EX
SS2	-1.5	-1.0	-6.7		1				1	HT	EX	EX
SS3	-1.5	-1.0	-7.4	1	1				2	HT	EX	EX
SS4	-1.0	-0.7	-8.4	1	1				2	HT	EX	NR
SS5	-1.5	-0.7	-7.0		1	1		1	3	WR	EX	EX
SS6	-1.5	-0.7	-8.0		1				1	HT	EX	NR
SS7	-1.5	-0.5	-7.9	1	1				2	HT	EX	EX
SS8	-2.0	0.5	-7.1	1	1		1	1	4	HT	EX	EX
SS9	-1.5	0.8	-7.6	-1	-1	-1	-1	-1	5	HT	IN	NR
SS10	-1.5	0.8	-7.6	1	1		1	1	4	HT	EX	EX
SS11	-1.0	0.7	-7.8	-1	-1				2	HT	IN	EX
SS12	-1.5	0.7	-7.5		1		1	1	3	HT	EX	EX
SS13	-2.0	-0.7	-7.5		1	1	1	1	4	WR	EX	EX
SS14	-1.0	0.7	-7.5				1	1	2	HT	EX	NR
SS15	-1.5	-0.6	-7.7	1	1	1	1	1	5	WR	EX	EX
SS16	-1.0	-0.8	-7.3	1	1	1	1	1	5	HT	EX	EX
SS17	-1.0	-0.8	-7.6	1	1			1	3	HT	EX	NR
SS18	-1.0	0.8	-7.3	1	1	1	1	1	5	WR	EX	EX
SS19	-1.0	-0.8	-8.1	1	1	1	1	1	5	HT	EX	EX
SS20	-1.5	-0.8	-9.1	-1	-1	-1	-1	-1	5	WR	IN	IN
SS21	-1.5	0.7	-8.5		1	1			2	HT	EX	EX
SS22	-1.5	0.7	-7.5		1	1		1	3	HT	EX	EX
SS23	-1.5	-0.7	-8.3		1				1	HT	EX	EX
LS1	-1.5	0.8	-6.8	1	1	1		1	4	WR	EX	EX
LS2	-1.5	0.8	-7.4		1	1	1	1	4	WR	EX	EX
LS3	-1.5	0.8	-8.4		1	-1			2	HT	CX	IN
LS4	-1.5	-0.8	-7.1	1	1				2	HT	EX	EX
LS5	-1.0	0.7	-6.9		1	1			2	WR	EX	EX
LS6	-1.0	0.7	-7.2	1	1				2	HT	EX	EX
LS7	-1.0	0.7	-8.1	1	1	1		1	4	HT	EX	IN
LS8	-1.5	-0.8	-6.8		1	1			2	WR	EX	NR
LS9	-1.5	-0.8	-9.0	1	1				2	HT	EX	EX
SI1	-2.0	-0.8	-7.0		1				1	HT	EX	EX
SI2	-2.0	-0.8	-7.4		1	1			2	WR	EX	EX
SI3	-2.0	0.8	-6.5	1	1				2	HT	EX	EX
SI4	-2.0	0.8	-7.2		1	1	1		3	WR	EX	EX
SI5	-2.0	0.7	-8.1		1				1	HT	EX	IN
SI6	-2.0	-0.8	-7.4	1	1				2	HT	EX	EX
SI7	-2.0	-0.8	-8.0	1	1	1			3	HT	EX	IN
SI8	-2.0	-0.8	-8.4	1	1				2	HT	EX	EX
SI9	-2.5	-0.8	-7.5		1				1	HT	EX	EX
SI10	-2.0	0.7	-8.0		-1	-1			2	HT	IN	IN
SI11	-2.5	0.7	-7.2	1	1				2	HT	EX	EX
SI12	-2.5	0.7	-7.7		1				1	HT	EX	NR
SI13	-2.5	0.7	-8.2	-1	-1				2	HT	IN	IN
SI14	-2.5	-0.7	-8.1		1				1	HT	EX	EX
SI15	-2.0	0.6	-7.4	1	1				2	HT	EX	EX
SI16	-2.0	0.6	-8.2	1	1	1	1	1	5	HT	EX	EX
SI17	-2.5	0.7	-6.6	1	1				2	HT	EX	EX
SI18	-2.5	-0.7	-7.3	1	1	1			3	HT	EX	EX
SI19	-2.5	-0.7	-7.6	1	1	1			3	WR	EX	EX
SI20	-1.5	0.5	-7.8	1	1				2	HT	EX	NR
SI21	-1.5	-0.7	-7.9	1	1	1			3	HT	EX	NR
SI22	-1.0	0.7	-7.0	1	1				2	HT	EX	IN
SI23	-1.5	0.7	-7.7	1	1				2	HT	EX	NR
SI24	-1.5	0.7	-8.5	1	1	1			3	WR	EX	EX
SI25	-1.5	0.7	-8.0		1				1	HT	EX	EX
SI26	-1.5	-0.7	-8.5	-1	-1				2	HT	IN	IN
SI27	-2.0	-0.7	-7.9	1	1	1			3	HT	EX	NR
SI28	-1.5	-0.7	-7.9	-1	-1				2	HT	IN	IN
SI29	-1.5	-0.7	-7.5	1	1				2	HT	EX	EX
SI30	-1.5	-0.7	-7.2	1	1				2	HT	EX	EX
SI31	-1.5	0.8	-7.4		1				1	HT	EX	EX

TABLE A2: THERMAL RAMP STIMULI (0,15°C/s, 35-48°C)

CELL	TOTSP1	TOTSP2	MEANSP1	MEANRES	MAXSP2	MINSP2	DMAX	THRESH2	LATENCY2	TPEAK	LOCATION
RA1	432	1106	9.4	3.6	19	7	9.6	40.5	40	42	IPSI
RA2	706	779	5.9	5.1	13	5	7.1	42.8	54	18	IPSI
RA3	3	1022	0.0	15.0	29	0	29.0	38.4	22	58	IPSI
RA4	2	258	0.0	18.4	20	0	20.0	46.0	80	14	IPSI
RA5	1575	1259	16.1	-3.6	16	11	-5.1	35.2	2	70	IPSI
RA6	1334	1368	12.4	3.9	17	16	4.6	44.0	66	18	IPSI
RA7	848	1957	7.1	19.8	39	6	31.9	39.4	34	58	IPSI
RA8	1	772	0.0	18.4	24	0	24.0	42.4	52	22	IPSI
RA9	560	1141	5.2	8.7	18	2	12.8	37.8	22	60	IPSI
RA10	1	271	0.0	4.7	8	0	8.0	40.4	40	26	IPSI
RA11	906	877	8.1	2.1	14	6	5.9	41.6	48	6	IPSI
RA12	1320	1957	12.9	24.1	47	12	34.1	43.4	54	16	IPSI
RA13	1336	367	13.6	-12.0	19	0	-13.6	37.3	18	34	IPSI
RA14	621	1249	5.9	10.9	25	3	19.1	39.4	30	30	IPSI
RA15	2136	2144	21.4	0.1	27	16	5.6				IPSI
RA16	2	566	0.0	9.1	15	0	15.0	40.0	34	32	IPSI
RA17	939	868	10.2	-1.4	12	4	-6.2				IPSI
RA18	3460	1775	33.3	-14.7	35	5	-28.3	37.1	12	64	IPSI
RA19	708	1837	6.3	16.9	28	7	21.7	36.6	12	28	IPSI
RA20	3105	2997	31.1	2.3	40	20	8.9	39.5	30	32	IPSI
RA21	0	2304	0.0	27.4	37	0	37.0	36.5	8	54	IPSI
RA22	6	2434	0.1	36.8	48	0	47.9	38.7	22	28	IPSI
RA23	1241	1191	12.4	2.3	17	11	4.6	40.0	32	56	IPSI
RA24	15	377	0.1	5.5	9	0	8.9	39.6	32	44	IPSI
RA25	779	639	7.6	-1.3	9	5	-2.6	37.4	16	58	IPSI
RA26	51	75	0.5	2.1	4	0	3.5	46.7	70	14	IPSI
RA27	1295	1130	12.7	-0.0	14	12	1.3				IPSI
RA28	2833	2310	25.8	1.7	29	26	3.2				IPSI
RA29	1264	870	11.9	-3.1	12	6	-5.9	36.7	12	58	IPSI
RA30	1516	1209	14.3	-0.1	15	12	-2.3				IPSI
RA31	1	122	0.0	6.7	9	0	9.0	46.1	72	12	IPSI
RA32	545	667	5.1	3.1	11	4	5.9	36.4	8	32	IPSI
RA33	1	687	0.0	15.6	20	0	20.0	42.8	56	14	IPSI
RA34	1881	1712	18.1	-0.2	20	15	-3.1				IPSI
RA35	184	110	2.0	-1.4	7	0	5.0	41.0	40	4	IPSI
RA36	2429	1167	22.9	-19.7	22	3	-19.9	40.9	44	24	IPSI
RA37	2878	3089	27.7	10.3	47	27	19.3	43.2	54	10	IPSI
RA38	1384	1320	13.6	0.0	16	12	2.4				IPSI
RA39	986	1668	9.9	9.7	23	7	13.1	39.2	30	24	IPSI
RA40	2	148	0.0	6.1	10	0	10.0	46.8	76	8	IPSI
RA41	3764	3422	38.4	-4.0	43	31	-7.4	39.3	30	22	IPSI
RA42	1249	658	12.5	-13.4	15	0	-12.5	42.6	56	4	IPSI
RA43	5	1370	0.0	40.1	65	0	65.0	43.5	62	22	IPSI
RA44	1255	1418	13.1	3.3	22	11	8.9	44.1	66	22	IPSI
RA45	36	799	0.4	11.5	18	0	17.6	39.4	36	36	IPSI

TABLE A2: THERMAL RAMP STIMULI (0,15°C/s, 35-48°C)

CELL	TOTSP1	TOTSP2	MEANSP1	MEANRES	MAXSP2	MINSP2	DMAX	THRESH2	LATENCY2	TPEAK	LOCATION
RA46	1375	139	14.6	-14.1	17	0	-14.6	35.7	6	8	IPSI
RA47	995	1082	10.2	0.8	13	7	-3.2	36.4	12	64	IPSI
RA48	2	239	0.0	8.5	12	0	12.0	44.2	70	26	IPSI
RA49	2068	1813	23.0	-9.3	25	10	-13.0	41.3	48	46	IPSI
RA50	2	437	0.0	11.4	18	0	18.0	42.9	58	34	IPSI
RA51	4	286	0.0	7.4	11	0	11.0	43.0	60	22	IPSI
RA52	499	442	5.1	-0.1	7	4	1.9				IPSI
RA53	1129	1379	12.0	3.4	20	6	8.0	37.8	20	40	IPSI
RA54	72	587	0.8	11.8	22	0	21.2	42.0	48	38	IPSI
RA55	1672	2231	19.0	13.7	46	17	27.0	42.6	52	38	IPSI
RA56	422	1004	4.3	9.5	18	2	13.7	39.1	28	20	IPSI
RA57	657	1063	7.3	7.8	17	6	9.7	40.2	34	10	IPSI
RA58	2	1858	0.0	37.1	55	0	55.0	41.0	36	46	IPSI
RA59	2	1254	0.0	34.8	43	0	43.0	43.1	54	22	IPSI
RA60	639	239	6.3	-5.6	9	0	-6.3	39.7	32	8	IPSI
RA61	554	724	6.2	5.0	13	5	6.8	43.3	56	30	IPSI
RA62	515	847	5.7	11.1	19	6	13.3	43.5	54	18	IPSI
RA63	554	805	5.8	3.9	14	4	8.2	39.4	32	58	IPSI
RA64	2	265	0.0	6.6	11	0	11.0	42.4	48	14	IPSI
RA65	1579	1085	16.1	-4.2	23	3	-13.1	37.2	14	42	IPSI
RA66	1576	1333	15.8	-0.8	18	11	-4.8				IPSI
RA67	2	666	0.0	9.8	14	0	14.0	38.7	26	44	IPSI
RA68	9	388	0.1	9.0	16	0	15.9	41.8	46	36	IPSI
RA69	1192	1027	12.4	-2.7	14	8	-4.4	43.6	56	20	IPSI
RA70	2	52	0.0	5.0	7	0	7.0	47.3	78	10	IPSI
RA71	578	784	5.9	4.8	15	4	9.1	39.9	28	54	IPSI
RA72	28	84	0.3	10.2	22	0	21.7	47.9	80	8	IPSI
RA73	72	766	0.8	7.7	12	1	11.2	35.2	4	88	IPSI
RA74	1240	1627	12.2	12.1	31	12	18.8	40.8	34	42	IPSI
RA75	100	651	1.0	8.8	14	1	13.0	38.6	22	46	IPSI
RA76	5	492	0.0	13.5	17	0	17.0	43.0	60	8	IPSI
RA77	1106	1656	11.5	12.1	29	11	17.5	43.2	66	32	IPSI
RA78	586	842	6.5	2.1	10	5	3.5	41.8	50	44	IPSI
RA79	2	684	0.0	13.6	21	0	21.0	42.5	54	20	IPSI
RA80	645	350	7.0	-6.8	9	0	-7.0	41.5	48	18	IPSI
RA81	2	750	0.0	19.7	34	0	34.0	43.6	64	4	IPSI
RA82	860	1291	9.0	6.9	17	9	8.0	42.4	52	20	IPSI
RA83	98	1519	1.0	16.1	31	0	30.0	36.6	12	82	IPSI
RA84	2	653	0.0	19.1	23	0	23.0	43.1	68	12	IPSI
RA85	2	339	0.0	9.9	12	0	12.0	43.7	66	8	IPSI
RA86	680	554	7.6	-6.0	10	0	-7.6	43.1	64	10	IPSI
RA87	981	1934	10.0	21.7	39	9	29.0	42.6	60	8	IPSI
RA88	697	749	7.0	6.1	19	5	12.0	45.6	70	12	IPSI
RA89	2189	1721	22.3	-11.1	28	5	-17.3	43.6	60	22	IPSI
RA90	327	771	3.3	10.8	22	0	18.7	43.0	62	16	IPSI

TABLE A2: THERMAL RAMP STIMULI (0,15°C/s, 35-48°C)

CELL	TOTSP1	TOTSP2	MEANSP1	MEANRES	MAXSP2	MINSP2	DMAX	THRESH2	LATENCY2	TPEAK	LOCATION
RA91	1	367	0.0	14.1	23	0	23.0	45.3	74	20	IPSI
RA92	760	473	8.4	-8.1	9	0	-8.4	42.5	54	12	IPSI
RA93	348	470	3.6	2.6	14	2	10.4	43.3	60	32	IPSI
RA94	1016	1092	10.2	3.9	16	10	5.8	42.3	52		IPSI
RA95	926	1184	9.3	4.3	16	9	6.7	40.5	40	24	IPSI
RA96	710	829	7.7	2.1	12	7	4.3	43.5	64	14	IPSI
RA97	2	779	0.0	25.9	35	0	35.0	44.3	64	22	IPSI
RA98	4	356	0.0	11.7	15	0	15.0	44.0	64	18	IPSI
RA99	335	180	3.4	-4.1	4	0	-3.4	43.6	62	14	IPSI
RA100	1341	1272	13.4	-0.6	16	5	-8.4				IPSI
RA101	763	492	7.3	-3.7	9	1	-6.3	39.9	38	56	IPSI
RA102	137	1142	1.5	15.4	22	0	20.5	40.8	42	46	IPSI
RA103	676	1103	6.9	10.0	24	5	17.1	43.8	62	28	IPSI
RA104	715	496	7.9	-5.7	9	1	-6.9	42.2	50	32	IPSI
RA105	4082	2065	46.4	-26.9	44	0	-46.4	36.3	10	52	IPSI
RA106	4	356	0.0	11.7	15	0	15.0	44.0	64	18	IPSI
RA107	2043	2436	21.3	10.1	39	20	17.7	45.7	82	18	IPSI
RA108	1164	906	11.6	-3.2	12	5	-6.6	37.8	20	70	IPSI
RA109	1091	1620	11.6	5.6	20	11	8.4	39.6	36	44	IPSI
RA110	7	99	0.1	1.2	8	0	7.9	39.0	26	4	IPSI
RA111	1220	1631	13.6	4.4	22	12	8.4	41.4	46	54	IPSI
RA112	2	761	0.0	19.0	30	0	30.0	43.4	56	36	IPSI
RA113	1131	1251	11.5	4.2	20	8	8.5	42.9	54	34	IPSI
RA114	786	919	8.5	2.3	15	6	6.5	44.9	72	28	IPSI
RA115	2200	2388	23.4	2.4	31	21	7.6	40.2	36	60	IPSI
RA116	2720	2115	27.8	-13.8	31	6	-21.8	42.3	54	26	IPSI
RA117	2	834	0.0	15.4	22	0	22.0	41.6	46	50	IPSI
RA3			0.0	10.5	24	0	24.0	38.4	24	62	IPSI2
RA6			12.7	1.7	18	12	5.3	36.6	12	82	IPSI2
RA7			6.6	11.3	30	4	23.4	43.9	62	32	IPSI2
RA20			14.1	11.1	37	11	22.9	41.0	40	44	IPSI2
RA21			0.0	11.3	20	0	20.0	40.8	42	24	IPSI2
RA23			13.8	5.9	22	12	8.2	43.0	50	22	IPSI2
RA29			6.6	-5.4	7	1	-5.6	44.6	64	22	IPSI2
RA34			8.7	4.0	14	7	5.3	44.1	62	26	IPSI2
RA38			9.6	7.0	20	8	10.4	40.0	36	36	IPSI2
RA69			0.0	8.3	12	0	12.0	44.8	64	22	IPSI2
RA71			0.0	5.9	10	0	10.0	42.8	48	34	IPSI2
RA74			13.0	10.7	35	13	22.0	36.9	10	70	IPSI2
RA75			0.0	6.3	9	0	9.0	41.7	40	26	IPSI2
RA76			0.1	8.0	16	0	15.9	39.4	32	38	IPSI2
RA77			12.7	4.7	23	12	10.3	41.2	46	50	IPSI2
RA79			0.0	9.0	17	0	17.0	43.9	64	22	IPSI2

TABLE A2: THERMAL RAMP STIMULI (0,15°C/s, 35-48°C)

CELL	TOTSP1	TOTSP2	MEANSP1	MEANRES	MAXSP2	MINSP2	DMAX	THRESH2	LATENCY2	TPEAK	LOCATION
RA82			8.1	5.8	17	8	8.9	39.9	40	38	IPSI2
RA83			0.0	2.8	6	0	6.0	44.5	68	24	IPSI2
RA84			0.0	11.4	20	0	20.0	41.5	56	44	IPSI2
RA85			0.0	7.1	11	0	11.0	37.6	20	60	IPSI2
RA86			8.6	-7.4	11	0	-8.6	42.2	54	12	IPSI2
RA87			11.2	8.4	27	10	15.8	43.7	62	30	IPSI2
RA90			2.0	3.1	11	0	9.0	44.4	78	22	IPSI2
RA93			3.4	0.3	14	3	10.6	42.2	52	40	IPSI2
RA96			7.8	2.4	11	8	3.2	43.7	62	18	IPSI2
RA97			0.0	14.6	24	0	24.0	45.0	72	16	IPSI2
RA103			8.9	9.5	25	8	16.1	42.6	52	12	IPSI2
RA104			8.4	-2.9	12	1	-7.4	43.4	64	32	IPSI2
RA105			32.5	-17.6	38	1	-31.5	45.0	68	16	IPSI2
RA107			22.9	14.5	48	22	25.1	44.0	66	30	IPSI2
RA110			0.0	1.8	7	0	7.0	38.1	22	4	IPSI2
RA111			30.3	-1.2	32	26	-4.3	40.8	38	66	IPSI2
RA112			0.1	8.2	13	0	12.9	45.2	70	22	IPSI2
RA116			34.6	-18.1	38	8	-26.6	42.1	50	34	IPSI2
RA117			0.0	6.0	13	0	13.0	45.6	76	20	IPSI2
RA8	0	397	0.0	10.4	17	0	17.0	43.3	60	10	CONTRA
RA9	696	1198	7.3	8.2	20	8	12.7	41.1	46	42	CONTRA
RA10	2	431	0.0	7.2	9	0	9.0	39.9	36	40	CONTRA
RA12	1200	1778	12.5	18.5	37	12	24.5	43.5	58	16	CONTRA
RA13	1408	471	13.5	-11.6	15	0	-13.5	38.7	26	26	CONTRA
RA14	1364	1458	13.6	2.0	22	12	8.4	42.8	54	6	CONTRA
RA15	2167	1735	20.4	-2.9	25	13	-7.4	39.3	30	20	CONTRA
RA18	3126	1189	31.3	-21.7	33	1	-30.3	37.4	16	44	CONTRA
RA19	620	1629	6.1	15.5	30	6	23.9	37.5	20	50	CONTRA
RA20	1644	2112	16.1	17.4	46	15	29.9	43.3	52	28	CONTRA
RA21	0	826	0.0	17.2	31	0	31.0	41.3	40	38	CONTRA
RA22	2	1600	0.0	24.2	37	0	37.0	39.2	28	44	CONTRA
RA23	1494	1618	14.1	6.7	24	13	9.9	42.7	50	12	CONTRA
RA24	5	477	0.0	10.3	12	0	12.0	42.0	48	26	CONTRA
RA25	785	555	7.7	-2.1	9	4	-3.7	41.7	40	26	CONTRA
RA26	216	245	2.2	0.8	6	0	3.8	37.8	18	24	CONTRA
RA27	1221	1050	11.7	0.2	13	12	1.3				CONTRA
RA28	2252	2100	21.7	3.7	29	21	7.3	36.6	8	78	CONTRA
RA31	0	22	0.0	1.8	4	0	4.0	46.9	80	10	CONTRA
RA32	2	356	0.0	5.0	10	0	10.0	38.0	20	56	CONTRA
RA33	3	251	0.0	7.8	11	0	11.0	44.2	66	22	CONTRA
RA34	4	382	0.0	14.6	18	0	18.0	44.0	60	22	CONTRA
RA35	208	212	2.2	0.7	5	0	2.8	45.7	70		CONTRA
RA38	1041	1109	10.2	3.0	19	9	8.8	43.9	62	34	CONTRA

TABLE A2: THERMAL RAMP STIMULI (0,15°C/s, 35-48°C)

CELL	TOTSP1	TOTSP2	MEANSP1	MEANRES	MAXSP2	MINSP2	DMAX	THRESH2	LATENCY2	TPEAK	LOCATION
RA39	1053	1236	10.5	4.0	20	8	9.5	42.8	54	12	CONTRA
RA41	4006	3492	38.5	-3.0	41	29	-9.5	38.9	28	56	CONTRA
RA44	4	650	0.0	14.7	20	0	20.0	42.4	56	16	CONTRA
RA45	1	871	0.0	12.1	20	0	20.0	38.3	22	68	CONTRA
RA47	1076	1089	10.8	0.1	12	10	1.2				CONTRA
RA48	2	374	0.0	12.4	17	0	17.0	44.4	70	28	CONTRA
RA49	1236	632	13.1	-6.7	13	2	-11.1	35.8	4	70	CONTRA
RA50	2	238	0.0	9.1	12	0	12.0	44.6	72	20	CONTRA
RA51	5	213	0.0	4.7	10	0	10.0	42.2	54	14	CONTRA
RA52	411	553	5.1	2.5	9	4	3.9	45.7	78	6	CONTRA
RA53	566	595	6.6	-1.7	11	4	4.4	45.1	74	20	CONTRA
RA54	325	1210	3.6	12.8	22	1	18.4	38.8	26	44	CONTRA
RA55	2298	2450	23.4	11.4	45	16	21.6	43.2	54	12	CONTRA
RA56	309	582	3.0	5.5	20	1	17.0	39.8	34	16	CONTRA
RA57	686	1250	7.6	8.8	21	7	13.4	38.8	26	16	CONTRA
RA58	2	2074	0.0	33.0	40	0	40.0	36.9	14	58	CONTRA
RA59	18	1245	0.2	20.5	30	0	29.8	39.8	32	54	CONTRA
RA62	536	771	5.8	5.6	16	3	10.2	41.8	46	22	CONTRA
RA63	69	346	0.1	5.5	9	0	8.9	40.6	38	36	CONTRA
RA64	3	49	0.0	1.4	5	0	5.0	43.3	58	8	CONTRA
RA65	1609	1381	17.5	-4.2	21	6	-11.5	40.6	38	30	CONTRA
RA67	2	113	0.0	2.5	6	0	6.0	41.6	44	28	CONTRA
RA68	100	772	1.1	11.2	19	0	17.9	39.5	30	50	CONTRA
RA69	2	434	0.0	10.8	14	0	14.0	42.6	48	28	CONTRA

TABLE A3: STEP SERIES (60 s, 2°C/s), ASCENDING

CELL	MEANT1	MEANT2	MEANT3	MEANT4	TOTSP1	TOTSP2	TOTSP3	TOTSP4	MEANSP1	MEANSP2	MEANSP3	MEANSP4	DMEAN2	DMEAN3	DMEAN4
DS1	34.9	39.7	44.6	35.5	1399	1518	1624	1384	22.9	25.3	27.1	23.1	2.4	4.1	0.1
DS2	34.8	39.6	44.5	35.5	411	433	506	508	6.7	7.2	8.4	8.5	0.5	1.7	1.7
DS3	34.9	39.7	44.7	35.6	363	329	362	396	6.0	5.5	6.0	6.6	-0.4	0.1	0.6
DS4	35.1	39.9	44.8	35.6	1301	1234	2216	2492	21.3	20.6	43.5	41.5	-0.7	22.1	20.2
DS5	35.4	40.3	45.2	36.0	767	680	974	996	10.8	11.3	16.2	16.9	0.5	5.4	6.1
DS6	35.0	39.7	44.7	35.4	543	1666	2686	3090	9.1	27.3	44.8	51.5	18.3	35.7	42.5
DS7	35.0	39.8	44.8	35.8	0	0	676	851	0.0	0.0	11.1	14.2	0.0	11.1	14.2
DS8	35.0	39.8	44.9	35.7	2039	2151	2295	1191	34.0	35.9	38.3	33.2	1.9	4.3	-0.7
DS9															
DS10	35.6	40.4	43.4	36.1	1745	1736	574	622	29.1	28.9	9.4	10.4	-0.1	-19.6	-18.6
DS11	35.8	40.6	43.7	36.3	378	608	1069	714	6.3	10.1	17.8	11.9	3.8	11.5	5.6
DS12	35.7	40.5	43.6	36.2	1	0	1236	1498	0.0	0.0	20.6	25.0	0.0	20.6	25.0
DS13															
DS14	35.0	39.8	42.9	35.5	1060	1118	1208	1071	17.7	18.3	20.5	17.9	0.7	2.8	0.2
DS15	34.9	39.7	42.8	35.4	1	0	737	826	0.0	0.0	12.3	13.8	0.0	12.3	13.8
DS16	35.0	39.8	42.9	35.5	901	998	1081	1223	15.0	16.6	18.0	20.4	1.6	3.0	5.4
DS17	35.0	39.8	42.9	35.5	322	494	498	416	5.3	8.2	8.6	6.9	3.0	3.3	1.7
DS18	35.1	39.9	43.0	35.7	637	618	584	588	10.6	10.3	9.7	9.8	-0.2	-0.8	-0.7
DS19	35.0	39.8	42.9	35.5	1585	1629	1493	1514	26.4	26.7	25.3	25.2	0.3	-1.0	-1.1
DS20	34.9	39.6	42.8	35.4	1438	1505	1782	1537	24.0	24.7	30.2	25.6	0.7	6.2	1.7
DS21	35.0	39.8	42.8	35.5	1116	1122	1116	1136	18.6	18.7	18.6	18.9	0.1	0.0	0.3
DS22	35.0	39.9	42.9	35.4	975	998	987	924	16.3	16.6	16.5	15.4	0.4	0.2	-0.8
DS23	35.0	39.8	42.9	35.6	2638	2160	1023	1714	44.0	36.0	17.1	28.6	-7.9	-26.8	-15.3
DS24	35.0	39.8	42.9	35.6	731	770	966	938	12.0	13.1	15.8	15.6	1.1	3.9	3.6
DS25	35.0	39.8	42.8	35.3	784	979	1181	1009	13.1	16.3	19.7	16.8	3.3	6.6	3.8
DS26	35.0	39.5	42.5	35.4	0	117	442	599	0.0	2.0	7.4	10.0	2.0	7.4	10.0
DS27															
DS28															
DS29	35.0	39.5	42.4	35.5	292	260	495	338	4.9	4.3	8.3	5.6	-0.4	3.4	0.8
DS30															
DS31	34.8	39.3	42.3	35.4	465	457	1019	674	7.8	7.6	17.0	11.2	0.0	9.2	3.5
DS32	35.0	39.5	42.5	35.5	310	325	836	599	5.2	5.4	13.9	10.0	0.3	8.8	4.8
DS33															
DS34	35.0	39.5	42.5	35.5	2477	2672	3149	943	41.3	44.5	52.5	15.7	3.3	11.2	-25.5
DS35	35.0	39.5	42.5	35.5	59	58	1109	573	1.0	1.0	18.5	9.6	0.0	17.5	8.6
DS36	36.5	39.1	43.8	36.9	1300	1110	1015	1059	21.7	18.5	16.9	17.7	-3.1	-4.7	-3.9
DS37	36.5	39.1	43.8	36.9	0	0	0	277	0.0	0.0	0.0	4.6	0.0	0.0	4.6
DS38	36.5	39.1	43.8	36.9	206	225	315	237	3.4	3.8	5.3	4.0	0.3	1.8	0.5
DS39	36.5	39.1	43.8	36.9	2017	1974	1339	943	33.6	32.9	22.3	15.7	-0.6	-11.2	-17.8

TABLE A3:

CELL	MAXSP1	MAXSP2	MAXSP3	MAXSP4	MINSP1	MINSP2	MINSP3	MINSP4	LATENCY2	LATENCY3	LATENCY4	TIMEPK21	TIMEPK31	TIMEPK41
DS1	24	26	29	28	22	22	24	21	4	3	2	7	6	33
DS2	8	9	10	11	5	6	7	7	36	35	13			65
DS3	7	7	8	8	4	3	4	5						
DS4	23	22	52	47	19	19	21	32		2	2		8	8
DS5	18	15	23	22	7	7	7	12		9	1		47	51
DS6	12	36	59	64	7	8	25	35	4	3		35	8	1
DS7	0	0	18	20	0	0	0	6		8			20	0
DS8	38	39	41	42	32	34	35	27		3	7		10	9
DS9														
DS10	32	31	31	16	23	26	2	4		4	4		60	61
DS11	10	16	20	16	3	5	13	6	15	4	1	58	17	54
DS12	1	0	27	27	0	0	0	23		4			58	
DS13														
DS14	21	21	24	23	13	15	16	13		3	1		38	57
DS15	1	0	16	16	0	0	0	11		6			23	
DS16	18	19	22	23	12	14	14	17						
DS17	7	10	12	10	3	5	6	4	6	13	11	36	15	67
DS18	12	12	13	11	9	9	8	8						
DS19	27	28	28	26	25	26	23	23		17	9		40	13
DS20	26	27	34	33	22	22	23	22		3	1		14	59
DS21	21	22	22	21	17	15	15	16						
DS22	17	18	21	17	15	15	15	13						
DS23	50	50	36	35	37	24	4	19	11	4	1	32	5	69
DS24	14	16	18	17	9	10	12	15	12	11	1	16	21	61
DS25	15	18	22	21	11	12	16	13	4	3	10	34	12	62
DS26	0	6	13	12	0	0	1	8	18	5	2	51	21	64
DS27														
DS28														
DS29	6	6	10	10	4	3	5	4		2	4		38	68
DS30														
DS31	10	9	20	19	7	6	8	10		4	2		24	18
DS32	7	8	20	21	4	4	7	7	50	4	4		58	68
DS33														
DS34	44	48	57	52	39	39	40	0	8	4	2	26	8	32
DS35	3	4	23	22	0	0	0	3		4	2		28	68
DS36	29	22	22	24	11	12	11	9						
DS37	0	0	0	12	0	0	0	0						
DS38	6	7	11	8	0	0	0	0			6		19	
DS39	37	36	35	25	30	30	8	9		23			35	

TABLE A4: DOUBLE STEP SERIES (60 s, 2°C/s), DESCENDING

CELL	MEANT1	MEANT2	MEANT3	MEANT4	TOTSP1	TOTSP2	TOTSP3	TOTSP4	MEANSP1	MEANSP2	MEANSP3	MEANSP4	DMEAN2	DMEAN3	DMEAN4
DS1	34.9	44.3	40.1	35.1	1000	1218	1077	1008	16.4	20.3	18.0	16.8	3.9	1.6	0.4
DS2	35.0	44.4	40.3	35.2	459	497	503	441	7.5	8.3	8.4	7.4	0.8	0.9	-0.1
DS3															
DS4	35.1	44.6	40.3	35.4	935	2322	2037	1986	15.3	38.7	34.0	33.1	23.4	18.6	17.8
DS5															
DS6	35.0	44.5	40.2	35.2	401	2630	1760	768	6.6	43.8	29.3	12.8	37.3	22.8	6.2
DS7	35.0	44.4	40.2	35.3	1665	1437	1273	113	27.8	24.0	21.2	1.9	-3.7	-6.4	-25.8
DS8	35.0	44.5	40.3	35.2	881	1918	1881	1846	14.7	32.0	31.4	30.8	17.3	16.7	16.1
DS9	35.0	44.5	40.3	35.2	0	243	74	0	0.0	4.0	1.2	0.0	4.0	1.2	0.0
DS10	35.6	43.1	40.7	35.9	1943	771	730	1040	32.4	12.9	12.2	17.3	-19.4	-20.1	-15.0
DS11	35.8	43.5	41.0	36.1	974	1107	613	508	16.2	18.5	10.2	8.5	2.2	-5.9	-7.7
DS12															
DS13	35.0	42.6	40.2	35.2	1395	1426	1418	1423	23.3	23.8	23.6	23.7	0.5	0.4	0.5
DS14	35.0	42.7	40.2	35.2	0	335	451	609	0.0	5.7	7.5	10.2	5.7	7.5	10.2
DS15	34.9	42.6	40.2	35.2	0	197	566	142	0.0	3.3	9.4	2.4	3.3	9.4	2.4
DS16															
DS17	35.0	42.6	40.1	35.3	212	338	390	335	3.5	5.6	6.5	5.6	2.1	3.0	2.1
DS18															
DS19	35.0	42.5	40.2	35.2	1534	1554	1543	1501	25.6	25.9	25.7	25.0	0.3	0.1	-0.5
DS20	34.9	42.5	40.1	35.2	1540	1739	1506	1473	25.7	29.0	25.1	24.6	3.3	-0.5	-1.0
DS21	35.0	42.6	40.1	35.2	1198	865	976	1114	20.3	14.2	16.3	18.6	-6.0	-3.9	-1.6
DS22	35.0	42.4	40.2	35.3	905	932	937	1052	15.1	15.5	15.6	17.5	0.5	0.5	2.5
DS23	35.1	42.6	40.2	35.2	2758	2584	2761	2575	46.0	43.1	41.8	42.9	-0.3	-4.0	-3.0
DS24	35.0	42.7	40.1	35.4	907	899	913	877	15.1	15.0	15.2	14.6	0.0	0.1	-0.4
DS25	35.0	42.6	40.1	35.2	469	878	969	791	7.8	14.6	16.2	13.2	6.8	8.3	5.4
DS26	34.9	42.4	39.7	35.0	218	611	612	412	3.5	10.2	10.2	6.9	6.7	6.7	3.4
DS27	34.8	42.0	39.7	35.1	482	172	4	38	8.0	2.9	0.1	0.6	-5.1	-7.9	-7.3
DS28	35.0	42.2	39.9	35.3	2000	1659	1462	1688	33.3	27.7	24.4	28.1	-5.6	-8.9	-5.1
DS29															
DS30	35.0	42.2	39.9	35.3	937	1504	1312	1091	15.6	25.1	21.9	18.2	9.5	6.3	2.6
DS31															
DS32															
DS33	35.0	42.5	40.2	35.3	4	1	1	1	0.0	0.0	0.0	0.0	0.0	0.0	0.0
DS34															
DS35	35.0	42.2	39.9	35.3	12	7.99	542	382	0.2	13.3	9.0	6.4	13.1	8.8	6.2
DS36	36.5	43.6	39.5	36.6	1897	1216	1210	1925	31.6	20.3	20.2	32.1	-11.3	-11.4	0.5
DS37															
DS38	36.5	43.6	39.5	36.6	259	356	298	211	4.3	5.9	5.0	3.5	1.6	0.7	-0.7
DS39	36.5	43.6	39.5	36.6	1638	900	890	903	27.3	15.0	14.8	15.1	-12.2	-12.4	-12.2

TABLE A4:

CELL	MAXSP1	MAXSP2	MAXSP3	MAXSP4	MINSP1	MINSP2	MINSP3	MINSP4	LATENCY	LATENCY	LATENCY	TIMEPK21	TIMEPK31	TIMEPK41
DS1	18	22	22	18	15	16	16	16	4	3		19	28	
DS2	13	10	10	9	6	5	6	6	5	36				
DS3														
DS4	18	49	42	39	13	16	28	24	4	1		15	12	42
DS5														
DS6	9	56	54	26	5	6	14	6	3	1	1	49	55	39
DS7	30	28	24	17	25	20	18	0	10		1	51	0	15
DS8	19	38	37	33	13	13	28	29	6	3		24	45	55
DS9	0	14	14	0	0	0	0	0	33	1		53	9	
DS10	35	37	15	24	27	6	7	11	6	3	7	47	38	68
DS11	19	21	19	14	13	16	7	5	2	3		19	31	
DS12														
DS13	25	27	25	26	21	21	21	21						
DS14	0	13	12	13	0	0	4	7	13	1		46	19	
DS15	0	13	12	9	0	0	6	0	38		5			
DS16														
DS17	6	8	8	7	1	3	5	3	20	35	19	49		49
DS18														
DS19	29	27	27	27	24	25	24	23						
DS20	28	32	29	29	24	24	22	22	3	1	1	19	23	59
DS21	24	22	19	22	16	9	11	12	4	5		9	58	
DS22	17	17	17	19	13	12	14	16						
DS23	54	49	49	48	40	32	32	36						
DS24	17	16	17	16	13	13	13	13						
DS25	10	18	18	16	6	7	14	10	5	9	7	53	43	35
DS26	5	15	15	9	2	1	7	5	8	2	2	40	10	66
DS27	10	10	1	3	6	0	0	0	8		26	54		68
DS28	35	36	28	31	30	21	21	22	18		22	54		32
DS29														
DS30	18	31	31	22	14	17	19	16	6	4	6	54	36	68
DS31														
DS32														
DS33	2	1	1	1	0	0	0	0						
DS34														
DS35	1	19	19	12	0	0	4	4	4	4		60	36	
DS36	47	30	23	54	21	16	17	20	1		1	14		
DS37														
DS38	7	8	10	6	2	2	2	1	16	2		33	47	45
DS39	30	27	21	28	24	4	9	6	13			20		

TABLE A5: SINGLE STEP SERIES (30 s, 2°C/s)

CELL	TEMP	TOTSP1	TOTSP2	TOTSP3	MEANSP1	MEANSP2	MEANSP3	DMEAN2	DMEAN3	MAXSP1	MAXSP2	MAXSP3
SS1	40	143	152	122	4.8	5.1	4.1	0.3	-0.6	11	14	11
SS2	40	282	286	270	9.4	9.5	9	0.1	-0.3	10	10	9
SS3	40	630	611	604	21	20.4	20.1	-0.5	-0.8	21	22	21
SS4	40	426	407	400	14.2	13.6	13.3	-0.5	-0.8	14	14	14
SS5	40	0	0	1	0	0	0	0	0	0	0	1
SS6	40	259	260	275	8.6	8.7	9.2	0.8	0.5	9	9	10
SS7	40	297	261	230	9.4	8.7	8.1	-0.5	-1.2	11	14	14
SS8	40	3	2	3	0.1	0.1	0.1	0	0	3	2	3
SS9	40	256	249	237	8.2	8.2	8.3	0.1	0.2	11	14	11
SS10	40	367	380	318	11.9	12.4	11.2	0.6	-0.6	17	19	14
SS11	40	776	706	629	25.1	23.1	22.1	-1.9	-2.8	31	25	28
SS12	40	999	948	956	31.9	32.1	32.8	0.2	0.9	36	36	39
SS13	40	352	409	440	11.2	13.7	15.3	2.4	4	17	19	19
SS14	40	526	466	438	16.8	15.6	15.2	-1.1	-1.5	19	19	19
SS15	40	71	77	80	2.3	2.6	2.8	0.3	0.5	8	6	6
SS16	40	443	450	409	14.1	14.9	14.4	0.7	0.2	22	22	22
SS17	40	450	395	39	14.2	13.2	14	-0.9	-0.1	17	17	17
SS18	40											
SS19	40											
SS20	40											
SS21	40											
SS22	40											
SS23	40											
SS1	42	145	239	162	4.9	8	5.4	3.1	0.6	14	17	14
SS2	42	257	269	250	8.6	9	8.3	0.4	-0.1	9	10	9
SS3	42	572	575	542	19.1	19.2	18.1	0.1	-0.9	20	21	20
SS4	42	390	396	399	13	13.2	13.3	0.2	0.3	13	13	14
SS5	42	0	0	10	0	0	0.3	0	0.3	0	0	2
SS6	42	269	279	284	9	9.3	9.5	0.3	0.5	9	10	10
SS7	42	263	282	240	8.4	9.3	8.4	0.9	0	14	14	11
SS8	42	4	0	3	0.1	0	0.1	0	0	3	0	3
SS9	42	242	200	184	7.6	6.8	6.4	-0.8	-1.2	11	11	11
SS10	42	413	392	300	13.2	13.1	10.4	0	-2.7	19	19	17
SS11	42	580	588	575	18.7	19.4	20	0.7	1.2	22	22	22
SS12	42	1038	1051	999	33.1	34.8	35.1	1.6	2	36	39	39
SS13	42	606	604	568	19.3	20	20	0.6	0.6	22	22	25
SS14	42	420	422	380	13.4	14	13.4	0.5	0	17	17	19
SS15	42	92	95	100	2.9	3.1	3.5	0.2	0.6	8	6	8
SS16	42	474	514	486	15.1	17	17.1	1.9	2	22	28	31
SS17	42	568	549	524	17.9	18.4	18.4	0.4	0.5	19	19	22
SS18	42	502	487	446	15.8	16.1	15.9	0.3	0	19	19	19
SS19	42	293	264	251	9.4	8.7	8.8	-0.5	-0.4	14	14	17
SS20	42	301	440	431	9.6	14.6	15.2	4.9	5.5	14	25	19
SS21	42	278	209	176	8.9	6.9	6.2	-1.9	-2.6	14	11	11
SS22	42	475	444	483	15.2	14.7	17	-0.4	1.8	19	19	22
SS23	42	72	70	59	2.3	2.3	2.1	0	-0.1	8	8	11
SS1	44	152	275	70	5.1	9.2	2.3	4.1	-2.6	17	17	11
SS2	44	244	258	264	8.1	8.6	8.8	0.5	0.7	9	9	10
SS3	44	571	572	577	19	19.1	19.2	0	0.2	20	20	20
SS4	44	403	410	408	13.4	13.7	13.6	0.2	0.2	14	14	14
SS5	44	0	0	1	0	0	0	0	0	0	0	1
SS6	44	266	290	295	8.9	9.7	9.8	0.8	1	9	10	10

TABLE A5:

CELL	TEMP	MINSP1	MINSP2	MINSP3	LATENCY2	LATENCY3	TIMEPK21	TIMEPK31
SS1	40	0	0	0	7.9			
SS2	40	9	9	8				
SS3	40	21	19	19				
SS4	40	14	13	13				
SS5	40	0	0	0				
SS6	40	8	8	9				
SS7	40	6	6	3				
SS8	40	0	0	0				
SS9	40	6	6	6				
SS10	40	8	8	8				
SS11	40	19	19	19				
SS12	40	28	31	31				
SS13	40	8	11	8				
SS14	40	14	14	14				
SS15	40	0	0	0				
SS16	40	8	8	6				
SS17	40	11	11	11				
SS18	40							
SS19	40							
SS20	40							
SS21	40							
SS22	40							
SS23	40							
SS1	42	0	0	0	3.2	1.8	4	
SS2	42	8	8	7	5			
SS3	42	18	18	17				
SS4	42	13	13	13				
SS5	42	0	0	0				
SS6	42	9	9	9				
SS7	42	6	6	6				
SS8	42	0	0	0				
SS9	42	6	3	3				
SS10	42	8	6	6				
SS11	42	14	14	17	14.4	0.7		
SS12	42	31	31	33				
SS13	42	17	17	17				
SS14	42	11	11	11				
SS15	42	0	0	0				
SS16	42	8	8	8	9.4		23.4	11.9
SS17	42	14	17	14				
SS18	42	14	14	14				
SS19	42	6	6	3				
SS20	42	6	6	11	2.2	0.7	5.8	28.1
SS21	42	6	3	3				
SS22	42	11	11	14				
SS23	42	0	0	0				
SS1	44	0	3	0		3.2		
SS2	44	8	8	8				
SS3	44	18	19	19				
SS4	44	13	13	13				
SS5	44	0	0	0				
SS6	44	9	9	9				

TABLE A5: SINGLE STEP SERIES (30 s, 2°C/s)

CELL	TEMP	TOTSP1	TOTSP2	TOTSP3	MEANSP1	MEANSP2	MEANSP3	DMEAN2	DMEAN3	MAXSP1	MAXSP2	MAXSP3
SS7	44	280	422	434	8.8	14.1	15.3	5.3	6.4	14	25	19
SS8	44	1	1	2	0	0	0.1	0	0	1	1	1
SS9	44	0	0	0	0	0	0	0	0	0	0	0
SS10	44	401	413	269	12.8	13.7	9.5	0.9	-3.2	19	22	14
SS11	44	829	934	769	26.2	31.3	27	5.1	0.9	31	36	33
SS12	44	1126	1142	1099	35.5	38.2	38.6	2.7	3.1	39	44	44
SS13	44	676	674	650	21.8	22	22.9	0.2	1	25	25	28
SS14	44	345	359	343	11	11.9	12.1	0.9	1	14	17	14
SS15	44	147	164	226	4.7	5.5	7.8	0.8	3.2	8	8	11
SS16	44	781	899	858	24.7	30.1	30.2	5.4	5.5	33	36	39
SS17	44	646	616	607	20.6	20.4	21.3	-0.2	0.7	22	25	25
SS18	44	522	501	463	16.5	16.8	16.3	0.3	-0.1	22	22	19
SS19	44	255	238	229	8.1	8	8	-0.1	-0.1	14	11	11
SS20	44	624	418	421	19.9	14	14.6	-5.8	-5.2	22	22	19
SS21	44	150	258	231	4.8	8.5	8.1	3.7	3.3	8	11	11
SS22	44	442	592	626	14.1	19.8	21.7	5.7	7.6	17	22	25
SS23	44	51	68	70	1.6	2.2	2.5	0.6	0.8	11	8	8
SS1	46	266	341	244	8.9	11.4	8.2	2.5	0.6	17	17	14
SS2	46	253	312	276	8.4	10.4	9.2	2	0.8	9	11	11
SS3	46	540	557	576	18	18.6	19.2	0.6	1.2	19	20	20
SS4	46	406	414	411	13.5	13.8	13.7	0.3	0.2	14	14	14
SS5	46	0	0	3	0	0	0.1	0	0.1	0	0	1
SS6	46	293	318	312	9.8	10.6	10.4	0.8	0.6	10	11	12
SS7	46	323	595	487	10.4	19.7	16.9	9.2	6.5	14	28	28
SS8	46	0	0	2	0	0	0.1	0	0.1	0	0	1
SS9	46											
SS10	46	351	460	231	11.2	15.2	8.1	4	-3	17	22	17
SS11	46	867	903	800	27.7	30.2	27.8	2.5	0.1	31	36	36
SS12	46	1138	1170	1154	36.3	39.2	40.1	2.8	3.7	39	44	44
SS13	46	716	716	678	22.9	24	23.5	1.1	0.7	28	31	28
SS14	46											
SS15	46	272	314	299	8.7	10.5	10.4	1.8	1.7	11	17	17
SS16	46	530	596	828	16.9	19.7	29.1	2.8	12.2	28	33	36
SS17	46	693	642	603	21.9	21.5	21.2	-0.3	-0.6	25	25	25
SS18	46	529	518	498	16.9	17.3	17.3	0.4	0.4	19	22	22
SS19	46	255	236	185	8.1	7.8	6.5	-0.2	-1.5	11	14	14
SS20	46	550	257	376	17.6	8.6	13.1	-8.9	-4.4	22	22	19
SS21	46	275	291	269	8.8	9.6	9.5	0.8	0.7	11	14	11
SS22	46	602	693	680	19.2	22.9	23.9	3.7	4.7	22	28	28
SS23	46	140	183	159	4.5	6.1	5.5	1.7	1.1	11	11	11
SS1	48	99	298	241	3.3	10	8.1	6.7	4.8	19	17	14
SS2	48	212	294	275	7.1	9.8	9.2	2.7	2.1	8	11	10
SS3	48	527	568	570	17.6	18.9	19	1.4	1.4	19	19	19
SS4	48	408	421	413	13.6	14	13.8	0.4	0.2	14	14	14
SS5	48	0	141	57	0	4.7	1.9	4.7	1.9	0	9	9
SS6	48	252	264	308	8.4	8.8	10.3	0.4	1.9	9	11	12
SS7	48	316	703	591	10.2	23.2	20.5	13	10.3	14	33	31
SS8	48	0	74	18	0	2.4	0.6	2.4	0.6	0	14	14
SS9	48											
SS10	48	302	494	230	9.6	16.3	8.1	6.7	-1.5	14	22	19
SS11	48	850	915	771	27.1	30.6	26.8	3.5	-0.3	31	36	36
SS12	48	1011	1090	1122	32.3	36.5	39	4.2	6.7	36	42	44

TABLE A5:

CELL	TEMP	MINSP1	MINSP2	MINSP3	LATENCY2	LATENCY3	TIMEPK21	TIMEPK31
SS7	44	6	6	11	6.1	0.4	22.3	17.6
SS8	44	0	0	0				
SS9	44	0	0	0				
SS10	44	8	6	6	5.8		8.6	19.4
SS11	44	22	25	22	3.2	0.4	20.9	8.3
SS12	44	33	33	36	4.3	0.4	29.5	15.1
SS13	44	19	19	19				
SS14	44	8	8	8				
SS15	44	3	3	3	16.2		24.5	7.9
SS16	44	8	22	22				
SS17	44	19	17	19				
SS18	44	14	14	11				
SS19	44	3	6	3				
SS20	44	17	6	8	7.6	4	16.9	11.2
SS21	44	3	3	6	3.2	0.4	4.3	22.7
SS22	44	11	14	19	1.1	0.4	18.4	19.1
SS23	44	0	0	0				
SS1	46	6	6	3	2.5	0.4	8.3	16.2
SS2	46	8	9	8	5	5		
SS3	46	16	17	19				
SS4	46	13	14	13				
SS5	46	0	0	0				
SS6	46	9	10	10				
SS7	46	8	8	11	4.7	0.4	23	14
SS8	46	0	0	0				
SS9	46							
SS10	46	8	11	3	3.6	0.4	5	11.5
SS11	46	22	25	22	5.8	0.7	11.9	10.1
SS12	46	33	33	36	1.8	0.4	3.2	5
SS13	46	19	17	22				
SS14	46							
SS15	46	6	3	6	3.6	0.7	25.6	22.3
SS16	46	6	8	11	15.8		30.2	
SS17	46	19	19	17				
SS18	46	11	14	14				
SS19	46	3	3	0				
SS20	46	11	0	6	5	0.7	15.1	6.5
SS21	46	6	6	8				
SS22	46	17	17	22	5.8	0.4	16.9	24.5
SS23	46	0	0	0	5	0.4	29.5	21.6
SS1	48	0	0	6	2.9	0.4	5.4	9
SS2	48	6	7	8	5		15	15
SS3	48	16	19	18				
SS4	48	13	13	13				
SS5	48	0	0	0	10	5	30	15
SS6	48	8	7	9	20	5	30	30
SS7	48	6	6	14	1.8	0.4	2.9	19.4
SS8	48	0	0	0	21.2	0.4	29.9	2.5
SS9	48							
SS10	48	3	8	3	2.9	0.7	12.2	6.8
SS11	48	22	25	22	4.7	0.4	29.5	21.2
SS12	48	28	28	36	3.6	0.4	27.4	4.7

TABLE A5: SINGLE STEP SERIES (30 s, 2°C/s)

CELL	TEMP	TOTSP1	TOTSP2	TOTSP3	MEANSP1	MEANSP2	MEANSP3	DMEAN2	DMEAN3	MAXSP1	MAXSP2	MAXSP3
SS13	48	744	763	706	23.8	25.5	24.5	1.8	0.8	28	28	31
SS14	48											
SS15	48	179	290	264	5.7	9.6	9.3	3.9	3.6	8	17	17
SS16	48	3	576	548	0.1	19.5	19	19.4	18.9	1	31	31
SS17	48	687	696	622	21.9	23	21.9	1.1	0	25	28	25
SS18	48	546	614	501	17.4	20.5	17.4	3.1	0	22	25	25
SS19	48	278	320	268	8.9	10.7	9.3	1.8	0.4	14	14	17
SS20	48	494	169	449	15.8	5.6	15.8	-10.1	0	19	19	22
SS21	48	277	394	262	8.9	13	9.1	4.1	0.2	11	17	14
SS22	48											
SS23	48	143	376	279	4.6	12.6	9.7	8	5.1	11	25	25
SS1	50											
SS2	50											
SS3	50											
SS4	50											
SS5	50											
SS6	50											
SS7	50											
SS8	50											
SS9	50											
SS10	50											
SS11	50											
SS12	50											
SS13	50											
SS14	50											
SS15	50											
SS16	50											
SS17	50											
SS18	50	509	612	499	16.3	20.5	17.3	4.2	1.1	19	25	25
SS19	50	222	261	268	7.1	8.6	9.4	1.5	2.3	11	14	14
SS20	50	511	145	497	16.3	4.9	17.3	-11.4	0.9	22	22	22
SS21	50	175	288	220	5.7	9.4	7.7	3.8	2.1	8	14	11
SS22	50											
SS23	50	105	329	303	3.4	10.9	10.7	7.5	7.3	11	22	22

TABLE A5:

CELL	TEMP	MINSP1	MINSP2	MINSP3	LATENCY2	LATENCY3	TIMEPK21	TIMEPK31
SS13	48	19	22	17	6.5	0.7	7.6	11.2
SS14	48							
SS15	48	3	3	3	4.3	0.4	8.3	23.8
SS16	48	0	0	11	5.4	0.4	23.4	20.5
SS17	48	19	19	19				
SS18	48	8	17	11	4	1.1	19.4	7.9
SS19	48	0	6	3	4.3	0.7	11.9	13
SS20	48	11	0	3	4.7	1.1	9.7	10.8
SS21	48	6	8	6	5.8	0.4	12.6	13.7
SS22	48							
SS23	48	0	0	3	4.7	0.4	23	18.7
SS1	50							
SS2	50							
SS3	50							
SS4	50							
SS5	50							
SS6	50							
SS7	50							
SS8	50							
SS9	50							
SS10	50							
SS11	50							
SS12	50							
SS13	50							
SS14	50							
SS15	50							
SS16	50							
SS17	50							
SS18	50	14	14	14	1.8	0.7	4.3	22
SS19	50	0	0	3	4.3	0.7	9	14.4
SS20	50	8	0	6	4.7	0.4	8.3	11.5
SS21	50	3	3	6	4.3	0.4	6.5	13.7
SS22	50							
SS23	50	0	0	3	6.1	0.4	29.2	24.1